In the Name of Allah, The Most beneficiary,
The Most Gracious, The Most Merciful

Unsteady Flow and Heat Transfer Over an Exponentially Stretching Surface.

By

Maryam Subhani.

Department of Mathematics
Quaid-i-Azam University
Islamabad, Pakistan
2015

Unsteady Flow and Heat Transfer Over an Exponentially Stretching Surface.

By

Maryam Subhani.

Supervised By

Dr. Sohail Nadeem.

Department of Mathematics
Quaid-i-Azam University
Islamabad, Pakistan
2015

Unsteady Flow and Heat Transfer Over an Exponentially Stretching Surface.

By

Maryam Subhani.

A DISSERTATION SUBMITTED IN THE PARTIAL FULFILLMENT OF THE REQUIREMENT FOR THE DEGREE OF

MASTER OF PHILOSOPHY

IN

MATHEMATICS

Supervised By

Dr. Sohail Nadeem.

Department of Mathematics
Quaid-i-Azam University
Islamabad, Pakistan
2015

Dedicated

To

My Parents

Who

Always loved me

And

Encouraged me

In

Every Step of my Life

Acknowledgement

*I pay heartiest gratitude to Almighty **Allah** who conferred His countless blessings upon me to accomplish this hectic task of compiling my research findings in the form of this dissertation. Thanks to **Allah** for making us the ummah of His **Prophet** ﷺ and follow his teachings to seek the light of knowledge to enlighten our mind and soul.*

*I forward thanks from the core of my heart to my mentor and supervisor **Dr. Sohail Nadeem** who has been affectionately considerate and patronizing with his unprecedented guidance and consistent encouragement for providing a condusive atmosphere and motivating spirit throughout my research work. His inspiring genius, helpful assistance and meek guidance enabled me to overcome all the difficulties that came in my way from the preliminary to the concluding level.*

*My humble thankfulness to my **teachers** who strengthened my knowledge to embark on this tideous task of contributing my share into this vast ocean of knowledge by conducting research and opening up new horizons for the ones to follow.*

It is worth mentioning to acknowledge the cooperation of my seniors and fellow students namely Muhammad Awais, Salman Saleem Jaffery, Raja Rashid, Syed Tayyab Hussain, Hina, Shagufta, Muhammad Haji Farooq and Noor Muhammad who always lent a hand whenever I was stuck up in an enigmatic situation.

I extend my heartfelt regards to my friends Parsa, Beenish, Summiya, Faiza, Sarah, Humaira, Shahida, Irum, Aisha and Madiha who have been exuberant and energizing to boost up my morale and provided the friendly and supportive environment to conduct the research.

*Last but not the least, the supportive role of my **parents** and **sister** is undenieable. They provided me courage and perseverance during my weak moments. I specially thank my **mother** who was a torch bearer for me in this journey of the pursuit of knowledge.*

Maryam Subhani

Preface

In view of the substantial practical applications in industrial and manufacturing fields, a lot of work has been done on boundary layer flow over a stretching surface. The interminable list of its engineering applications comprise extrusion of polymer sheet, paper production, manufacturing of metal wires and plastic sheets, annealing and tinning of copper wires, cooling of metallic plate inside a cooling reservoir and so forth. Sakiadis [1] propounded the idea of the boundary layer flow over a continuous stretched surface and devised the boundary layer equations for two-dimensional flows. Tsou et al. [2] extended the idea of the effects of heat transfer on boundary layer flow over a stretching surface. Gupta et al. [3] incorporated mass transfer analysis over stretching sheet by considering suction or blowing. Later many researchers have further probed into boundary layer flows over stretching surfaces [4-5].

In the contemporary period, boundary layer flow over an exponentially stretching sheet is gaining much importance due to its vast applications. For instance; in the process of drawing and tinning of copper wires, the rate of heat transfer past a continuously stretching surface which has exponential modifications in its stretching velocity and temperature, influences the form of the final product. In this regard, Magyari and Keller [6] forwarded the comparison of numerical and analytical solutions. Nadeem et al. [7] discussed the heat transfer analysis of nanofluid over an exponentially stretching sheet. Ibrahim et al. [8] considered the MHD effects on nanofluid over an exponentially stretching sheet.

At the same time, the study of heat transfer gained momentum due to its importance in the industry for maintaining the quality of final product which significantly depends on the rate of cooling. Grubka and Bobba [9] presented the analysis of heat transfer over a linearly stretching surface with power law variations of surface temperature. Char [10] extended this work by considering the effects of suction or blowing. Elbashbeshy [11] presented the heat transfer analysis over an unsteady stretching surface. Lately Malvandi [12] analyzed the heat transfer of nanofluid over a permeable stretching sheet. Later on, researchers embarked on the effects of viscous dissipation in different fluids. Partha et al. [13] contemplated these effects on mixed convection heat transfer. Currently, investigation is being sought on the influence of viscous dissipation on nanofluids by different researchers [14-15]. Along with viscous dissipation, heat generation/absorption results on nanofluid have also been explored by Pal et al. [16]. Awais et al. [17] evaluated the heat generation/absorption effects on third grade nanofluid.

A substantial research has been done on thermal radiation and heat transfer due to its ample significance in electrical power generation, solar energy, space vehicles, astrophysical flows, cooling of nuclear reactors and industrial sector. Moreover, thermal radiation is the pivot around which the polymer industry moves. Initially radiation effects were studied by Hayat et al. [18] and Biliana et al. [19]. Nowadays the impact of thermal radiation on nanofluid is vastly being investigated. Prominent work has been done by Hayat et al. [20] and Sheikholeslami et al. [21].

Fluids which allow electrical conduction are frequently used in power generators, in the pattern of heat exchanges, MHD accelerators and electrostatic filters. This factor is of vital importance especially in metallurgical procedures for example, the process of cooling of filaments and strips being pulled out

from an inert fluid and exclusion of non-metallic materials from molten metals. The filaments are being drawn through an electrically conducting fluid exposed to a magnetic field; this helps in controlling the cooling rate. Therefore, MHD fluid flows are of great importance, which were analyzed by Andersson [22] in 1992, after that by Damseh et al. [23] in 2006 and then by Ishak [24] in 2011. Currently research is being sought on MHD flows over exponentially stretching sheets [25-26].

It is worth mentioning that unsteady flow conditions are also encountered in case when flow becomes time dependent due to unusual change in temperature or stretching of the sheet or heat flux of the sheet. Elbashbeshy [27] discussed the thermal radiation and magnetic field effects on unsteady flow. Mansur et al. [28] discussed the unsteady boundary layer flow over a stretching sheet.

Fluid particle suspension or dusty fluid deals with the motion of liquid or gas comprising inert, immiscible solid particles such as dust in gas cooling systems, blood flow in arteries etc. Their immense application is traced in cement process and steel manufacturing industry, fluidized bed, magneto hydrodynamic generators (MHG), gas purification, sedimentation pipe flows and bio fluids. The foremost task of formulating the governing equations for the flow of dusty fluids was undertaken by Saffman [29] who also brought into consideration the stability of the laminar flow of dusty fluid with uniformly distributed dust particles. Vajravelu et al. [30] carried out investigation on hydro magnetic flow of dusty fluid and highlighted the outcome of fluid particle interaction and suction on fluid properties. Extensive research has been done on fluid with dust particles by Gireesha et al. [31-33], on various aspects such as for nanofluids, convective boundary conditions, unsteady flow over an exponentially stretching sheet, and MHD flow with heat transfer analysis.

It was the need of the hour to enhance the thermal conductivity of some important conventional heat transfer fluids such as water, mineral oil and ethylene glycol which possess poor heat transfer characteristics. A novel solution was found by introducing small metallic solid particles in the fluid; this revolutionized the realm of technology and industry. These nanoparticles elevate the thermal conductivity of fluids improving the heat transfer properties. The fluids so obtained were termed as nanofluids. Therefore, nanofluids are characterized as a solid-fluid mixture with base fluid of low conductivity and nano-meter sized particles with high thermal conductivity. This fluid was first introduced by Choi [34] in 1995. A comprehensive study of convective transport within nanofluid was done by Buongiorno [35]. Boundary layer flow over an exponentially stretching sheet of nanofluid was initially investigated by Nadeem et al. [36]. Bachok et al. [37] examined the unsteady boundary layer flow of nanofluid. Nanoparticles with their low volume fraction, stability and remarkable useful applications in optical, biomedical and electronic fields have opened up new horizons of research recently. Naramgari et al. [38] conducted the research on dual solutions of MHD nanofluid flow on an exponentially stretching sheet. Nadeem et al. [39-40] investigated nanofluid model in different geometries with pertinent physical properties of fluid. Gireesha et al. [41] put forward the solution for MHD flow and heat transfer of a dusty nanofluid over a stretching sheet.

HAM is a frequently used approach among scientists to find explicit analytical solutions of non-linear problems. The optimal HAM (OHAM) is a modified and advanced version of HAM. OHAM uses the technique of minimizing the squared residual error through which the optimal values of the

convergence control parameters are obtained. Yubashita et al. [42] were the first to propose the optimization method for finding convergence control parameters. Then, it was Liao [43] who suggested that by minimized squared residual error one can acquire the optimized value of convergence control parameters.

In the vast field of literature, there is hardly any research conducted on the effects of nanoparticles on an unsteady flow of dusty fluid over an exponentially stretching sheet. In the present thesis, effect of dust particles on an unsteady boundary layer flow and heat transfer characteristics of a viscous nanofluid over an exponentially stretching sheet have been critically examined. Moreover, thermal radiation, viscous dissipation and internal heat generation absorption effects are also brought into consideration. For heat transfer analysis, two heating processes (i) Variable Exponential order Surface Temperature (VEST) case and (ii) Variable Exponential order Heat Flux (VEHF) case have been profoundly studied. Similarity transformations are defined to reduce governing equations to coupled non-linear Ordinary Differential Equations. Solution of the resulting ODE's is computed by OHAM. The Optimal Convergence Control parameters are acquired. Finally, non-dimensional velocities, temperature and concentration profiles and the effects of various physical parameters on them are exhibited by plotting graphs and are also presented in tabular form.

Contents

Chapter 1

Introduction

1.1 Preliminaries

This chapter comprises some fundamental definitions and pertinent governing equations with thorough mathematical algorithms related to the subsequent chapters.

1.2 Basic definitions

1.2.1 Fluid

An amorphous matter, in the state of a liquid or gas, that has the ability to flow and the tendency to change its shape continuously under an applied shear stress is known as a fluid.

1.2.2 Flow

It is a continuous phenomenon which tends to move the constituent components smoothly and steadily deforming their shape.

1.2.3 Fluid mechanics

Fluid mechanics deals with the profound study of fluids, both in dynamic and static form and also pertains to the application of the laws of force and motion to fluids.

1.3 Some physical properties of fluids

1.3.1 Density

Mass (m) per unit volume (V) of a fluid at a given temperature and pressure or stress conditions, is called density. Mathematically, the density ρ at a point may be defined as

$$\rho = \lim_{\delta V \to 0} \frac{\delta m}{\delta V}. \tag{1.1}$$

Dimension of density is $\left[ML^{-3}\right]$ and unit is kg/m^3.

1.3.2 Viscosity

It is the measure of a fluid's ability to resist gradual deformation, subjected to the action of applied shear stresses. Mathematically, it is defined as

$$\text{Viscosity} = \mu = \frac{\text{shear stress}}{\text{rate of shear strain}}. \tag{1.2}$$

where μ represents the coefficient of viscosity or dynamic viscosity or simply viscosity having dimension $\left[ML^{-1}T^{-1}\right]$.

1.3.3 Kinematic viscosity

The ratio of dynamic viscosity to the density of a fluid is known as kinematic viscosity and is denoted by ν. Mathematically

$$\nu = \frac{\mu}{\rho}, \tag{1.3}$$

where density of the fluid is defined by ρ and dimension of kinematic viscosity is $\left[L^2T^{-1}\right]$.

1.4 Classification of fluids

1.4.1 Ideal / Inviscid fluids

Ideal or inviscid fluids are those which offer no resistance to external forces due to vanishing viscosity. Gases are usually treated as ideal fluids for engineering purposes.

1.4.2 Real fluids

All the fluids in reality have some viscosity ($\mu > 0$) and hence are called real fluids. These fluids can either be compressible or incompressible, depending upon the relationship between the shear stress and the rate of shear strain.

1.4.3 Newtonian fluids

Fluids in which shear stress has a linear relationship with the local strain rate (the rate of change of its deformation over time) are called Newtonian fluids. These fluids observe the Newton's law of viscosity, which is given by

$$\tau_{yx} = \mu \frac{du}{dy}, \tag{1.4}$$

where τ_{yx} is the shear stress acting on a plane which is normal to $y-$axis, u is the velocity in $x-$direction, du/dy is the shear rate and μ is the constant of proportionality which is called the dynamic viscosity. Water and gasoline are common examples of Newtonian fluids.

1.4.4 Non-Newtonian fluids

Non-Newtonian fluids are those for which the shear stress is not directly proportional to the rate of deformation. These fluids obey power law model, which is given by

$$\tau_{yx} = k \left(\frac{du}{dy} \right)^n, \quad n \neq 1, \tag{1.5}$$

where k is the consistency index and n is the flow behavior index.

For $n = 1$ with $k = \mu$, the above equation reduces to the Newton's law of viscosity. Examples of non-Newtonian fluids include ketchup, tooth paste, blood, paints, biological fluids and so on.

1.5 Types of flows

1.5.1 Laminar flow

A flow in which particles move in a particular framework of their own and do not cross one another is known as laminar flow.

1.5.2 Turbulent flow

A flow in which particles do not move in a particular framework of their own and can cross one another is called turbulent flow. In this case particles move randomly.

1.5.3 Steady flow

A flow in which fluid properties at each point in a flow field do not change with time. For such a flow, we can write

$$\frac{\partial \zeta}{\partial t} = 0, \tag{1.6}$$

where ζ represents any fluid property that may be velocity, density etc.

1.5.4 Unsteady flow

A flow in which fluid properties at each point in a flow field differ with time is called unsteady flow. For such a flow, we can write

$$\frac{\partial \zeta}{\partial t} \neq 0. \tag{1.7}$$

1.5.5 Incompressible flow

It is a flow in which the density of the flowing fluid is uniform and remains constant throughout the flow. Therefore, when the flow is incompressible, the volume of every part of fluid remains unchanged during the course of its motion.

Mathematically, in an incompressible flow, the density ρ of a fluid particle remains constant throughout the flow field, i.e.,

$$\rho \neq \rho\,(x, y, z, t) \text{ or } \rho = \text{constant}. \tag{1.8}$$

or

$$\frac{d\rho}{dt} = 0, \tag{1.9}$$

where d/dt is the total derivative, which is equal to the sum of local and convective derivatives. All the liquids generally exhibit incompressible flow.

1.5.6 Compressible Flow

A flow in which the density is not uniform and does not remain constant during the flow, i.e.,

$$\rho = \rho\left(x, y, z, t\right). \tag{1.10}$$

1.6 Magnetohydrodynamics

Magnetohydrodynamics (MHD) is a branch of fluid dynamics that undertakes the study of magnetic characteristics of electrically conducting fluids. Liquid metals, plasmas and salt waters are examples of such fluids. Maxwell equations have an important role in MHD studies.

1.6.1 The Maxwell equations

James Clerk Maxwell derived a set of equations describing the behavior of both magnetic and electric fields known as Maxwell equations. In electromagnetism, Maxwell equations enlist four partial differential equations describing the salient features of electrical and magnetic fields. These equations are independently termed as Gauss's law, Gauss's law for magnetism, Faraday's law and Ampere's law. These equations are

$$\boldsymbol{\nabla} \cdot \mathbf{E} = \frac{\rho_e}{\varepsilon}, \qquad \text{(Gauss's law)} \tag{1.11}$$

$$\boldsymbol{\nabla} \cdot \mathbf{B} = 0, \qquad \text{(Gauss's law for magnetism)} \tag{1.12}$$

$$\boldsymbol{\nabla} \times \mathbf{E} = -\frac{\partial \mathbf{B}}{\partial t}, \qquad \text{(Faraday's law of induction)} \tag{1.13}$$

$$\boldsymbol{\nabla} \times \mathbf{B} = \mu_e \mathbf{J} + \mu_e \varepsilon \frac{\partial \mathbf{E}}{\partial t}, \qquad \text{(Ampere's law with Maxwell correction)} \tag{1.14}$$

where $\mathbf{E}$ is the electric field, $\mathbf{B}$ is the total magnetic field, $\mathbf{J}$ is the total current density, ρ_e is the charge density, ε is the permittivity of the free space and μ_e is the magnetic permeability.

1.6.2 The generalized Ohm's law

For an electrically conducting fluid the generalized Ohm's law is

$$\mathbf{J} = \sigma \left(\mathbf{E} + \mathbf{V} \times \mathbf{B} \right), \tag{1.15}$$

where σ is the electric conductivity and $\mathbf{V}$ is the velocity vector.

1.7 Governing laws

1.7.1 Law of conservation of mass

According to the conservation of mass law, which is also termed as continuity equation, mass can neither be created nor destroyed in any system. In the vector form, it can be written as follows

$$\frac{\partial \rho}{\partial t} + \boldsymbol{\nabla} \cdot (\rho \mathbf{V}) = 0, \tag{1.16}$$

where

$$\boldsymbol{\nabla} = \left(\frac{\partial}{\partial x}, \frac{\partial}{\partial y}, \frac{\partial}{\partial z} \right), \tag{1.17}$$

is a three dimensional differential operator, ρ is the density of the fluid, t is the time and $\mathbf{V}$ denotes the velocity of the fluid. For an incompressible fluid, the density is constant and thus Eq. (1.16) becomes

$$\boldsymbol{\nabla} \cdot \mathbf{V} = 0. \tag{1.18}$$

1.7.2 Law of conservation of momentum

Every particle of fluid, either at rest or in steady state or accelerated motion obeys Newton's second law of motion according to which, the total sum of all external forces acting upon a system is equivalent to the rate of variation of linear momentum of that particular system. In

vector form, it can be written as

$$\rho\frac{d\mathbf{V}}{dt} = \text{div}\,\boldsymbol{\tau}+\rho\mathbf{b}, \tag{1.19}$$

where d/dt is material time derivative, $\mathbf{b}$ is the body force per unit mass and $\boldsymbol{\tau}$ is the Cauchy stress tensor.

1.7.3 Law of conservation of energy

Law of conservation of energy is essential to study the heat transfer phenomenon in fluid dynamics problems. It states that in a secluded system, energy can change its form but cannot be created or destroyed and the overall energy of the system is conserved. Mathematically

$$\rho c_p\frac{dT}{dt} = k\boldsymbol{\nabla}^2T + \boldsymbol{\tau}\cdot\mathbf{L}, \tag{1.20}$$

where c_p is specific heat at constant pressure,$\boldsymbol{\tau}\cdot\mathbf{L}$ is viscous dissipation term and k is the thermal conductivity which describes that how fast a particular material conducts heat.

1.7.4 Law of conservation of concentration

Fick's Law

In 1855, Adolf Engen Fick, a German physiologist developed Fick's law of diffusion, which governs the diffusion of a gas across a fluid membrane. It relates the diffusive flux to concentration. It states that the flux of diffusion goes from higher concentration region to low concentration. In Mathematical form, we have

$$\mathbf{J}^* = -D\ \nabla C. \tag{1.21}$$

Fick's 2^{nd} law governs how diffusion causes the concentration to change with time,

$$\frac{\partial C}{\partial t} = D\ \nabla^2 C, \tag{1.22}$$

where C the concentration, $\mathbf{J}^*$ the diffusion flux, D is the diffusivity, which gives the rate of diffusion, how slow or fast an object diffuses.

1.8 Heat transfer

It is the branch of thermal science that deals with the production, conversion, utilization and exchange of thermal energy and heat between physical processes.

1.8.1 Conduction

The transfer of energy between objects that are in physical contact is called conduction.

1.8.2 Convection

The transfer of energy between an object and its environment due to fluid motion is called convection. It occurs in gas molecules.

1.8.3 Viscous Dissipation

Viscous dissipation refers to the work done by the fluid due to the action of viscous forces on adjacent layers resulting in the irreversible change of mechanical energy into thermal energy.

1.8.4 Thermal Radiation

Thermal radiation is the outcome of the thermal movement of the charged particles in matter. In this process electromagnetic radiation is generated from a heated surface in all directions.

1.9 Mass transfer

It is the gross movement of mass from one location to another as a side effect of physically moving an object containing that mass.

1.10 Boundary layer

Ludwig Prandtl a German astronomer discovered the idea of boundary layer, in 1904, in his paper which he presented in mathematical congress. It is a layer that fluid forms close to the solid boundary, where the viscosity effects are dominant in determining the flow field. The viscous effects are considered which have significant role on fluid motion. Thus a fluid flow

is upheld in the vicinity of the wall and a finite slow moving boundary layer is formed. The thickness of the boundary layer is taken to be the distance from the wall to the point at which the velocity is equivalent to 99% of the free-stream velocity. As the solution of the Navier-Stokes equation is expensive, so this technique helps us to reduce equations.

1.11 Dimensionless numbers

1.11.1 Reynolds number

Having no dimensions this number represents the relationship between inertial forces ($V\rho$) and viscous forces ($\frac{\mu}{L}$). Mathematically

$$\mathrm{Re} = \frac{UL}{\nu}, \tag{1.23}$$

where L is characteristic length, U is the free stream velocity. Laminar flow exists at low Reynolds number, where viscous forces are influential, while turbulent flow exists at high Reynolds number and it is dominated by inertial forces.

1.11.2 Skin friction

The amount of friction produced by a fluid when it passes through a surface is known as skin friction. It arises between the fluid and the surface, which tends to stress-free the fluid's motion. The skin friction coefficient is mathematically written as

$$C_f = \frac{\tau_w}{\rho U^2} \tag{1.24}$$

where τ_w is the shear stress at the wall, ρ is the density and U is free-stream velocity.

1.11.3 Nusselt number

It is a non-dimensional number, used in heat transfer, it is the fraction between convective heat transfer and conductive heat transfer which is normal to the boundary introduced by German mathematician Nusselt. In Mathematical form, we one can write

$$Nu = \frac{hL}{k}, \tag{1.25}$$

where h is coefficient of convective heat transfer and k is the thermal conductivity of the fluid.

1.11.4 Sherwood number

It is a dimensionless number, used in mass transfer analysis which gives the measure of the ratio of convective to diffusive mass transport. Mathematically

$$Sh = \frac{K_c L}{D}, \tag{1.26}$$

where D is component diffusion coefficient and K_c is convective mass transfer coefficient.

1.11.5 Prandtl number

It is a number having no dimension exhibiting the relationship between momentum diffusivity and thermal diffusivity. It governs the respective thickness of momentum and thermal boundary layer. In Mathematical form, we have

$$\mathrm{Pr} = \frac{\text{viscous diffusion rate}}{\text{thermal diffusion rate}} = \frac{\nu}{\alpha} = \frac{\mu/\rho}{k/\rho c_p} = \frac{\mu c_p}{k}. \tag{1.27}$$

1.11.6 Schmidt number

It is the ratio of rate of momentum diffusivity to mass diffusivity. It is a dimensionless number, used to characterize fluid flows in which there are simultaneous momentum and mass diffusion convection process. Mathematically we have

$$Sc = \frac{\text{rate of viscous diffusion}}{\text{rate of molecular diffusion}} = \frac{\nu}{D}. \tag{1.28}$$

1.11.7 Eckert Number

It is a number having no dimension illustrating the ratio of kinetic energy to enthalpy. Mathematically

$$Ec = \frac{u^2}{c_p \Delta T}, \tag{1.29}$$

where u is the local velocity, c_p is the specific heat and ΔT is the difference between temperature.

1.11.8 Brownian motion

Brownian motion in nanofluid is the random motion of the nanoparticles in the base fluid due to the collision of nanoparticles with the particles of base fluid. In Mathematical form, we have

$$N_B = \frac{(\rho c_p)_p D_B (C_w - C_\infty)}{\rho c_p \nu},$$

In the above equation, $(\rho c_p)_p$ is the heat capacity of nanoparticles, ρc_p denotes the fluid heat capacity, D_B symbolizes Brownian diffusion coefficient, C_w and C_∞ are the wall and fluid concentration and ν is the kinematic viscosity.

1.11.9 Thermophoresis parameter

For cold and hot surface this parameter is positive and negative respectively. In the process of thermophoresis, for hot surface, the nanoparticle concentration boundary layer flow is moved away from the wall. Resulting in the formation of particle free layer at the boundary. Mathematically

$$N_T = \frac{(\rho c_p)_p D_T (T_w - T_\infty)}{\rho c_p \nu T_\infty},$$

where D_T symbolizes thermophoretic diffusion coefficient, T_w and T_∞ are the wall and fluid temperature.

Chapter 2

Unsteady Boundary Layer Flow and Heat Transfer of a Fluid Particle Suspension over an Exponentially Stretching Surface

2.1 Introduction

In this chapter we have discussed the analytical solution of the unsteady boundary layer flow and heat transfer of a fluid with dust particles suspended in it. An external magnetic field is employed transverse to the plate. Heat generation or absorption, viscous dissipation and thermal radiation effects are also considered. First of all, by employing similarity transformations, modelled partial differential equations are converted to ordinary differential equations by using similarity transformations for the following cases of boundary conditions (i) Variable exponential order surface temperature (VEST) (ii) Variable exponential order heat flux (VEHF) and then by using OHAM (Optimal Homotopy Analysis Method) the series solutions are calculated. At the end, the impact of the relevant parameters over velocity and temperature distributions are examined in detail. The physical idea of this work was solved numerically by Pavithra and Gireesha [31] . However, its analytical solutions through OHAM have been computed by us.

2.2 Problem formulation

For the above considered problem the equation of continuity, equation of conservation of linear momentum and equation of conservation of energy for the fluid respectively are,

$$\text{div } \mathbf{V} = 0, \tag{2.1}$$

$$\rho \left[\frac{d\mathbf{V}}{dt}\right] = \boldsymbol{\nabla} \cdot \boldsymbol{\tau} + KN \left[\mathbf{V}_P - \mathbf{V}\right] + \mathbf{J} \times \mathbf{B}, \tag{2.2}$$

$$\begin{aligned} \rho c_p \left[\frac{dT}{dt}\right] &= k \left(\nabla \cdot \nabla T\right) + \frac{N c_p}{\tau_T} \left(T_p - T\right) + \frac{N}{\tau_\nu} (\mathbf{V}_p - \mathbf{V}) \cdot (\mathbf{V}_p - \mathbf{V}) \\ &\quad - \frac{\partial q_r}{\partial y} + \boldsymbol{\tau} \cdot \mathbf{L} + Q(T - T_\infty). \end{aligned} \tag{2.3}$$

Similarly the equation of continuity, equation of conservation of linear momentum and equation of conservation of energy for dust particle phase are,

$$\text{div } \mathbf{V}_p = 0, \tag{2.4}$$

$$\rho \left[\frac{d\mathbf{V}_p}{dt}\right] = \frac{K}{m} \left[\mathbf{V} - \mathbf{V}_P\right], \tag{2.5}$$

$$\rho c_m \left[\frac{dT_p}{dt}\right] = -\frac{N c_p}{\tau_T} \left(T_P - T\right). \tag{2.6}$$

For an electrically conducting fluid, the Maxwell equations are

$$\boldsymbol{\nabla} \cdot \mathbf{B} = 0, \quad \boldsymbol{\nabla} \times \mathbf{B} = \mu_e \mathbf{J}, \quad \boldsymbol{\nabla} \times \mathbf{E} = \mathbf{0}, \tag{2.7}$$

$$\mathbf{J} = \sigma \left(\mathbf{E} + \mathbf{V} \times \mathbf{B}\right), \tag{2.8}$$

where μ_e is the magnetic permeability, σ denotes the electrical conductivity and $\mathbf{E}$ is the total electric field, which is neglected. Further the Hall effects and electric magnetic fields induced by the fluid motion are also ignored. So that the Lorentz force in Eq. (2.2) becomes

$$\mathbf{J} \times \mathbf{B} = \sigma \left(\mathbf{V} \times \mathbf{B}\right) \times \mathbf{B}. \tag{2.9}$$

We consider the velocity and the magnetic fields of the form

$$\mathbf{V} = [(u(x,y), v(x,y), 0)], \tag{2.10}$$

$$\mathbf{B} = [0, B, 0]. \tag{2.11}$$

Now

$$\mathbf{V} \times \mathbf{B} = \begin{bmatrix} \hat{i} & \hat{j} & \hat{k} \\ u & v & 0 \\ 0 & B & 0 \end{bmatrix}, \tag{2.12}$$

$$\mathbf{V} \times \mathbf{B} = Bu\hat{k}. \tag{2.13}$$

Then we have

$$(\mathbf{V} \times \mathbf{B}) \times \mathbf{B} = \begin{bmatrix} \hat{i} & \hat{j} & \hat{k} \\ 0 & 0 & Bu \\ 0 & B & 0 \end{bmatrix}. \tag{2.14}$$

Using Eq. (2.14) in Eq. (2.9), we have

$$\mathbf{J} \times \mathbf{B} = \left[-\sigma B^2 u, 0, 0\right]. \tag{2.15}$$

The Cauchy stress tensor $\boldsymbol{\tau}$ for the Newtonian fluid is defined as

$$\boldsymbol{\tau} = -p\mathbf{I} + \mu\mathbf{A}_1, \tag{2.16}$$

where p represents the pressure, $\mathbf{I}$ symbolizes the identity tensor and $\mathbf{A}_1$ is the first Rivlin-Erickson tensor, that gives us the rate of strain, which is defined as

$$\mathbf{A}_1 = \mathbf{L} + \mathbf{L}^{T_1}, \tag{2.17}$$

where

$$\mathbf{L} = \operatorname{grad} \mathbf{V}, \tag{2.18}$$

$$\mathbf{L} = \begin{bmatrix} \frac{\partial u}{\partial x} & \frac{\partial u}{\partial y} & 0 \\ \frac{\partial v}{\partial x} & \frac{\partial v}{\partial y} & 0 \\ 0 & 0 & 0 \end{bmatrix}, \tag{2.19}$$

and

$$\mathbf{L}^{T_1} = \begin{bmatrix} \frac{\partial u}{\partial x} & \frac{\partial v}{\partial x} & 0 \\ \frac{\partial u}{\partial y} & \frac{\partial v}{\partial y} & 0 \\ 0 & 0 & 0 \end{bmatrix}, \tag{2.20}$$

with T_1 represents as the transpose. After substituting Eqs. (2.19) and (2.20) in Eq. (2.17), the first Rivlin-Erickson tensor is

$$\mathbf{A}_1 = \begin{bmatrix} 2\frac{\partial u}{\partial x} & \frac{\partial u}{\partial y} + \frac{\partial v}{\partial x} & 0 \\ \frac{\partial v}{\partial x} + \frac{\partial u}{\partial y} & 2\frac{\partial v}{\partial y} & 0 \\ 0 & 0 & 0 \end{bmatrix}. \tag{2.21}$$

Invoking Eq. (2.21) into Eq. (2.16), we obtain

$$\boldsymbol{\tau} = \begin{bmatrix} -p + 2\mu\frac{\partial u}{\partial x} & \mu\left(\frac{\partial u}{\partial y} + \frac{\partial v}{\partial x}\right) & 0 \\ \mu\left(\frac{\partial v}{\partial x} + \frac{\partial u}{\partial y}\right) & -p + 2\mu\frac{\partial v}{\partial y} & 0 \\ 0 & 0 & -p \end{bmatrix}. \tag{2.22}$$

The first term on the R.H.S of Eq. (2.2) can be attained by taking the divergence of Eq.(2.22) and is given as

$$\boldsymbol{\nabla} \cdot \boldsymbol{\tau} = \left[-\frac{\partial p_1}{\partial x} + \mu\left(2\frac{\partial^2 u}{\partial x^2} + \frac{\partial^2 u}{\partial y^2} + \frac{\partial^2 v}{\partial y \partial x}\right), -\frac{\partial p_1}{\partial y} + \mu\left(2\frac{\partial^2 v}{\partial y^2} + \frac{\partial^2 v}{\partial x^2} + \frac{\partial^2 u}{\partial x \partial y}\right), 0 \right]. \tag{2.23}$$

Using continuity equation, we get

$$\boldsymbol{\nabla} \cdot \boldsymbol{\tau} = \left[-\frac{\partial p_1}{\partial x} + \mu\left(\frac{\partial^2 u}{\partial x^2} + \frac{\partial^2 u}{\partial y^2}\right), -\frac{\partial p_1}{\partial y} + \mu\left(\frac{\partial^2 v}{\partial y^2} + \frac{\partial^2 v}{\partial x^2}\right), 0 \right]. \tag{2.24}$$

Making use of Eqs. (2.10), (2.15) and (2.24) in the continuity and momentum equations in component form, we have

$$\frac{\partial u}{\partial x}+\frac{\partial v}{\partial y}=0, \tag{2.25}$$

$$\frac{\partial u}{\partial t}+u\frac{\partial u}{\partial x}+v\frac{\partial u}{\partial y}=-\frac{1}{\rho}\frac{\partial p}{\partial x}+\nu\left(\frac{\partial^2 u}{\partial x^2}+\frac{\partial^2 u}{\partial y^2}\right)-\frac{\sigma}{\rho}B^2u+KN\left(u_p-u\right), \tag{2.26}$$

$$\frac{\partial v}{\partial t}+u\frac{\partial v}{\partial x}+v\frac{\partial v}{\partial y}=-\frac{1}{\rho}\frac{\partial p}{\partial y}+\nu\left(\frac{\partial^2 v}{\partial x^2}+\frac{\partial^2 v}{\partial y^2}\right)+KN\left(v_p-v\right). \tag{2.27}$$

Similarly the velocity vector for dust particles is defined as

$$\mathbf{V}_p=\left[\left(u_p\left(x,y\right),v_p\left(x,y\right),0\right)\right]. \tag{2.28}$$

Substituting the above equation into Eqs.(2.4) and (2.5), we get equation of continuity and equation of momentum for dust particles in component form, as follows

$$\frac{\partial u_p}{\partial x}+\frac{\partial v_p}{\partial y}=0, \tag{2.29}$$

$$\frac{\partial u_p}{\partial t}+u_p\frac{\partial u_p}{\partial x}+v_p\frac{\partial u_p}{\partial y}=\frac{K}{m}\left(u-u_p\right), \tag{2.30}$$

$$\frac{\partial v_p}{\partial t}+u_p\frac{\partial v_p}{\partial x}+v_p\frac{\partial v_p}{\partial y}=\frac{K}{m}\left(v-v_p\right). \tag{2.31}$$

Using the boundary layer assumptions by considering x, u and p be $O\left(1\right)$ while y, v be $O\left(\delta\right)$ and ν being $O\left(\delta^2\right)$, where δ is the boundary layer thickness, Eqs. $(2.25-2.27)$ and $(2.29-2.31)$ reduce to

$$\frac{\partial u}{\partial x}+\frac{\partial v}{\partial y}=0, \tag{2.32}$$

$$\frac{\partial u}{\partial t}+u\frac{\partial u}{\partial x}+v\frac{\partial u}{\partial y}=\nu\frac{\partial^2 u}{\partial y^2}-\frac{\sigma}{\rho}B^2u+KN\left(u_p-u\right), \tag{2.33}$$

$$\frac{\partial u_p}{\partial x}+\frac{\partial v_p}{\partial y}=0, \tag{2.34}$$

$$\frac{\partial u_p}{\partial t}+u_p\frac{\partial u_p}{\partial x}+v_p\frac{\partial u_p}{\partial y}=\frac{K}{m}\left(u-u_p\right). \tag{2.35}$$

The corresponding boundary conditions are

$$\begin{aligned} u &= U_w(x,t),\ v = -V_w(x,t),\ \text{at } y = 0, \\ u &\to 0, u_p \to 0,\ v_p \to v,\ \text{as } y \to \infty, \end{aligned} \tag{2.36}$$

where $U_w(x,t) = \frac{U_o}{(1-\alpha t)} e^{\frac{x}{L}}$ denotes the velocity of the sheet, $V_w(x,t) = -S\sqrt{\frac{U_o \nu}{2L(1-\alpha t)}} e^{\frac{x}{2L}}$ represents the suction velocity, U_o illustrates the reference velocity, L is the reference length and $S > 0$ is a suction parameter.

Introducing the following similarity transformations

$$\begin{aligned} \eta &= \sqrt{\frac{U_o}{2\nu L(1-\alpha t)}} e^{\frac{x}{2L}} y,\ u = \frac{U_o}{(1-\alpha t)} e^{\frac{x}{L}} f'(\eta), \\ v &= -\sqrt{\frac{U_o \nu}{2L(1-\alpha t)}} e^{\frac{x}{2L}} \left[f(\eta) + \eta f'(\eta) \right],\ u_p = \frac{U_o}{(1-\alpha t)} e^{\frac{x}{L}} F'(\eta), \\ v_p &= -\sqrt{\frac{U_o \nu}{2L(1-\alpha t)}} e^{\frac{x}{2L}} \left[F(\eta) + \eta F'(\eta) \right], B = \frac{B_o}{\sqrt{(1-\alpha t)}} e^{\frac{x}{2L}}. \end{aligned} \tag{2.37}$$

Making use of Eq. (2.37), equations of continuity are identically satisfied and Eqs. (2.33 and 2.35) take the following form

$$f'''(\eta) + f(\eta) f''(\eta) - 2f'(\eta)^2 + 2l\beta \left[F'(\eta) - f'(\eta) \right] - A \left[2f'(\eta) + \eta f''(\eta) \right] - Mf' = 0, \tag{2.38}$$

$$F(\eta)F''(\eta) - 2F'(\eta)^2 + 2\beta[f'(\eta) - F'(\eta)] - A[\eta F''(\eta) + 2F'(\eta)] = 0, \tag{2.39}$$

where prime signifies the differentiation with respect to η and $l = \frac{m\mathbf{N}}{\rho}$ represents the mass concentration, $\beta = \frac{L}{\boldsymbol{\tau}_\nu U_o}(1-\alpha t) e^{-\frac{x}{L}}$ represents the fluid-particle interaction parameter for velocity, where $\boldsymbol{\tau}_\nu = \frac{m}{K}$ is the relaxation time of dust phase, $A = \frac{\alpha L}{U_o e^{\frac{x}{L}}}$ is the unsteady parameter which determines the unsteadiness and $M = \frac{2\sigma B_o^2 L}{\rho U_o}$ is the magnetic parameter.

Making use of the similarity transformations on boundary conditions they will reduce to

$$\begin{aligned} f'(\eta) &= 1, f(\eta) = S \text{ at } \eta = 0, \\ f'(\eta) &= 0, F'(\eta) = 0, F(\eta) = f(\eta) + \eta f'(\eta) - \eta F'(\eta) \text{ as } \eta \to \infty. \end{aligned} \tag{2.40}$$

The Expression for the skin friction coefficient is

$$C_f = \frac{\boldsymbol{\tau}_w}{\rho U_w^2}, \tag{2.41}$$

where the skin friction $\boldsymbol{\tau}_w$ is given by,

$$\boldsymbol{\tau}_w = \mu \left(\frac{\partial u}{\partial y} \right)_{y=0}. \tag{2.42}$$

Employing the non-dimensional variables on Eq.(2.41), one obtains,

$$\sqrt{2\,\mathrm{Re}} C_f = f''(0). \tag{2.43}$$

where $\mathrm{Re} = \frac{U_0 L}{\nu}$ is the Reynolds number.

2.3 Heat Transfer Analysis

Energy equation for fluid

$$\begin{aligned} \rho c_p \left(\frac{dT}{dt} \right) &= k(\nabla . \nabla T) + \frac{N c_p}{\tau_T} (T_p - T) + \frac{N}{\tau_\nu} (\mathbf{V}_p - \mathbf{V}) \cdot (\mathbf{V}_p - \mathbf{V}) \\ &\quad - \frac{\partial q_r}{\partial y} + \boldsymbol{\tau} \cdot \mathbf{L} + Q(T - T_\infty), \end{aligned} \tag{2.44}$$

5th term of R.H.S can be calculated using τ, the Cauchy stress tensor.

$$\boldsymbol{\tau} = \mu \begin{bmatrix} \tau_{xx} & \tau_{xy} & 0 \\ \tau_{yx} & \tau_{yy} & 0 \\ 0 & 0 & 0 \end{bmatrix}, \tag{2.45}$$

$$\mathbf{L} = \operatorname{grad} \mathbf{V}, \tag{2.46}$$

$$\boldsymbol{\tau} \cdot \mathbf{L} = \begin{bmatrix} \tau_{xx} & \tau_{xy} & 0 \\ \tau_{yx} & \tau_{yy} & 0 \\ 0 & 0 & 0 \end{bmatrix} . \begin{bmatrix} \frac{\partial u}{\partial x} & \frac{\partial u}{\partial y} & 0 \\ \frac{\partial v}{\partial x} & \frac{\partial v}{\partial y} & 0 \\ 0 & 0 & 0 \end{bmatrix}, \tag{2.47}$$

$$\boldsymbol{\tau}\cdot\mathbf{L}=2\mu\left(\left(\frac{\partial u}{\partial x}\right)^2+\left(\frac{\partial v}{\partial y}\right)^2\right)+\mu\left(\frac{\partial u}{\partial y}\right)^2+\mu\left(\frac{\partial v}{\partial x}\right)^2+2\mu\left(\frac{\partial u}{\partial y}\frac{\partial v}{\partial x}\right). \tag{2.48}$$

Using the above values and under the boundary layer assumptions, energy equation for fluid phase takes the form

$$\begin{aligned}\rho c_p\left(\frac{\partial T}{\partial t}+u\frac{\partial T}{\partial x}+v\frac{\partial T}{\partial y}\right) &= k\frac{\partial^2 T}{\partial y^2}+\frac{Nc_p}{\tau_T}\left(T_p-T\right)+\frac{N}{\tau_\nu}\left(u_p-u\right)^2 \\ &\quad -\frac{\partial q_r}{\partial y}+\mu\left(\frac{\partial u}{\partial y}\right)^2+Q(T-T_\infty).\end{aligned} \tag{2.49}$$

Similarly for dust particles, we get the equation

$$Nc_m\left(\frac{\partial T_p}{\partial t}+u_p\frac{\partial T_p}{\partial x}+v_p\frac{\partial T_p}{\partial y}\right)=-\frac{Nc_p}{\tau_T}\left(T_p-T\right). \tag{2.50}$$

Involving Rosseland approximation for thermal radiation, heat flux is simplified to

$$q_r=-\frac{4\sigma^*}{3k^*}\frac{\partial T^4}{\partial y}, \tag{2.51}$$

where σ^* symbolizes the Stefan-Boltzmann constant and k^* represents the mean absorption coefficient. T^4 can be written in terms of a linear function of temperature by using Taylor series expansion about T_∞

$$T^4=4T_\infty^3T-3T_\infty^4. \tag{2.52}$$

Substituting Eq.(2.51) in Eq.(2.49), we get

$$\begin{aligned}\rho c_p\left(\frac{\partial T}{\partial t}+u\frac{\partial T}{\partial x}+v\frac{\partial T}{\partial y}\right) &= \left(k+\frac{16\sigma^*T_\infty^3}{3k^*}\right)\frac{\partial^2 T}{\partial y^2}+\frac{\partial^2 T}{\partial y^2}+\frac{Nc_p}{\tau_T}\left(T_p-T\right) \\ &\quad +\frac{N}{\tau_\nu}\left(u_p-u\right)^2+\mu\left(\frac{\partial u}{\partial y}\right)^2+Q(T-T_\infty).\end{aligned} \tag{2.53}$$

The phenomenon of heat transfer is discussed for two different types of heating procedures, i.e.,

Case 1: Variable exponential order surface temperature (VEST).

Case 2: Variable exponential order heat flux (VEHF).

2.3.1 Case 1: Variable exponential order surface temperature (VEST):

In this case the boundary conditions employed, are defined as

$$\begin{aligned} T &= T_w(x,t) \text{ at } y=0, \\ T &\to T_\infty,\ T_p \to T_\infty \text{ as } y\to\infty, \end{aligned} \tag{2.54}$$

where $T_w = T_\infty + \frac{\mathbf{T}_o}{(1-\alpha t)^2} e^{\frac{c_1 x}{2L}}$ is the temperature of stretching surface, c_1 is a constant and T_0 is a reference temperature. Introducing the dimensionless variables for the fluid temperature $\theta(\eta)$ and dust particles temperature $\theta_p(\eta)$,

$$\theta(\eta) = \frac{T-T_\infty}{T_w - T_\infty},\ \theta_p(\eta) = \frac{T_p - T_\infty}{T_w - T_\infty}, \tag{2.55}$$

where $T - T_\infty = \frac{T_0}{(1-\alpha t)^2} e^{\frac{c_1 x}{2L}} \theta(\eta)$. Using the similarity variable (η) and Eq. (2.55) into Eqs.(2.50) and (2.53) , the following set of equations is achieved

$$\left(1+\frac{4R}{3}\right)\theta''(\eta) + \Pr\left[f(\eta)\theta'(\eta) - c_1 f'(\eta)\theta(\eta)\right] + 2\lambda\Pr\theta(\eta) + \Pr Ec\left[f'(\eta)\right]^2 \tag{2.56}$$

$$+2\frac{N}{\rho}\beta_T \Pr\left[\theta_p(\eta) - \theta(\eta)\right] + 2\frac{N}{\rho}\beta \Pr Ec\left[F'(\eta) - f'(\eta)\right]^2 - A\Pr\left[\eta\theta'(\eta) + 4\theta(\eta)\right] = 0,$$

$$c_1 F'(\eta)\theta_p(\eta) - F(\eta)\theta_p'(\eta) + 2\gamma\beta_T\left[\theta_p(\eta) - \theta(\eta)\right] + A[\eta\theta_p'(\eta) + 4\theta_p(\eta)] = 0, \tag{2.57}$$

where $\Pr = \frac{\mu c_p}{k}$ portrays the Prandtl number, $R = \frac{4\sigma^* T_\infty^3}{kk^*}$ is the parameter for radiation, $\gamma = \frac{c_p}{c_m}$ is the specific heat ratio, $Ec = \frac{U_0^2 e^{\frac{2x}{L}}}{c_p T_0 e^{\frac{c_1 x}{2L}}}$ is the Eckert number, $A = \frac{\alpha L}{U_0 e^{\frac{x}{L}}}$ is the unsteady parameter, $\beta = \frac{L}{\tau_\nu U_0 e^{\frac{x}{L}}}(1-\alpha t)$ and $\beta_T = \frac{L}{\tau_T U_0 e^{\frac{x}{L}}}(1-\alpha t)$ are the fluid and particle interaction parameters for velocity and heat transfer respectively, $\lambda = \frac{QL^2}{\mu c_p \operatorname{Re}}$ denotes the dimensionless heat source/sink parameter where $\operatorname{Re} = \frac{U_0 L e^{\frac{x}{L}}}{\nu(1-\alpha t)}$ is the Reynolds number.

Subsequent thermal boundary conditions become

$$\begin{aligned} \theta(\eta) &= 1 \text{ at } \eta = 0 \\ \theta(\eta) &\to 0,\ \theta_p(\eta) \to 0 \text{ as } \eta\to\infty. \end{aligned} \tag{2.58}$$

2.3.2 Case 2: Variable exponential order heat flux (VEHF):

For this thermal procedure, the boundary conditions considered are defined as

$$\begin{aligned} \frac{\partial T}{\partial y} &= -\frac{q_w(x,t)}{k} \text{ at } y=0, \\ T &\rightarrow T_\infty, T_p \rightarrow T_\infty \text{ as } y \rightarrow \infty, \end{aligned} \tag{2.59}$$

where $T_w = T_\infty + \frac{q_w}{k}\left(\frac{2\nu L}{U_w}\right)^{\frac{1}{2}}$, $q_w = \frac{T_1}{(1-\alpha t)^{\frac{5}{2}}} e^{\frac{(c_1+1)x}{2L}}$ and T_1 is the reference temperature. Now by using the similarity variable (η) and Eq. (2.55) we get the same system of equations with $Ec = \frac{kU_o^2}{c_p T_1}\sqrt{\frac{U_0}{2\nu L}}$, which is different from the VEST case, all the other parameters are same as in VEST.

The boundary conditions for above case take the following form,

$$\begin{aligned} \theta'(\eta) &= -1 \text{ at } \eta = 0 \\ \theta(\eta) &\rightarrow 0,\ \theta_p(\eta) \rightarrow 0 \text{ as } \eta \rightarrow \infty. \end{aligned} \tag{2.60}$$

The Nusselt number is defined as,

$$Nu_x = \frac{x q_w}{k(T - T_\infty)}, \tag{2.61}$$

where q_w is the heat transfer from the sheet, which is given by

$$q_w = -k\left(\frac{\partial T}{\partial y}\right)_{y=0}. \tag{2.62}$$

Making use of non-dimensional variables, one obtains,

$$\frac{Nu_x}{\sqrt{2\,\mathrm{Re}}} = -\frac{x}{2L}\theta'(0) \text{ (VEST Case)}, \tag{2.63}$$

and.

$$\frac{Nu_x}{\sqrt{2\,\mathrm{Re}}} = \frac{x}{2L}\frac{1}{\theta(0)} \text{ (VEHF Case)}. \tag{2.64}$$

2.4 Solutions by Optimal Homotopy Analysis Method (OHAM)

The coupled nonlinear ordinary differential equations for VEST and VEHF cases are analytically solved by the method commonly known as Optimal Homotopy Analysis Method (OHAM). According to the procedure, we express the set of basic functions $f(\eta)$, $F(\eta)$, $\theta(\eta)$ and $\theta_p(\eta)$ by

$$\left\{\eta^k \exp(-n\eta) \mid k \geq 0,\ \eta \geq 0\right\}, \tag{2.65}$$

in the form

$$f(\eta) = \sum_{n=0}^{\infty}\sum_{k=0}^{\infty} a_{m,n}^{k}\ \eta^k \exp(-n\eta), \tag{2.66}$$

$$F(\eta) = \sum_{n=0}^{\infty}\sum_{k=0}^{\infty} b_{m,n}^{k}\ \eta^k \exp(-n\eta), \tag{2.67}$$

$$\theta(\eta) = \sum_{n=0}^{\infty}\sum_{k=0}^{\infty} c_{m,n}^{k}\ \eta^k \exp(-n\eta), \tag{2.68}$$

$$\theta_p(\eta) = \sum_{n=0}^{\infty}\sum_{k=0}^{\infty} d_{m,n}^{k}\ \eta^k \exp(-n\eta). \tag{2.69}$$

in which $a_{m,n}^{k}$, $b_{m,n}^{k}, c_{m,n}^{k}$ and $d_{m,n}^{k}$ are coefficients. Taking up the rule of solution expressions and utilizing the given boundary conditions, the initial guesses $f_0, F_0, \theta_0, \theta_{p_0}$ can be chosen as follows

$$f_0(\eta) = (1+s) - \exp(-\eta), \tag{2.70}$$

$$F_0(\eta) = (1+s) - \exp(-\eta), \tag{2.71}$$

$$\theta_0(\eta) = \exp(-\eta), \tag{2.72}$$

$$\theta_{p_0}(\eta) = \exp(-\eta). \tag{2.73}$$

The auxiliary linear operators are

$$\mathcal{L}_f = \frac{d^3}{d\eta^3} - \frac{d}{d\eta}, \tag{2.74}$$

$$\mathcal{L}_F = \frac{d^2}{d\eta^2} - \frac{d}{d\eta}, \tag{2.75}$$

$$\mathcal{L}_\theta = \frac{d^2}{d\eta^2} - 1, \tag{2.76}$$

$$\mathcal{L}_{\theta_p} = \frac{d}{d\eta} - 1, \tag{2.77}$$

which satisfy

$$\mathcal{L}_f \left[c_1 + c_2 \exp(\eta) + c_3 \exp(-\eta)\right] = 0, \tag{2.78}$$

$$\mathcal{L}_F \left[c_4 + c_5 \exp(\eta)\right] = 0, \tag{2.79}$$

$$\mathcal{L}_\theta \left[c_6 \exp(\eta) + c_7 \exp(-\eta)\right] = 0, \tag{2.80}$$

$$\mathcal{L}_{\theta_p} \left[c_8 \exp(\eta)\right] = 0, \tag{2.81}$$

where $c_i \, (i = 1 - 8)$ are arbitrary constants.

If the embedding parameter is defined by $p \in [0, 1]$ and the non-zero auxiliary parameters are indicated by $\hbar_f, \hbar_F, \hbar_\theta$ and $\hbar_{\theta_p}$, then following are the zeroth order deformation problems

$$(1-p)\,\mathcal{L}_f \left[\widehat{f}(\eta;p) - \widehat{f}_0(\eta)\right] = p\hbar_f N_f \left[\widehat{f}(\eta;p), \widehat{F}(\eta;p)\right], \tag{2.82}$$

$$(1-p)\,\mathcal{L}_F \left[\widehat{F}(\eta;p) - \widehat{F}_0(\eta)\right] = p\hbar_F N_F \left[\widehat{f}(\eta;p), \widehat{F}(\eta;p)\right], \tag{2.83}$$

$$(1-p)\,\mathcal{L}_\theta \left[\widehat{\theta}(\eta;p) - \widehat{\theta}_0(\eta)\right] = p\hbar_\theta N_\theta \left[\widehat{f}(\eta;p), \widehat{F}(\eta;p), \widehat{\theta}(\eta;p), \widehat{\theta_p}(\eta;p)\right], \tag{2.84}$$

$$(1-p)\,\mathcal{L}_{\theta_p} \left[\widehat{\theta_p}(\eta;p) - \widehat{\theta_p}_0(\eta)\right] = p\hbar_{\theta_p} N_{\theta_p} \left[\widehat{F}(\eta;p), \widehat{\theta}(\eta;p), \widehat{\theta_p}(\eta;p)\right], \tag{2.85}$$

with boundary conditions as

CASE 1:

$$\widehat{f}'(0;p) = 1 = \widehat{\theta}(0;p) \;,\; \widehat{f}(0;p) = S \tag{2.86}$$

$$\begin{aligned} \widehat{f}'(\infty;p) &= 0 = \widehat{F}'(\infty;p) = \widehat{\theta}(\infty;p) = \widehat{\theta_p}(\infty;p) \;, \\ \widehat{F}(\infty;p) &= \widehat{f}(\infty;p) + \eta\widehat{f}'(\infty;p) - \eta\widehat{F}'(\infty;p)\Big|_{\eta=\infty} \end{aligned} \tag{2.87}$$

CASE 2:

$$\widehat{f}'(0;p) = 1,\; \widehat{f}(0;p) = S,\; \widehat{\theta}'(0;p) = -1 \tag{2.88}$$

$$\widehat{f}'(\infty;p) = 0 = \widehat{F}'(\infty;p) = \widehat{\theta}(\infty;p) = \widehat{\theta}_p(\infty;p)\ , \tag{2.89}$$

$$\widehat{F}(\infty;p) = \widehat{f}(\infty;p) + \eta\widehat{f}'(\infty;p) - \eta\widehat{F}'(\infty;p)\Big|_{\eta=\infty}. \tag{2.90}$$

in which

$$\begin{aligned} N_f\left[\widehat{f}(\eta;p),\widehat{F}(\eta;p)\right] = {} & \frac{\partial^3\widehat{f}(\eta;p)}{\partial\eta^3} + \widehat{f}(\eta;p)\frac{\partial^2\widehat{f}(\eta;p)}{\partial\eta^2} - 2\left(\frac{\partial\widehat{f}(\eta;p)}{\partial\eta}\right)^2 \\ & +2l\beta\left[\frac{\partial\widehat{F}(\eta;p)}{\partial\eta} - \frac{\partial\widehat{f}(\eta;p)}{\partial\eta}\right] - M\left(\frac{\partial\widehat{f}(\eta;p)}{\partial\eta}\right) \\ & -A\left[2\left(\frac{\partial\widehat{f}(\eta;p)}{\partial\eta}\right) + \eta\left(\frac{\partial^2\widehat{f}(\eta;p)}{\partial\eta^2}\right)\right], \end{aligned} \tag{2.91}$$

$$\begin{aligned} N_F\left[\widehat{F}(\eta;p),\widehat{f}(\eta;p)\right] = {} & \widehat{F}(\eta;p)\frac{\partial^2\widehat{F}(\eta;p)}{\partial\eta^2} - 2\left(\frac{\partial\widehat{F}(\eta;p)}{\partial\eta}\right)^2 \\ & +2\beta\left[\frac{\partial\widehat{f}(\eta;p)}{\partial\eta} - \frac{\partial\widehat{F}(\eta;p)}{\partial\eta}\right] \\ & -A\left[\eta\left(\frac{\partial^2\widehat{F}(\eta;p)}{\partial\eta^2}\right) + 2\left(\frac{\partial\widehat{F}(\eta;p)}{\partial\eta}\right)\right], \end{aligned} \tag{2.92}$$

$$\begin{aligned} N_\theta\left[\widehat{\theta}(\eta;p),\widehat{f}(\eta;p),\widehat{F}(\eta;p),\widehat{\theta}_p(\eta;p)\right] = {} & \left(1+\frac{4R}{3}\right)\frac{\partial^2\widehat{\theta}(\eta;p)}{\partial\eta^2} + \Pr Ec\left[\frac{\partial^2\widehat{f}(\eta;p)}{\partial\eta^2}\right]^2 \\ & +\Pr\left[\widehat{f}(\eta;p)\frac{\partial\widehat{\theta}(\eta;p)}{\partial\eta} - c_1\frac{\partial\widehat{f}(\eta;p)}{\partial\eta}\widehat{\theta}(\eta;p)\right] \\ & +2\frac{N}{\rho}\beta_T\Pr\left[\widehat{\theta}_p(\eta;p) - \widehat{\theta}(\eta;p)\right] \\ & +2\frac{N}{\rho}\beta\Pr Ec\left[\frac{\partial\widehat{F}(\eta;p)}{\partial\eta} - \frac{\partial\widehat{f}(\eta;p)}{\partial\eta}\right]^2 \\ & -A\Pr\left[\eta\frac{\partial\widehat{\theta}(\eta;p)}{\partial\eta} + 4\widehat{\theta}(\eta;p)\right] + 2\lambda\Pr\widehat{\theta}(\eta;p), \end{aligned} \tag{2.93}$$

$$
\begin{aligned}
N_{\theta_p}\left[\widehat{\theta}_p(\eta;p),\widehat{\theta}(\eta;p),\widehat{F}(\eta;p)\right] &= c_1\frac{\partial\widehat{F}(\eta;p)}{\partial\eta}\widehat{\theta}_p(\eta;p)-\widehat{F}(\eta;p)\frac{\partial\widehat{\theta}(\eta;p)}{\partial\eta} \\
&\quad +2\gamma\beta_T\left[\widehat{\theta}_p(\eta;p)-\widehat{\theta}(\eta;p)\right] \\
&\quad +A\left[\eta\frac{\partial\widehat{\theta}_p(\eta;p)}{\partial\eta}+4\widehat{\theta}_p(\eta;p)\right].
\end{aligned} \tag{2.94}
$$

For $p=0$ and $p=1$, we have,

$$
\widehat{f}(\eta;0)=f_0(\eta)\ ,\ \widehat{f}(\eta;1)=f(\eta), \tag{2.95}
$$

$$
\widehat{F}(\eta;0)=F_0(\eta)\ ,\ \widehat{F}(\eta;1)=F(\eta), \tag{2.96}
$$

$$
\widehat{\theta}(\eta;0)=\theta_0(\eta)\ ,\ \widehat{\theta}(\eta;1)=\theta(\eta), \tag{2.97}
$$

$$
\widehat{\theta_p}(\eta;0)=\theta_{p_0}(\eta)\ ,\ \widehat{\theta_p}(\eta;1)=\theta_p(\eta), \tag{2.98}
$$

By Taylor theorem

$$
\widehat{f}(\eta;0)=f_0(\eta)+\sum_{m=1}^{\infty}f_m(\eta)p^m, \tag{2.99}
$$

$$
\widehat{F}(\eta;0)=F_0(\eta)+\sum_{m=1}^{\infty}F_m(\eta)p^m, \tag{2.100}
$$

$$
\widehat{\theta}(\eta;0)=\theta_0(\eta)+\sum_{m=1}^{\infty}\theta_m(\eta)p^m, \tag{2.101}
$$

$$
\widehat{\theta_p}(\eta;0)=\theta_{p_0}(\eta)+\sum_{m=1}^{\infty}\theta_{p_m}(\eta)p^m. \tag{2.102}
$$

$$
f_m(\eta)=\frac{1}{m!}\left.\frac{\partial^m\widehat{f}(\eta;p)}{\partial\eta^m}\right|_{p=0},F_m(\eta)=\frac{1}{m!}\left.\frac{\partial^m\widehat{F}(\eta;p)}{\partial\eta^m}\right|_{p=0}, \tag{2.103}
$$

$$
\theta_m(\eta)=\frac{1}{m!}\left.\frac{\partial^m\widehat{\theta}(\eta;p)}{\partial\eta^m}\right|_{p=0},\theta_{p_m}(\eta)=\frac{1}{m!}\left.\frac{\partial^m\widehat{\theta_p}(\eta;p)}{\partial\eta^m}\right|_{p=0}, \tag{2.104}
$$

and

$$
f(\eta)=f_0(\eta)+\sum_{m=1}^{\infty}f_m(\eta), \tag{2.105}
$$

$$F(\eta) = F_0(\eta) + \sum_{m=1}^{\infty} F_m(\eta), \tag{2.106}$$

$$\theta(\eta) = \theta_0(\eta) + \sum_{m=1}^{\infty} \theta_m(\eta), \tag{2.107}$$

$$\theta_p(\eta) = \theta_{p_0}(\eta) + \sum_{m=1}^{\infty} \theta_{p_m}(\eta). \tag{2.108}$$

The mth-order deformation problems are defined as

$$\mathcal{L}[f_m(\eta) - \chi_m f_{m-1}(\eta)] = \hbar_f R_m^f(\eta), \tag{2.109}$$

$$\mathcal{L}[F_m(\eta) - \chi_m F_{m-1}(\eta)] = \hbar_F R_m^F(\eta), \tag{2.110}$$

$$\mathcal{L}[\theta_m(\eta) - \chi_m \theta_{m-1}(\eta)] = \hbar_\theta R_m^\theta(\eta), \tag{2.111}$$

$$\mathcal{L}[\theta_{p_m}(\eta) - \chi_m \theta_{p_{m-1}}(\eta)] = \hbar_{\theta_p} R_m^{\theta p}(\eta), \tag{2.112}$$

CASE 1:

$$f_m(0) = f_m'(0) = \theta_m(0) = 0, \tag{2.113}$$

$$f_m'(\infty) = F_m'(\infty) = \theta_m(\infty) = \theta_{p_m}(\infty) = 0, \tag{2.114}$$

$$F_m(\infty) - f_m(\infty) + \eta f_m'(\infty) - \eta F_m'(\infty)\big|_{\eta=\infty} = 0. \tag{2.115}$$

CASE 2:

$$f_m(0) = f_m'(0) = \theta_m'(0) = 0, \tag{2.116}$$

$$f_m'(\infty) = F_m'(\infty) = \theta_m(\infty) = \theta_{p_m}(\infty) = 0, \tag{2.117}$$

$$F_m(\infty) - f_m'(\infty) + \eta f_m'(\infty) - \eta F_m'(\infty)\big|_{\eta=\infty} = 0. \tag{2.118}$$

where

$$\begin{aligned} R_m^f(\eta) \;=\; & f_{m-1}''' + \sum_{k=0}^{m-1} f_k' f_{m-1-k}'' - 2\sum_{k=0}^{m-1} f_k' f_{m-1-k}' + 2l\beta[F_{m-1}' - f_{m-1}'] \\ & -A[2f_{m-1}' + \eta f_{m-1}''] - M f_{m-1}', \end{aligned} \tag{2.119}$$

$$
\begin{aligned}
R_m^F(\eta) &= \sum_{k=0}^{m-1} F_k' F_{m-1-k}'' - 2\sum_{k=0}^{m-1} F_k' F_{m-1-k}' + 2\beta[f_{m-1}' - F_{m-1}'] \\
&\quad -A[2F_{m-1}' + \eta F_{m-1}''],
\end{aligned} \tag{2.120}
$$

$$
\begin{aligned}
R_m^\theta(\eta) &= \left(1+\frac{4R}{3}\right)\theta_{m-1}'' + \Pr\left[\sum_{k=0}^{m-1} f_k\theta_{m-1-k}' - c_1\sum_{k=0}^{m-1}\theta_k f_{m-1-k}'\right] \\
&\quad +2\frac{N}{\rho}\beta_T \Pr\left[\theta_{p_{m-1}} - \theta_{m-1}\right] - A\Pr\left[\eta\theta_{m-1}' + 4\theta_{m-1}\right] \\
&\quad +2\frac{N}{\rho}\beta \Pr Ec\left[\sum_{k=0}^{m-1} F_k' F_{m-1-k}' - \sum_{k=0}^{m-1} f_k' F_{m-1-k}' + \sum_{k=0}^{m-1} f_k' f_{m-1-k}'\right] \\
&\quad +2\lambda\Pr\theta_{m-1} + \Pr Ec\left[\sum_{k=0}^{m-1} f_k'' f_{m-1-k}''\right],
\end{aligned} \tag{2.121}
$$

$$
\begin{aligned}
R_m^{\theta_p}(\eta) &= c_1\sum_{k=0}^{m-1}\theta_{p_k} F_{m-1-k}' - \sum_{k=0}^{m-1} F_k\theta_{p_{m-1-k}}' + 2\gamma\beta_T\left[\theta_{p_{m-1}} - \theta_{m-1}\right] \\
&\quad +A\left[\eta\theta_{p_{m-1}}' + 4\theta_{p_{m-1}}\right],
\end{aligned} \tag{2.122}
$$

$$
\chi_m = \begin{cases} 0; & m \le 1, \\ 1; & m > 1. \end{cases} \tag{2.123}
$$

The general solutions of equations can be expressed as

$$
f_m(\eta) = f_m^*(\eta) + c_1 + c_2\exp(\eta) + c_3\exp(-\eta), \tag{2.124}
$$

$$
F_m(\eta) = F_m^*(\eta) + c_4 + c_5\exp(\eta), \tag{2.125}
$$

$$
\theta_m(\eta) = \theta_m^*(\eta) + c_6\exp(\eta) + c_7\exp(-\eta), \tag{2.126}
$$

$$
\theta_{p_m}(\eta) = \theta_{p_m}^*(\eta) + c_8\exp(\eta), \tag{2.127}
$$

where $f_m^*(\eta), F_m^*(\eta), \theta_m^*(\eta)$, and $\theta_{p_m}^*(\eta)$ are the special solutions.

2.5 Optimal convergence-control parameters

Homotopy analysis solutions comprise the non-zero auxiliary parameters c_0^f, c_0^F, c_0^θ and $c_0^{\theta_p}$, which act as a helping tool in determining the area of convergence and rate of the homotopy series solution. In order to obtain the optimal values of c_0^f, c_0^F, c_0^θ and $c_0^{\theta_p}$ we need to find the so-called average residual error [43]. Tables (2.1) and (2.2) present the values for several optimal convergence control parameters for the VEST and VEHF cases respectively. These tables reveal that the total averaged squared residual errors decrease as we increase the order of approximation, which proves that the solution is convergent at higher order approximations. Hence, Optimal Homotopy Analysis Method provides us a proper way to select any family of local convergence control parameters to attain the convergent solutions.

$\frac{values\rightarrow}{m\downarrow}$	c_0^f	c_0^F	c_0^θ	$c_0^{\theta_p}$	ε_m^t	CPU time $[s]$
2	-0.689	-0.483	-0.506	0.455	9.704×10^{-3}	11.12
4	-0.702	-0.569	-0.601	0.459	2.246×10^{-4}	49.19
6	-0.682	-0.610	-0.713	0.451	2.721×10^{-5}	429.0
8	-0.648	-0.605	-0.791	0.510	6.608×10^{-6}	3359.3

Table.2.1. Total averaged squared residual errors using BVPh2.0. (VEST Case)

$\frac{values\rightarrow}{m\downarrow}$	c_0^f	c_0^F	c_0^θ	$c_0^{\theta_p}$	ε_m^t	CPU time $[s]$
2	-0.724	-0.482	-0.514	0.389	7.295×10^{-3}	11.55
4	-0.646	-0.560	-0.694	0.419	8.059×10^{-4}	81.33
6	-0.697	-0.573	-0.752	0.420	6.685×10^{-5}	590.84
8	-0.615	-0.563	-0.865	0.451	5.510×10^{-6}	6161.65

Table.2.2. Total averaged squared residual errors using BVPh2.0. (VEHF Case)

where ε_m^t is the total squared residual error.

Table.(2.3) and Fig.(2.1) exhibit that the individual averaged squared residual errors also decrease as the order of approximation increases, proving that the solution is convergent.

$\frac{values\rightarrow}{m\downarrow}$	ε_m^f	ε_m^F	ε_m^θ	$\varepsilon_m^{\theta_p}$	CPU time $[s]$
4	6.375×10^{-5}	1.333×10^{-4}	1.908×10^{-4}	4.806×10^{-4}	7.30
8	1.435×10^{-6}	8.246×10^{-6}	2.604×10^{-5}	2.288×10^{-5}	52.08
12	1.263×10^{-7}	6.647×10^{-7}	5.104×10^{-6}	5.517×10^{-6}	184.53
16	1.574×10^{-8}	6.942×10^{-8}	1.232×10^{-6}	1.370×10^{-6}	470.92

Table.2.3. Individual averaged squared residual errors using optimal values at $m = 2$. (VEST Case)

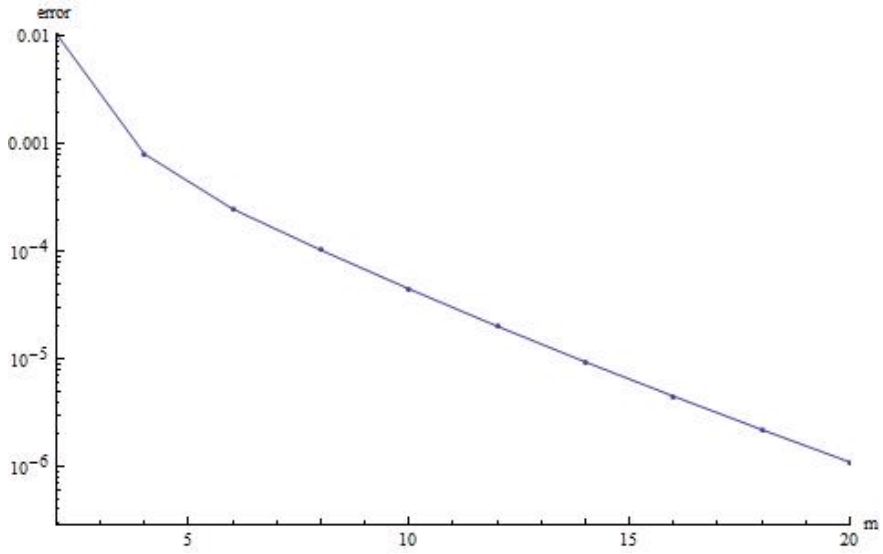

Fig 2.1 Individual squared residual error when m=2

2.6 Graphical results and discussion

The non-linear ordinary differential equations (2.38, 2.39, 2.56 and 2.57) along with the boundary conditions (2.40, 2.58 and 2.60) have been solved analytically by using the OHAM. The influence of various important parameters on velocity and temperature fields are presented graphically in *Figs*.2.2 − 2.15 and in *Table*2.4. The values of $\beta_T = 0.6, c_1 = 1, \rho = 1, \gamma = 1.4$ and $l = 0.1$ are used in our calculations.

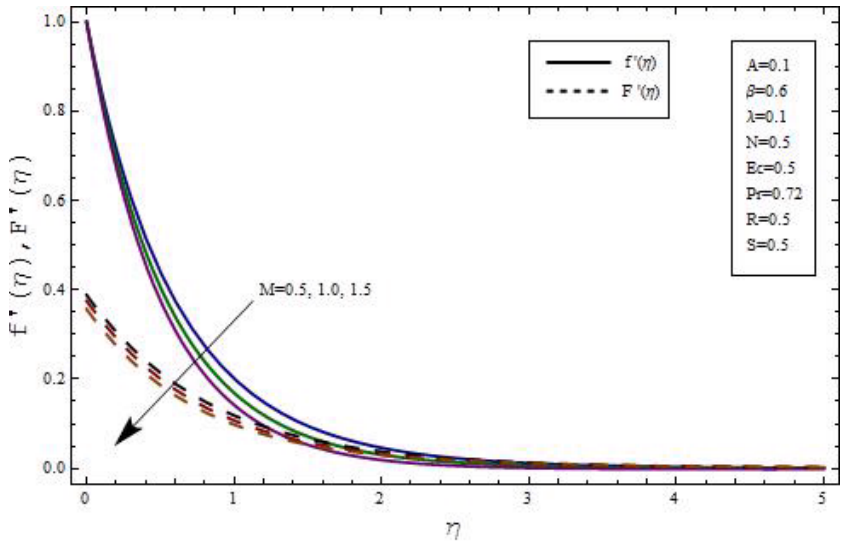

Fig 2.2 Influence of M on velocity profiles

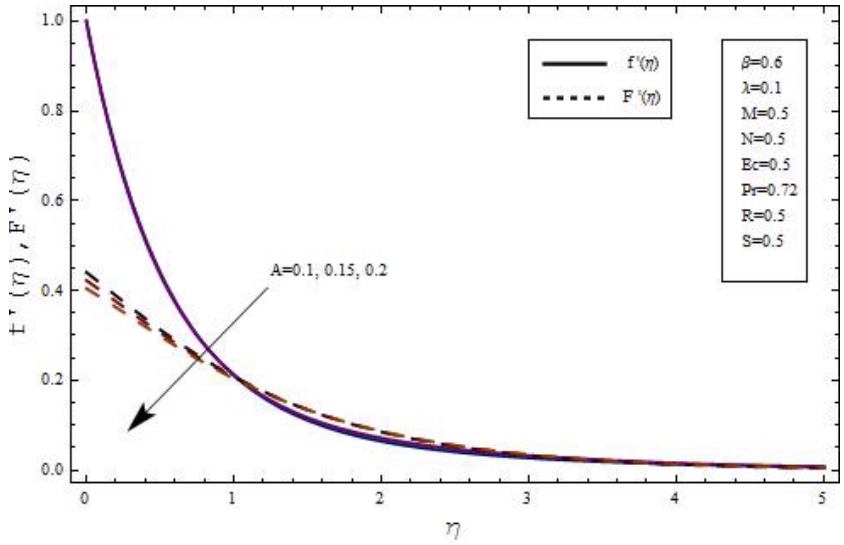

Fig. 2.3 Influence of A on velocity profiles

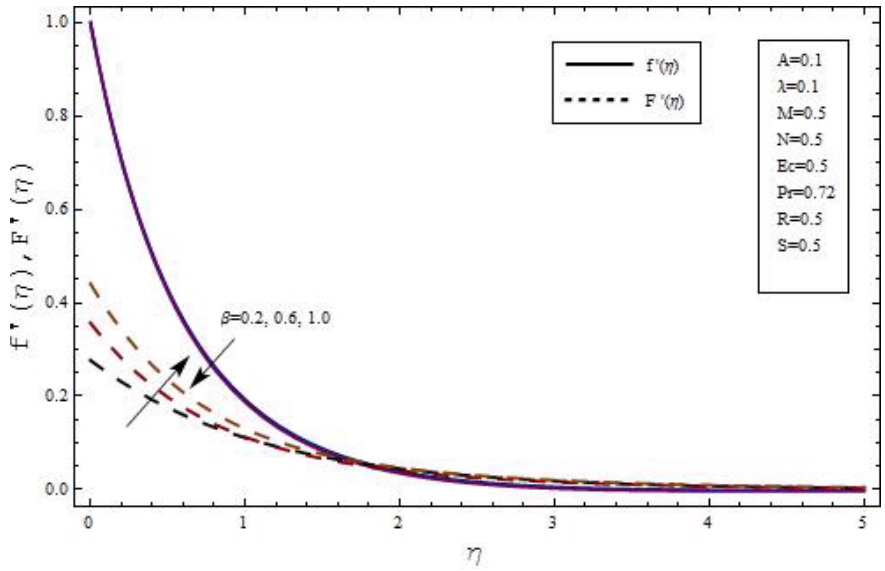

Fig 2.4 Influence of β on velocity profiles

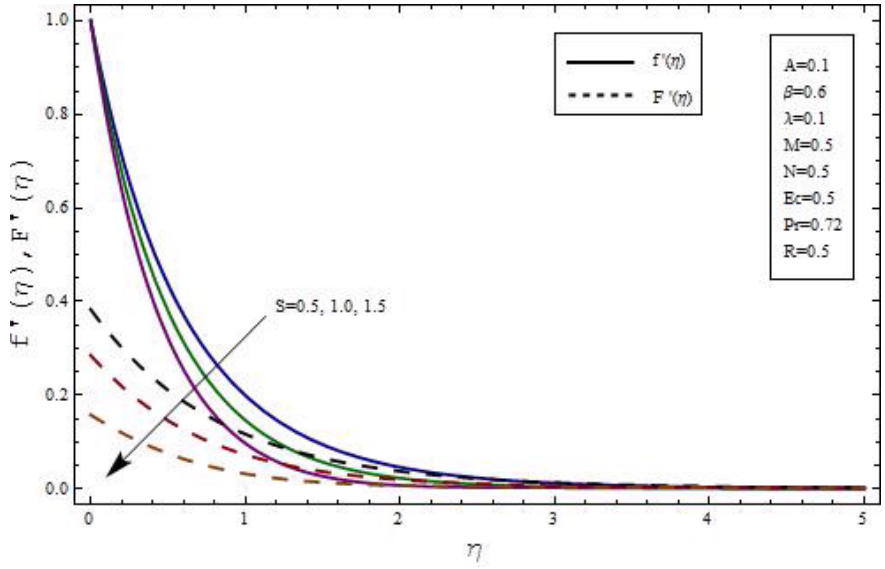

Fig 2.5 Influence of S on velocity profiles

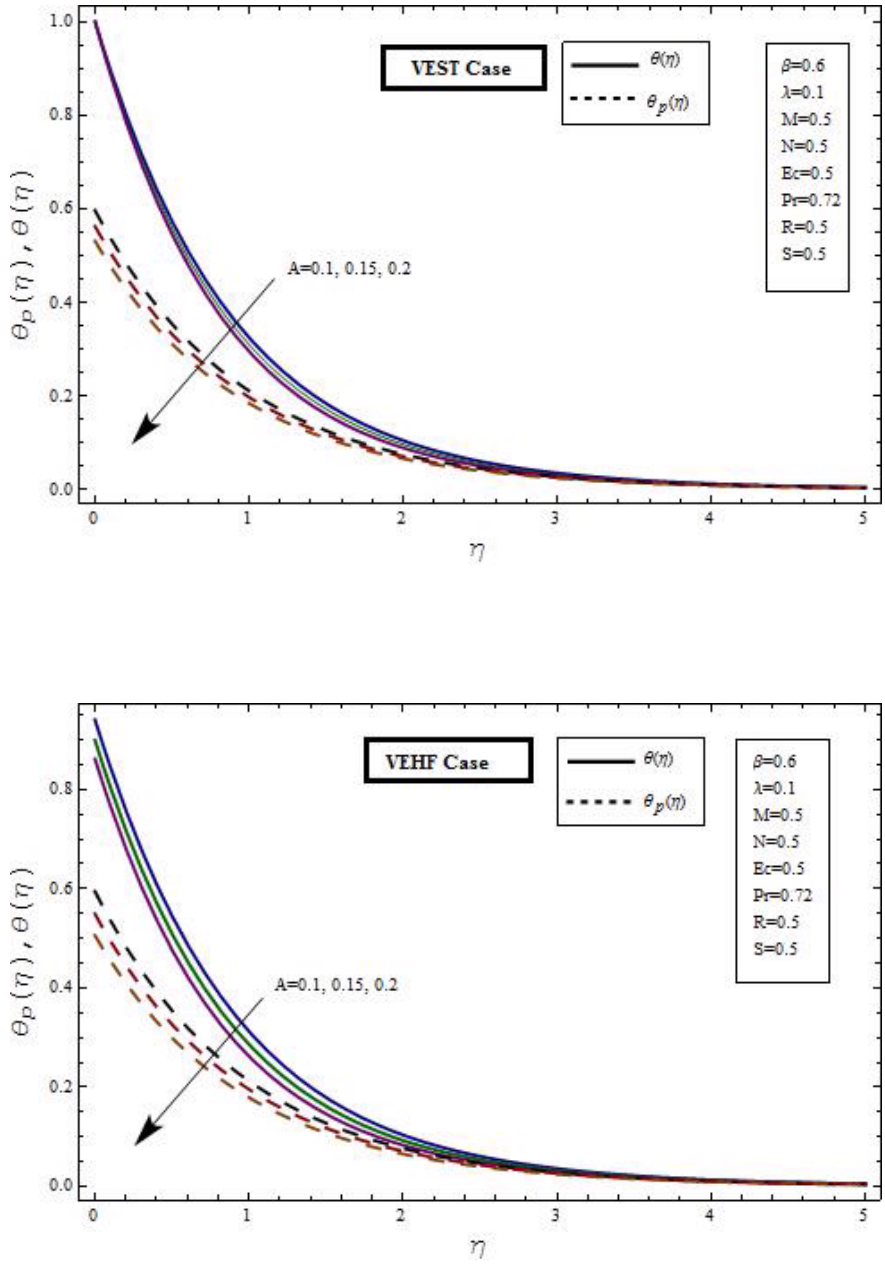

Fig.2.6 Influence of A on temperature distribution for both VEST and VEHF cases.

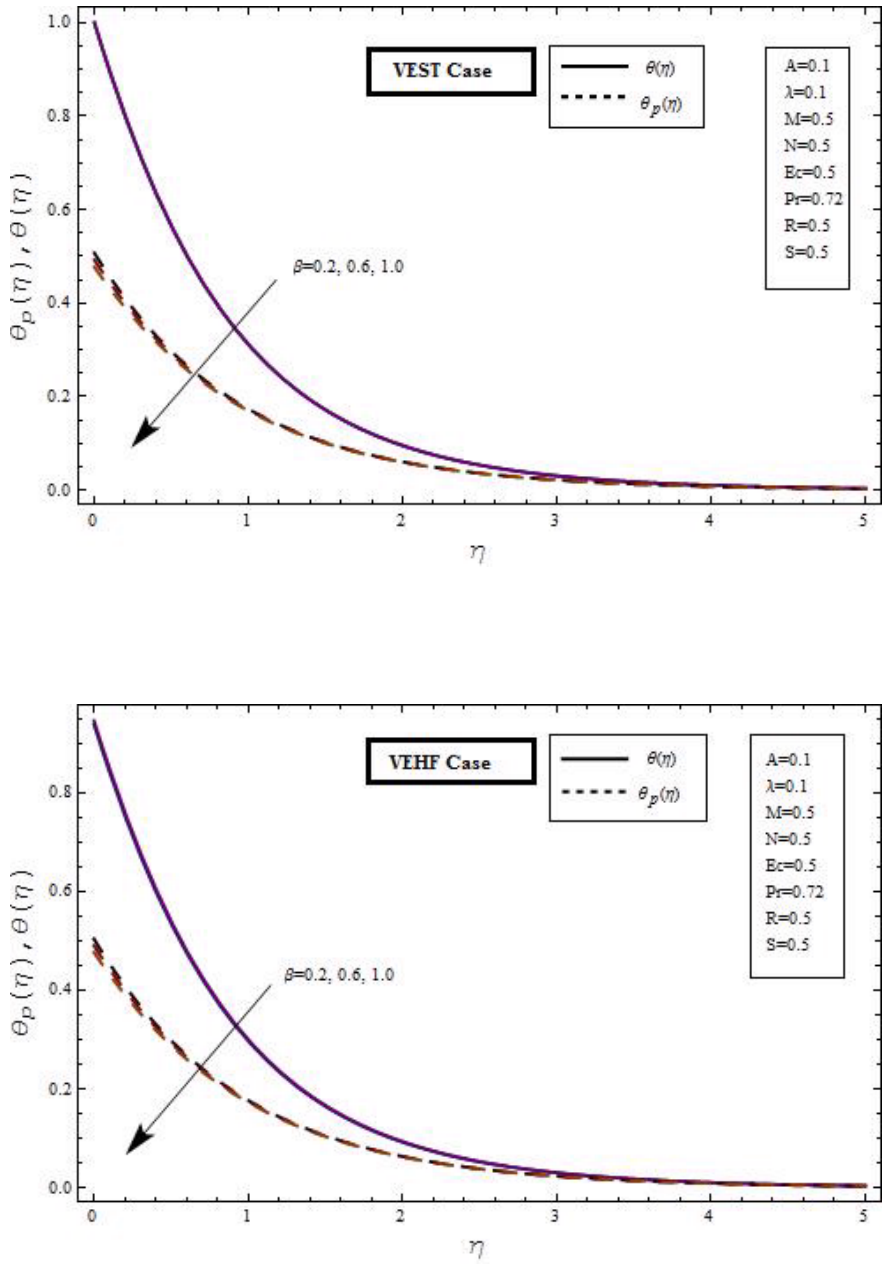

Fig.2.7 Influence of β on temperature distribution for both VEST and VEHF cases.

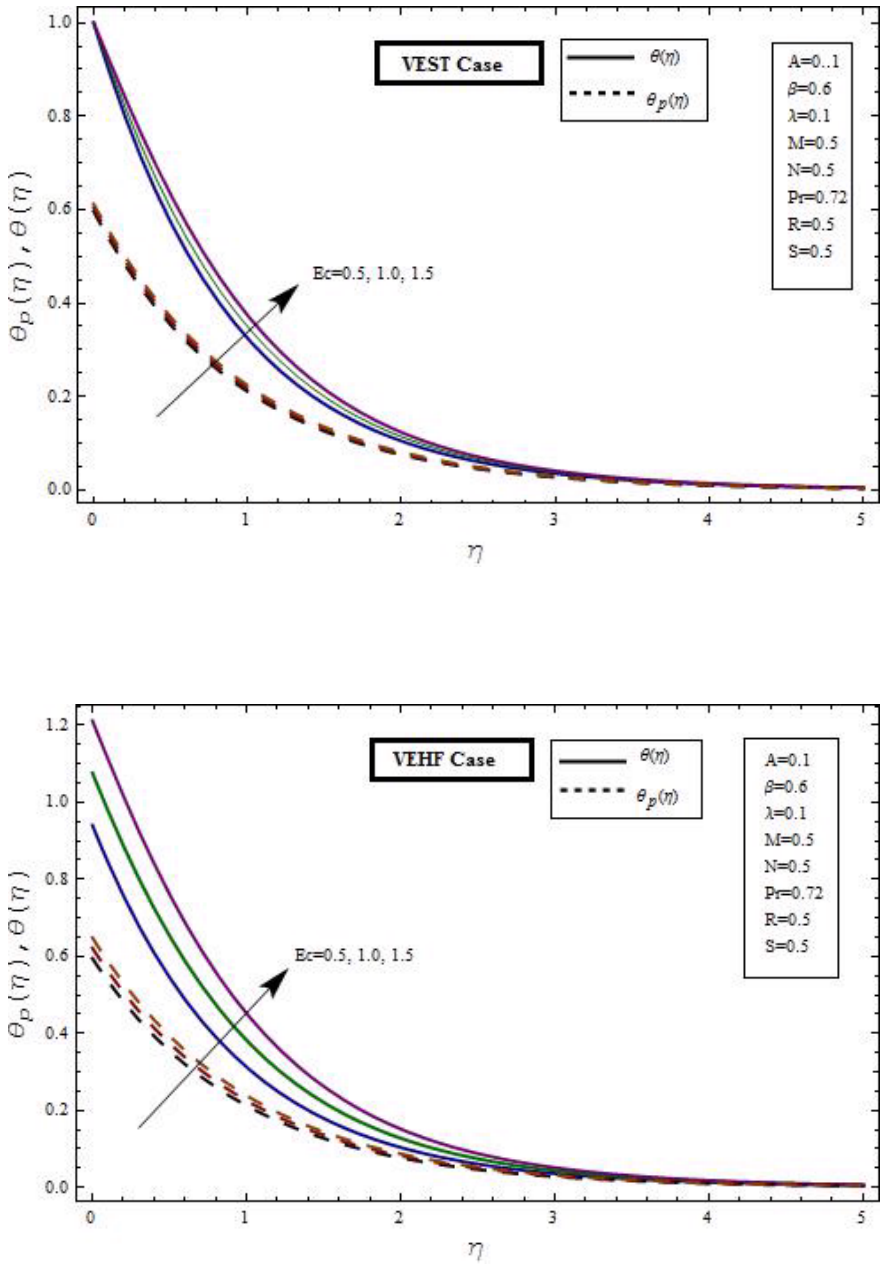

Fig. 2.8 Influence of Ec on temperature distribution for both VEST and VEHF cases.

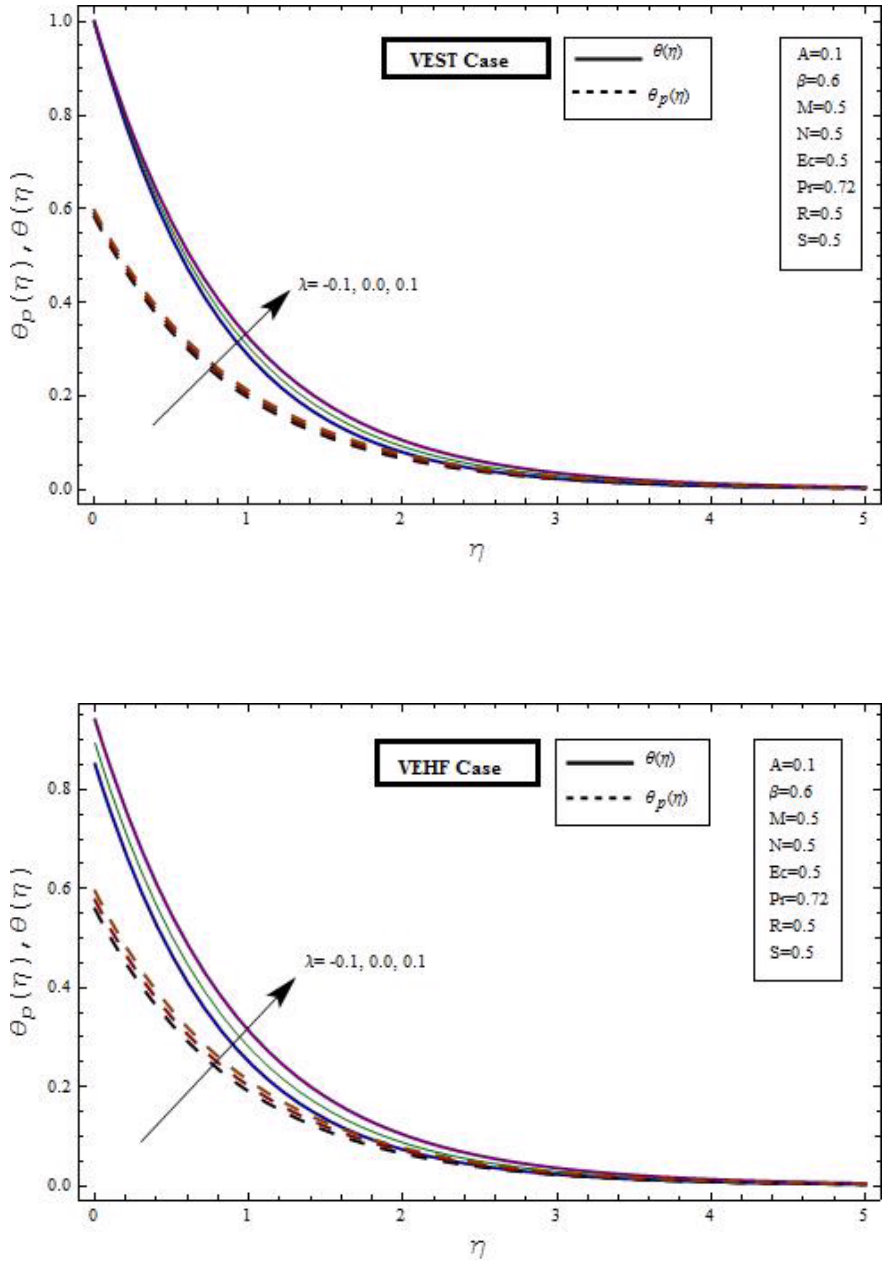

Fig. 2.9 Influence of λ on temperature distribution for both VEST and VEHF cases.

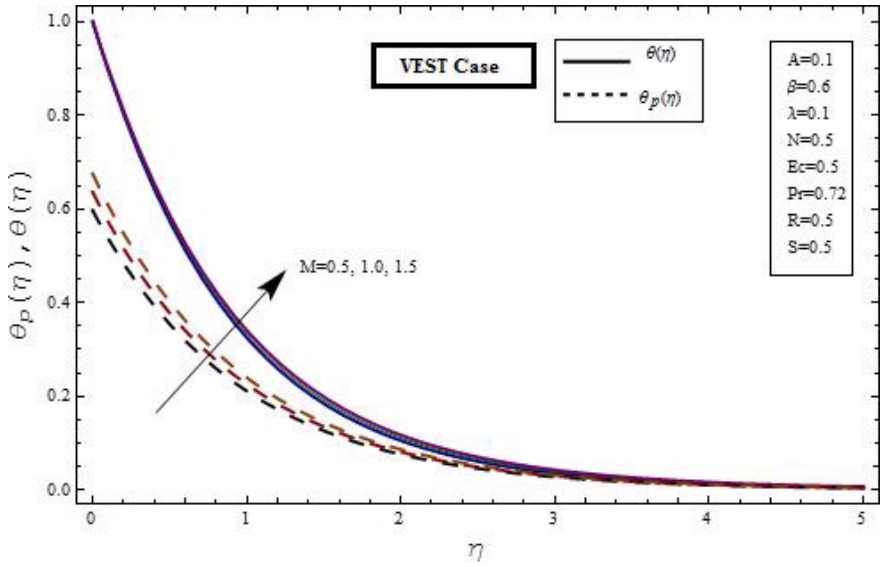

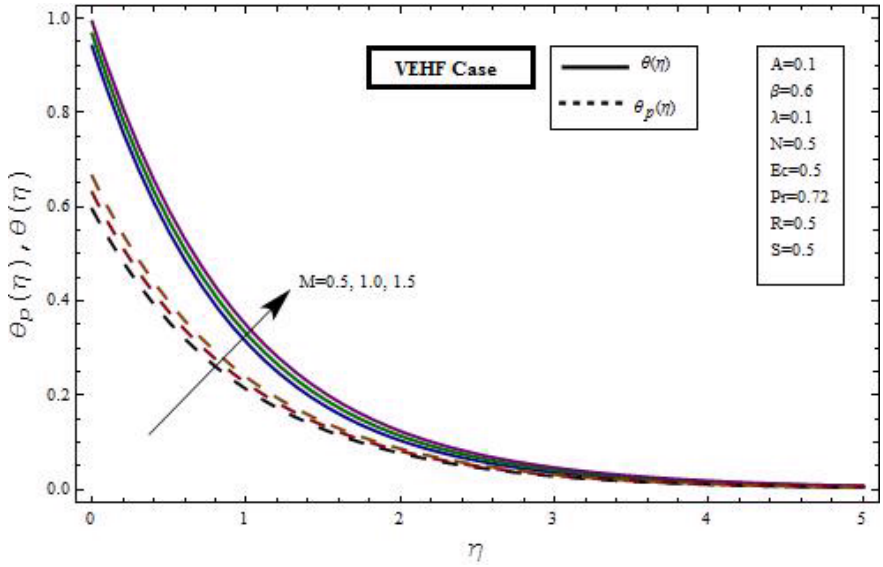

Fig.2.10 Influence of M on temperature distribution for both VEST and VEHF cases.

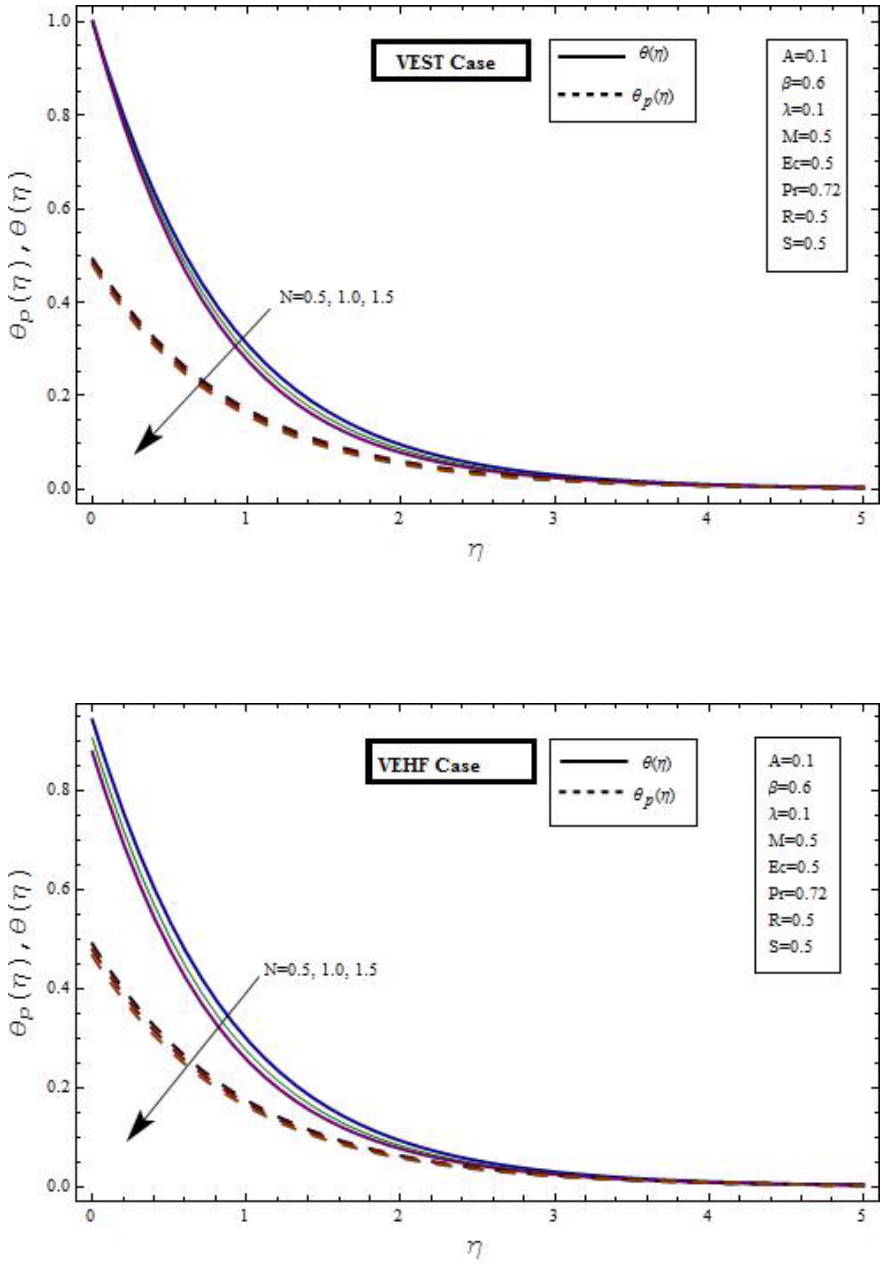

Fig 2.11 Influence of N on temperature distribution for both VEST and VEHF cases.

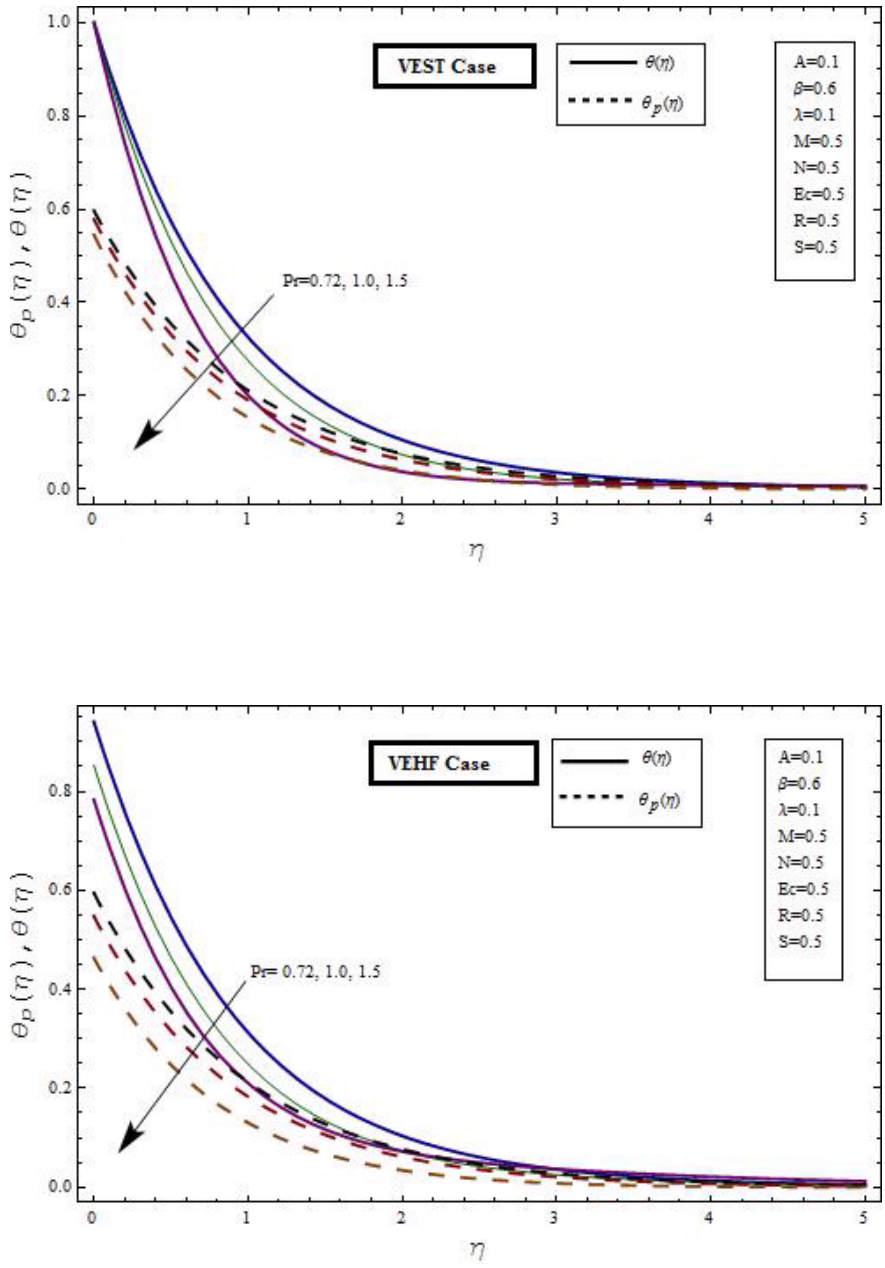

Fig 2.12 Influence of Pr on temperature distribution for both VEST and VEHF cases.

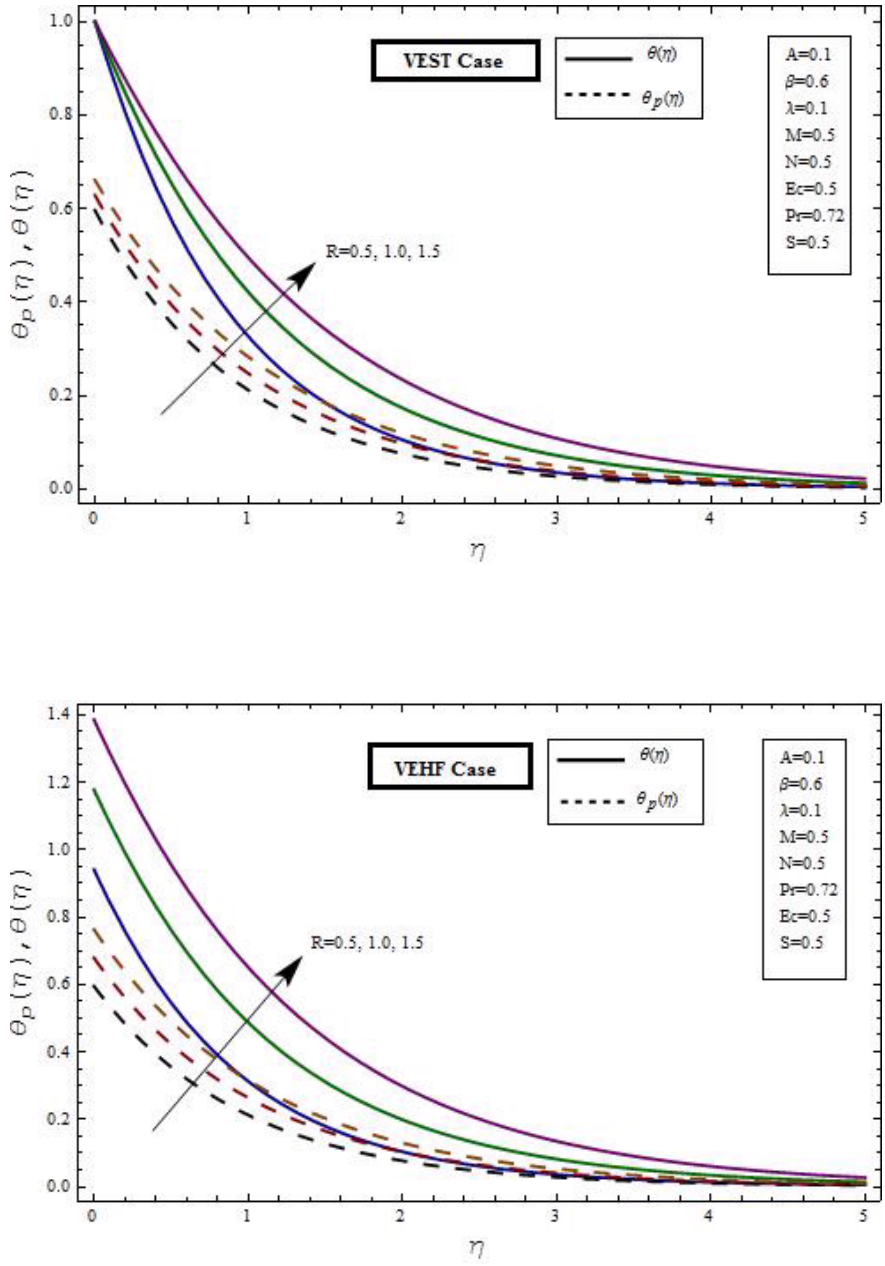

Fig 2.13 Influence of R on temperature distribution for both VEST and VEHF cases.

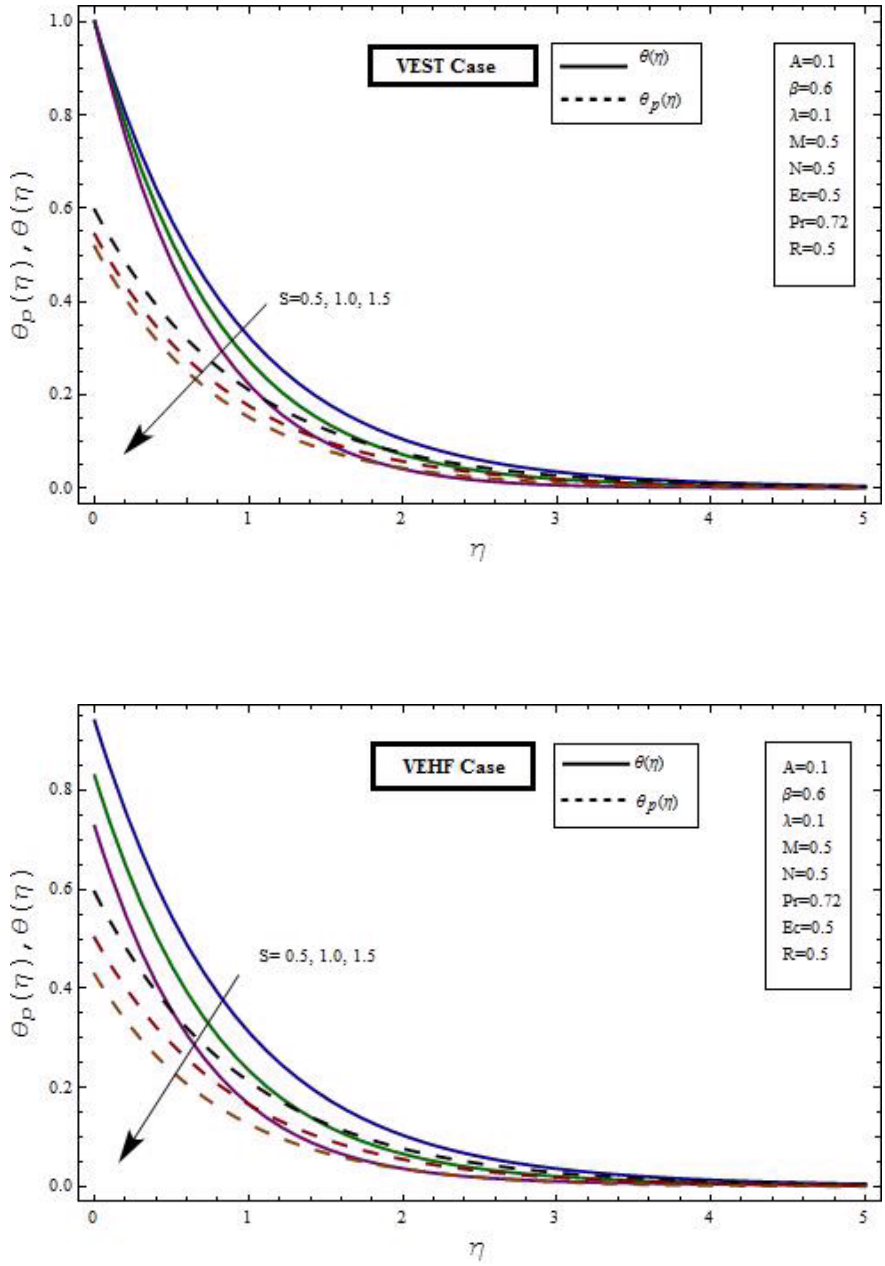

Fig 2.14 Influence of S on temperature distribution for both VEST and VEHF cases.

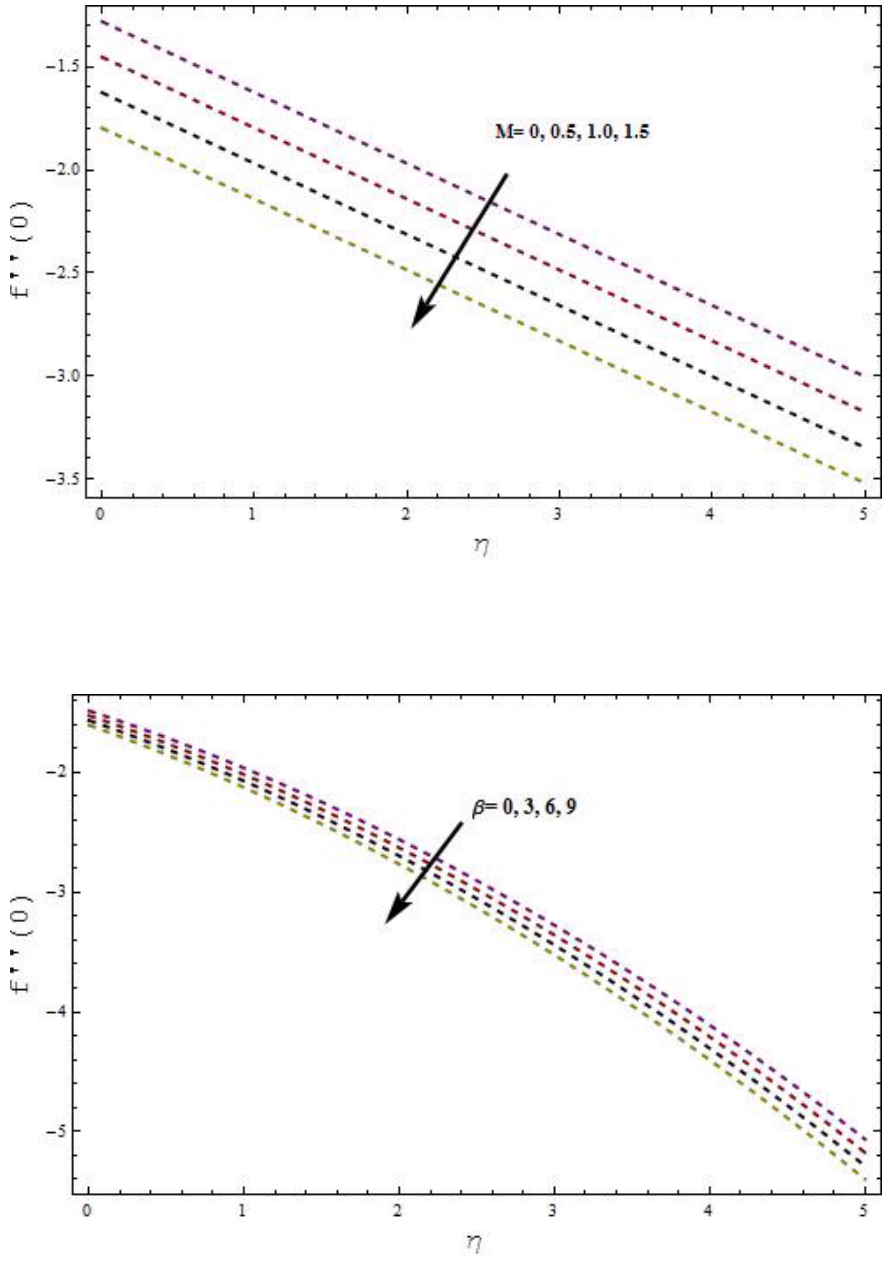

Fig 2.15 Influence of M and β on skin friction coefficient against S.

*Fig.*2.2 illustrates the nature of velocity profile with the variation of magnetic parameter (M). It shows that with an increase in M the velocity fields decrease. Reason being, the magnetic field is applied transversely, so when M increases a drag force, known as Lorentz force, is created increasing resistance to the flow. Boundary layer thickness increases with every higher value of M. *Fig.*2.3 depicts the behavior of velocity fields $f'(\eta)$ and $F'(\eta)$ for changing values of the unsteadiness parameter (A). It is noticed that both fluid and dust phase velocities decrease when we increase the unsteady parameter whereas the boundary layer thickness increases with increasing values of A. In *Fig.*2.4 the velocity profiles are plotted for different values of the fluid particle interaction parameter (β). It is observed that the fluid phase velocity profile decreases with increasing β while the dust phase velocity profile increases with increasing values of β. Momentum boundary layer increases with increase in β.

*Fig.*2.5 exhibits the effects of suction parameter S on velocity fields. With increasing S both of the velocity profiles decrease significantly and with this reduction in velocity fields boundary layer thickness also decreases.

Figs.$(2.6 - 2.14)$ represent the effects of various parameters on temperature distribution of fluid segment $\theta(\eta)$ and dust segment $\theta_p(\eta)$ phase for both VEST and VEHF cases. *Fig.*2.6 shows us the effects of unsteadiness parameter (A) on temperature profiles $\theta(\eta)$ and $\theta_p(\eta)$. As A increases there is a decrease in both temperature profiles because when we increase A the surface temperature gradient also increases resulting in higher rate of heat transfer. Thus for larger values of A the rate of cooling is very fast.

In *Fig.*2.7 the variation of temperature profiles due to the fluid-particle interaction parameter (β) is demonstrated. It is found that with an increase in β temperature profiles decrease.

Next in *Fig.*2.8 we analyze the impact on temperature distributions of Eckert number (Ec) which represents the viscous dissipation changes. The temperature increases when we increase Ec, as viscous dissipation plays the role of energy source because there is stored heat energy in the fluid because of frictional heating. *Fig.*2.9 displays the temperature distributions with varying heat source/sink parameter (λ). We conclude from this graphical representation that with an increase in λ temperature increases because energy is produced at thermal boundary layer in case of heat source. While the case is opposite for heat sink. *Fig.*2.10 shows the effect on temperature profiles due to the variation in magnetic parameter (M). In both VEST

and VEHF case the temperature profiles increase with increase in the value of M. It can also be seen that fluid and dust particle temperature profiles are parallel to each other. Effect on temperature distributions for variation in number density (N) is illustrated in $Fig.2.11$. When we increase N we notice a decrease in temperature profiles of both VEST and VEHF cases.

The influence of changing Prandtl number (Pr) on temperature profiles for fluid and particle phase is depicted in $Fig.2.12$. With increasing Pr decrease in temperature profiles is observed. This is because when we increase (Pr) thermal diffusion decreases as both are inversely related hence thermal boundary layer thickness reduces too. Now we discuss the effects of parameter of radiation (R) on temperature distributions of fluid and dust particles shown in $Fig.2.13$. In both VEST and VEHF cases when we increase R, there is an increase in both temperature profiles and the thermal boundary layer thickness. $Fig.2.14$ represents the impact of suction parameter (S) on temperature profiles. From here we can observe that when S increases the temperature profiles decrease and the boundary layer becomes thin. The nature of skin friction coefficient against suction parameter (S) for varying values of magnetic parameter (M) and fluid-particle interaction parameter (β) is displayed in $Fig.2.15$. Skin friction decreases with magnetic, suction and fluid-particle interaction parameters.

The thermal properties of fluid at the surface are investigated for skin friction coefficient, temperature gradient $\theta'(0)$ in case of VEST and temperature $\theta(0)$ in VEHF case, which are presented in $Table$ 2.4.

Table 2.4: Influence of various parameters on skin friction coefficient, temperature gradient $\theta'(0)$ for VEST Case and surface temperature $\theta(0)$ for VEHF Case.

β	A	M	S	λ	R	N	Pr	Ec	$f''(0)$	$\theta'(0)(VEST)$	$\theta(0)(VEHF)$
0.2									−1.7832	−0.6820	1.3745
0.6	0.1	0.5	0.5	0.1	0.5	0.5	0.72	0.5	−1.7971	−0.6745	1.3836
1									−1.8060	−0.6718	1.3869
	0								−1.7507	−0.5278	1.6721
0.6	0.1	0.5	0.5	0.1	0.5	0.5	0.72	0.5	−1.7971	−0.6745	1.3836
	0.2								−1.8430	−0.7906	1.2174
		0.5							−1.7971	−0.6745	1.3836
0.6	0.1	1.0	0.5	0.1	0.5	0.5	0.72	0.5	−1.9537	−0.6416	1.4302
		1.5							−2.0964	−0.6131	1.4718
			0						−1.5372	−0.5873	1.5674
0.6	0.1	1.0	0.5	0.1	0.5	0.5	0.72	0.5	−1.7971	−0.6745	1.3836
			1.0						−2.0985	−0.7731	1.2305
				−0.1					–	−0.8070	1.1978
0.6	0.1	1.0	0.5	0	0.5	0.5	0.72	0.5	–	−0.7442	1.2795
				0.1					–	−0.6745	1.3836
					0.5				–	−0.6745	1.3836
0.6	0.1	1.0	0.5	0.1	1.0	0.5	0.72	0.5	–	−0.5546	1.6538
					1.5				–	−0.4832	1.8866
						0.5			–	−0.6745	1.3836
0.6	0.1	1.0	0.5	0.1	0.5	1.0	0.72	0.5	–	−0.7922	1.2133
						1.5			–	−0.8954	1.0962
							0.72		–	−0.6745	1.3836
0.6	0.1	1.0	0.5	0.1	0.5	0.5	1.0	0.5	–	−0.8231	1.1669
							1.5		–	−1.0574	0.9589
								0	–	−0.8482	1.1788
0.6	0.1	1.0	0.5	0.1	0.5	0.5	0.72	0.5	–	−0.6745	1.3836
								1.0	–	−0.5009	1.5883

2.7 Concluding Remarks

- The temperature of dust phase is lower as compared to the fluid phase temperature.
- Increase in fluid particle interaction parameter increases the fluid segment velocity while decreases the dust segment velocity.
- Increase in unsteady parameter decreases the momentum and thermal boundary layer thickness.
- The effect of suction parameter is unfavorable in case of momentum boundary layer thickness.
- As the magnetic field increases, its impact becomes more significant causing the fluid to slow down.
- Viscous dissipation increases the temperature of the flow region.
- The thermal boundary layer becomes thinner for increasing Prandtl number.
- Increase in magnetic, unsteady, suction and fluid particle interaction parameter increases the skin friction.
- The Nusselt number increases when we increase Prandtl number, unsteadiness parameter, number density and suction parameter
- Thermal radiation, magnetic field, fluid particle interaction parameter, and heat generation absorption parameter decrease the Nusselt number

Chapter 3

Unsteady flow and heat transfer of nanofluid with dust particles suspended over an exponentially stretching surface

3.1 Introduction

In this chapter we have presented the analytical solution of the unsteady boundary layer flow and heat transfer of nanofluid with dust particles suspended in it. The external magnetic field is transverse to the plate. Considering the effects of heat generation or absorption, viscous dissipation and thermal radiation, partial differential equations are modelled. Then they are changed to ODE's by employing similarity transformations for the following two cases of boundary conditions (i) Variable exponential order surface temperature (VEST) (ii) Variable exponential order heat flux (VEHF) and then the series solutions are calculated using OHAM. At the end, the influence on the velocity, temperature and concentration profiles of various important physical parameters are explored in detail with graphical illustrations and tables.

3.2 Problem formulation

For the above considered problem the equation of continuity, equation of conservation of linear momentum and equation of conservation of energy for the fluid respectively are,

$$\text{div } \mathbf{V} = 0, \tag{3.1}$$

$$\rho \left[\frac{d\mathbf{V}}{dt}\right] = -\boldsymbol{\nabla}\mathbf{p} + \mu\boldsymbol{\nabla}^2\mathbf{V} + KN\left[\mathbf{V}_P - \mathbf{V}\right] + \mathbf{J}\times\mathbf{B}, \tag{3.2}$$

$$\begin{aligned}\rho c_p \left[\frac{dT}{dt}\right] &= k\left(\nabla\cdot\nabla T\right) + \frac{Nc_p}{\tau_T}\left(T_p - T\right) + \frac{N}{\tau_\nu}(\mathbf{V}_p - \mathbf{V})\cdot(\mathbf{V}_p - \mathbf{V}) \\ &\quad -\frac{\partial q_r}{\partial y} + \boldsymbol{\tau}\cdot\mathbf{L} + Q(T - T_\infty) - \left(c_p\right)_p \mathbf{j}_p \nabla T,\end{aligned} \tag{3.3}$$

$\boldsymbol{\tau}$ is Cauchy stress tensor, $\mathbf{L}$ is grad $\mathbf{V}$, Q represents heat source where $Q > 0$ and sink when $Q < 0$, $\left(c_p\right)_p$ is the nanoparticles specific heat and $\mathbf{j}_p$ is the nanoparticles diffusion mass flux.

$\mathbf{j}_p$ (the sum of Brownian and thermophoresis diffusion) is defined as

$$\mathbf{j}_p = \mathbf{j}_p, B + \mathbf{j}_p, T, \tag{3.4}$$

where

$$\mathbf{j}_p, B = -\rho_p D_B \nabla C,$$

where the Brownian diffusion coefficient D_B in view of Einstein equation is equal to

$$D_B = \frac{k_B T}{3\pi\mu d_p},$$

where k_B represents the Boltzmann's constant and d_p the diameter of nanoparticles.

Second term on RHS of Eq. (3.4) is defined as follows

$$\mathbf{j}_p, T = \rho_p C \mathbf{V}_T, \tag{3.5}$$

$$\mathbf{V}_T = -\tilde{\beta}\frac{\mu}{\rho}\frac{\nabla T}{T},$$

in which $\mathbf{V}_T$ represents the thermophoretic velocity and $\tilde{\beta}$ is the proportionality factor given by

$$\tilde{\beta} = 0.26\frac{k}{2k + k_p},$$

where k and k_p are the fluid and nanoparticle material thermal conductivities respectively.

Hence the thermophoresis diffusion flux can be expressed as follows

$$\mathbf{j}_p, T = -\rho_p D_T \frac{\nabla T}{T}, \tag{3.6}$$

where

$$D_T = \tilde{\beta}\frac{\mu C}{\rho},$$

represents thermophoretic diffusion coefficient. Thus

$$\mathbf{j}_p = -\rho_p D_B \nabla C - \rho_p D_T \frac{\nabla T}{T}. \tag{3.7}$$

Final form of energy equation (3.3) for the above problem takes the form

$$\begin{aligned} \rho c_p \left[\frac{dT}{dt}\right] &= k\left(\nabla \cdot \nabla T\right) + \frac{N c_p}{\tau_T}\left(T_p - T\right) + \frac{N}{\tau_\nu}(\mathbf{V}_p - \mathbf{V}).(\mathbf{V}_p - \mathbf{V}) \\ &\quad -\frac{\partial q_r}{\partial y} + \boldsymbol{\tau} \cdot \mathbf{L} + Q(T - T_\infty) + (\rho c_p)_p \left(D_B \nabla C.\nabla T + D_T \frac{\nabla T.\nabla T}{T_\infty}\right). \end{aligned} \tag{3.8}$$

Now, from Fick's law, the concentration equation for fluid phase is

$$\frac{\partial C}{\partial t} + \mathbf{V}.\nabla C = \frac{-1}{\rho_p}\nabla.\mathbf{j}_p, \tag{3.9}$$

in which C denotes the concentration, ρ_p is the mass density and $\mathbf{j}_p$ is the diffusion mass flux, using value of $\mathbf{j}_p$ we have,

$$\frac{\partial C}{\partial t} + \mathbf{V}.\nabla C = \nabla\left(D_B \nabla C + D_T \frac{\nabla T}{T_\infty}\right), \tag{3.10}$$

Governing equations for dust particles are

$$\nabla.\mathbf{V}_p = 0, \tag{3.11}$$

$$\frac{\partial \mathbf{V}_p}{\partial t} + (\mathbf{V}_p.\nabla)\,\mathbf{V}_p = \frac{K}{m}\,(\mathbf{V} - \mathbf{V}_p)\,, \tag{3.12}$$

$$NC_m\left(\frac{\partial T_p}{\partial t} + (\mathbf{V}_p.\nabla)\,T_p\right) = -\frac{Nc_p}{\tau_T}\,(T_p - T)\,, \tag{3.13}$$

$$\frac{\partial C_p}{\partial t} + (\mathbf{V}_{p.}\nabla)\,C_p = D\nabla^2 C_p \tag{3.14}$$

where C_p represents the concentration of dust particles, and D denotes the coefficient of mass diffusivity.

Continuity and momentum equations for fluid and dust particles phase can be written as

$$\frac{\partial u}{\partial x} + \frac{\partial v}{\partial y} = 0, \tag{3.15}$$

$$\frac{\partial u}{\partial t} + u\frac{\partial u}{\partial x} + v\frac{\partial u}{\partial y} = \nu\frac{\partial^2 u}{\partial y^2} - \frac{\sigma}{\rho}B^2 u + KN\,(u_p - u)\,, \tag{3.16}$$

$$\frac{\partial u_p}{\partial x} + \frac{\partial v_p}{\partial y} = 0, \tag{3.17}$$

$$\frac{\partial u_p}{\partial t} + u_p\frac{\partial u_p}{\partial x} + v_p\frac{\partial u_p}{\partial y} = \frac{K}{m}\,(u - u_p)\,. \tag{3.18}$$

The corresponding boundary conditions are

$$\begin{aligned} u &= U_w\,(x,t)\,,\ v = -V_w\,(x,t)\,,\ \text{at } y = 0, \\ u &\to 0, u_p \to 0,\ v_p \to v,\ \text{as } y \to \infty, \end{aligned} \tag{3.19}$$

where $U_w\,(x,t) = \frac{U_o}{(1-\alpha t)}e^{\frac{x}{L}}$ is the velocity of the sheet and $V_w\,(x,t) = -S\sqrt{\frac{U_o\nu}{2L(1-\alpha t)}}e^{\frac{x}{2L}}$ is the suction velocity, L is the reference length, U_o is the reference velocity and $S > 0$ is a suction parameter.

Similarity transformations are defined as

$$\begin{aligned}
\eta &= \sqrt{\frac{U_o}{2\nu L\left(1-\alpha t\right)}}e^{\frac{x}{2L}}y, \quad u=\frac{U_o}{\left(1-\alpha t\right)}e^{\frac{x}{L}}f'(\eta),\\
v &= -\sqrt{\frac{U_o\nu}{2L\left(1-\alpha t\right)}}e^{\frac{x}{2L}}\left[f\left(\eta\right)+\eta f'(\eta)\right],\ u_p=\frac{U_o}{\left(1-\alpha t\right)}e^{\frac{x}{L}}F'(\eta),\\
v_p &= -\sqrt{\frac{U_o\nu}{2L\left(1-\alpha t\right)}}e^{\frac{x}{2L}}\left[F\left(\eta\right)+\eta F'(\eta)\right], B=\frac{B_o}{\sqrt{\left(1-\alpha t\right)}}e^{\frac{x}{2L}}
\end{aligned} \tag{3.20}$$

Making use of Eq. (3.20), Equations of continuity (3.15 and 3.17) are identically satisfied and Eqs. (3.16) and (3.18) take the following form

$$f'''\left(\eta\right)+f\left(\eta\right)f''\left(\eta\right)-2f'\left(\eta\right)^2+2l\beta\left[F'\left(\eta\right)-f'(\eta)\right]-A\left[2f'(\eta)+\eta f''(\eta)\right]-Mf'=0, \tag{3.21}$$

$$F(\eta)F"(\eta)-2F'(\eta)^2+2\beta[f'(\eta)-F'(\eta)]-A[\eta F''(\eta)+2F'(\eta)]=0, \tag{3.22}$$

where prime signifies the differentiation with respect to η and $l=\frac{m\mathbf{N}}{\rho}$ represents the mass concentration, $\beta=\frac{L}{\boldsymbol{\tau}_\nu U_o}\left(1-\alpha t\right)e^{-\frac{x}{L}}$ represents the fluid-particle interaction parameter for velocity, where $\boldsymbol{\tau}_\nu=\frac{m}{K}$ is the relaxation time of dust phase, $A=\frac{\alpha L}{U_o e^{\frac{x}{L}}}$ is the unsteady parameter which determines the unsteadiness and $M=\frac{2\sigma B_o^2 L}{\rho U_o}$ is the magnetic parameter. Employing the similarity transformations on boundary conditions presented in Eq.(3.19) , we acquire

$$f'(\eta)=1, f(\eta)=S \text{ at } \eta=0, \tag{3.23}$$

$$f'(\eta)=0, F'(\eta)=0, F(\eta)=f(\eta)+\eta f'(\eta)-\eta F'(\eta) \text{ as } \eta\to\infty.$$

The expression for the skin friction coefficient is

$$C_f=\frac{\boldsymbol{\tau}_w}{\rho U_w^2}, \tag{3.24}$$

where the skin friction $\boldsymbol{\tau}_w$ is given by,

$$\boldsymbol{\tau}_w=\mu\left(\frac{\partial u}{\partial y}\right)_{y=0}, \tag{3.25}$$

Involving the non-dimensional variables, one obtains,

$$\sqrt{2\,\mathrm{Re}}C_f = f''(0). \tag{3.26}$$

3.3 Heat and Mass Transfer Analysis for Nanofluid

Energy equations for fluid phase and dust particles are

$$\begin{aligned}\rho c_p\left(\frac{\partial T}{\partial t}+u\frac{\partial T}{\partial x}+v\frac{\partial T}{\partial y}\right) &= k\frac{\partial^2 T}{\partial y^2}+\frac{Nc_p}{\tau_T}\left(T_p-T\right)+\frac{N}{\tau_v}\left(u_p-u\right)^2\\ &\quad +\mu\left(\frac{\partial u}{\partial y}\right)^2-\frac{\partial q_r}{\partial y}+Q(T-T_\infty)\\ &\quad +\left(\rho c_p\right)_p\left(D_B\frac{\partial C}{\partial y}\frac{\partial T}{\partial y}+\frac{D_T}{T_\infty}\left(\frac{\partial T}{\partial y}\right)^2\right),\end{aligned} \tag{3.27}$$

$$Nc_m\left(\frac{\partial T_p}{\partial t}+u_p\frac{\partial T_p}{\partial x}+v_p\frac{\partial T_p}{\partial y}\right)=-\frac{Nc_p}{\tau_T}\left(T_p-T\right). \tag{3.28}$$

Using Rosseland approximation for thermal radiation, radiative heat flux becomes

$$q_r=\frac{-4\sigma^*}{3k^*}\frac{\partial T^4}{\partial y}, \tag{3.29}$$

where σ^* symbolizes the Stefan-Boltzmann constant and k^* represents the mean absorption coefficient. T^4 is a function of temperature defined as

$$T^4=4T_\infty^3T-3T_\infty^4. \tag{3.30}$$

Using Eq.(3.29) in energy equation (3.27), we obtain

$$\begin{aligned}\rho c_p\left(\frac{\partial T}{\partial t}+u\frac{\partial T}{\partial x}+v\frac{\partial T}{\partial y}\right) &= \left(k+\frac{16\sigma^*T_\infty^3}{3k^*}\right)\frac{\partial^2 T}{\partial y^2}+\frac{Nc_p}{\tau_T}\left(T_p-T\right)\\ &\quad +\frac{N}{\tau_v}\left(u_p-u\right)^2+\mu\left(\frac{\partial u}{\partial y}\right)^2+Q\left(T-T_\infty\right)\\ &\quad +\left(\rho c_p\right)_p\left(D_B\frac{\partial C}{\partial y}\frac{\partial T}{\partial y}+\frac{D_T}{T_\infty}\left(\frac{\partial T}{\partial y}\right)^2\right),\end{aligned} \tag{3.31}$$

where ρ is the density of the base fluid. $(\rho c_p)_p$ is the effective heat capacity of nanoparticle material.

Concentration equations of fluid phase and dust particles are

$$\frac{\partial C}{\partial t} + u\frac{\partial C}{\partial x} + v\frac{\partial C}{\partial y} = D_B\frac{\partial^2 C}{\partial y^2} + \frac{D_T}{T_\infty}\left(\frac{\partial^2 T}{\partial y^2}\right), \tag{3.32}$$

$$\frac{\partial C_p}{\partial t} + u_p\frac{\partial C_p}{\partial x} + v_p\frac{\partial C_p}{\partial y} = D\frac{\partial^2 C_p}{\partial y^2}, \tag{3.33}$$

where D is the coefficient of mass diffusivity C is the concentration of fluid and C_p denotes concentration of dust particles.

We have discussed the heat and mass transfer phenomenon for two different types of heating procedures, i.e.,

1. Variable exponential order surface temperature and surface concentration (VEST).

2. Variable exponential order heat flux and mass flux (VEHF).

3.3.1 Case 1: Variable exponential order surface temperature (VEST):

In this case the boundary conditions employed, are defined as

$$\begin{aligned} T &= T_w(x,t) \text{ at } y = 0, \\ T &\to T_\infty, T_p \to T_\infty \text{ as } y \to \infty, \\ C &= C_w(x,t) \text{ at } y = 0, \\ C &\to C_\infty, C_p \to C_\infty \text{ as } y \to \infty, \end{aligned} \tag{3.34}$$

where $T_w = T_\infty + \frac{T_o}{(1-\alpha t)^2}e^{\frac{c_1 x}{2L}}$, $C_w = C_\infty + \frac{C_o}{(1-\alpha t)^2}e^{\frac{c_1 x}{2L}}$is the temperature distribution and concentration distribution respectively in the stretching surface, c_1 is a constant, T_0 is the reference temperature and C_o is the corresponding reference concentration. The dimensionless variables for the fluid temperature $\theta(\eta)$ and concentration $\phi(\eta)$ and dust particles temperature

$\theta_p(\eta)$ and concentration $\phi_p(\eta)$ are defined as

$$\begin{aligned} \theta(\eta) &= \frac{T-T_\infty}{T_w-T_\infty},\ \theta_p(\eta)=\frac{T_p-T_\infty}{T_w-T_\infty}, \\ \phi(\eta) &= \frac{C-C_\infty}{C_w-C_\infty},\ \phi_p(\eta)=\frac{C_p-C_\infty}{C_w-C_\infty}, \end{aligned} \tag{3.35}$$

where $T-T_\infty=\frac{T_0}{(1-\alpha t)^2}e^{\frac{c_1 x}{2L}}\theta(\eta)$ and $C-C_\infty=\frac{C_0}{(1-\alpha t)^2}e^{\frac{c_1 x}{2L}}\phi(\eta)$. Using the similarity variable (η) and Eq. (3.35) into Eqs.(3.28) and $(3.31-3.33)$, one can achieves the following system of equations

$$\left(1+\frac{4R}{3}\right)\theta''(\eta)+\Pr\left[f(\eta)\theta'(\eta)-c_1 f'(\eta)\theta(\eta)\right]+2\frac{N}{\rho}\beta_T\Pr\left[\theta_p(\eta)-\theta(\eta)\right]-A\Pr\left[\eta\theta'(\eta)+4\theta(\eta)\right]$$

$$+2\frac{N}{\rho}\beta\Pr Ec\left[F'(\eta)-f'(\eta)\right]^2+\Pr Ec\left[f'(\eta)\right]^2+2\lambda\Pr\theta(\eta)+\Pr[N_T\theta'^2+N_B\phi'\theta']=0, \tag{3.36}$$

$$c_1F'(\eta)\theta_p(\eta)-F(\eta)\theta_p'(\eta)+2\gamma\beta_T\left[\theta_p(\eta)-\theta(\eta)\right]+A[\eta\theta_p'(\eta)+4\theta_p(\eta)]=0, \tag{3.37}$$

$$\phi''+\frac{N_T}{N_B}\theta''+Sc[f\phi'-c_1f'\phi]-ASc[4\phi+\eta\phi']=0 \tag{3.38}$$

$$\phi_p''+Sc[F\phi_p'-c_1F'\phi_p]-ASc[4\phi_p+\eta\phi_p']=0 \tag{3.39}$$

where $\Pr=\frac{\mu c_p}{k}$ portrays the Prandtl number, $R=\frac{4\sigma^* T_\infty^3}{kk^*}$ is the parameter for radiation, $\gamma=\frac{c_p}{c_m}$ is the specific heat ratio, $Ec=\frac{U_0^2e^{\frac{2x}{L}}}{c_pT_0e^{\frac{c_1x}{2L}}}$ is the Eckert number, $A=\frac{\alpha L}{U_0e^{\frac{x}{L}}}$ is the unsteady parameter, $\beta=\frac{L}{\tau_\nu U_0e^{\frac{x}{L}}}(1-\alpha t)$ and $\beta_T=\frac{L}{\tau_T U_0e^{\frac{x}{L}}}(1-\alpha t)$ are the fluid and particle interaction parameters for velocity and heat transfer respectively, $\lambda=\frac{QL^2}{\mu c_p\,\mathrm{Re}}$ denotes the dimensionless heat source/sink parameter where $\mathrm{Re}=\frac{U_0Le^{\frac{x}{L}}}{\nu(1-\alpha t)}$ is the Reynolds number, $N_T=\frac{(\rho c_p)_p D_T(T_w-T_\infty)}{\rho c_p\nu T_\infty}$ represents the Thermophoresis parameter, $N_B=\frac{(\rho c_p)_p D_B(C_w-C_\infty)}{\rho c_p\nu}$ denotes the Brownian motion parameter and $Sc=\frac{\nu}{D_B}$ is the Schmidt number.

Subsequent thermal and concentration boundary conditions become

$$\begin{aligned}
\theta(\eta) &= 1 \text{ at } \eta = 0, \\
\theta(\eta) &\to 0,\ \theta_p(\eta) \to 0 \text{ as } \eta \to \infty, \\
\phi(\eta) &= 1 \text{ at } \eta = 0, \\
\phi(\eta) &\to 0,\ \phi_p(\eta) \to 0 \text{ as } \eta \to \infty.
\end{aligned} \tag{3.40}$$

3.3.2 Case 2: Variable exponential order heat flux (VEHF):

For this heat and mass transfer procedure, consider the following boundary conditions

$$\begin{aligned}
\frac{\partial T}{\partial y} &= -\frac{q_w(x,t)}{k} \text{ at } y = 0, \\
T &\to T_\infty, T_p \to T_\infty \text{ as } y \to \infty, \\
\frac{\partial C}{\partial y} &= -\frac{q_m(x,t)}{D_B} \text{ at } y = 0, \\
C &\to C_\infty, C_p \to C_\infty \text{ as } y \to \infty,
\end{aligned} \tag{3.41}$$

where $q_w = \frac{T_1}{(1-\alpha t)^{\frac{5}{2}}} e^{\frac{(c_1+1)x}{2L}}$, $q_m = \frac{C_1}{(1-\alpha t)^{\frac{5}{2}}} e^{\frac{(c_1+1)x}{2L}}$ are heat and mass fluxes, T_1 is the reference temperature and $C_1$is reference concentration. Now by using the similarity variable (η) and Eq.(3.41) , we get the same system of equations, with $Ec = \frac{kU_o^2}{c_p T_1}\sqrt{\frac{U_0}{2\nu L}}$, which is different from the VEST case, all the other parameters are same as in VEST.

The boundary conditions for above case transform to

$$\begin{aligned}
\theta'(\eta) &= -1 \text{ at } \eta = 0, \\
\theta(\eta) &\to 0,\ \theta_p(\eta) \to 0 \text{ as } \eta \to \infty, \\
\phi'(\eta) &= -1 \text{ at } \eta = 0, \\
\phi(\eta) &\to 0,\ \phi_p(\eta) \to 0 \text{ as } \eta \to \infty.
\end{aligned} \tag{3.42}$$

The Nusselt number and Sherwood number are defined as,

$$Nu_x = \frac{x q_w}{k(T - T_\infty)}, \tag{3.43}$$

$$Sh_x = \frac{xq_m}{D_B(C - C_\infty)}, \tag{3.44}$$

where q_w and q_m are the heat and mass transfer from the sheet respectively, which are given by,

$$q_w = -k\left(\frac{\partial T}{\partial y}\right)_{y=0}, \tag{3.45}$$

$$q_m = -D_B\left(\frac{\partial C}{\partial y}\right)_{y=0}. \tag{3.46}$$

Making use of non-dimensional variables, one obtains,

$$\frac{Nu_x}{\sqrt{2\,\mathrm{Re}}} = -\frac{x}{2L}\theta'(0),\ \frac{Sh_x}{\sqrt{2\,\mathrm{Re}}} = -\frac{x}{2L}\phi'(0)\ \text{(VEST Case)}, \tag{3.47}$$

and.

$$\frac{Nu_x}{\sqrt{2\,\mathrm{Re}}} = \frac{x}{2L}\frac{1}{\theta(0)}, \frac{Sh_x}{\sqrt{2\,\mathrm{Re}}} = \frac{x}{2L}\frac{1}{\phi(0)}\ \text{(VEHF Case)}.$$

3.4 The OHAM solutions

The nonlinear coupled ordinary differential equations for VEST and VEHF case are analytically solved by Optimal Homotopy Analysis Method (OHAM). According to the procedure, we express the set of basic functions $f(\eta)$, $F(\eta)$, $\theta(\eta)$, $\theta_p(\eta)$, $\phi(\eta)$ and $\phi_p(\eta)$ by

$$\left\{\eta^k \exp(-n\eta) \mid k \geq 0,\ \eta \geq 0\right\}, \tag{3.48}$$

in the form

$$f(\eta) = \sum_{n=0}^{\infty}\sum_{k=0}^{\infty} a_{m,n}^k\ \eta^k \exp(-n\eta), \tag{3.49}$$

$$F(\eta) = \sum_{n=0}^{\infty}\sum_{k=0}^{\infty} b_{m,n}^k\ \eta^k \exp(-n\eta), \tag{3.50}$$

$$\theta(\eta) = \sum_{n=0}^{\infty}\sum_{k=0}^{\infty} c_{m,n}^k\ \eta^k \exp(-n\eta), \tag{3.51}$$

$$\theta_p(\eta) = \sum_{n=0}^{\infty}\sum_{k=0}^{\infty} d_{m,n}^k\ \eta^k \exp(-n\eta), \tag{3.52}$$

$$\phi(\eta) = \sum_{n=0}^{\infty} \sum_{k=0}^{\infty} e_{m,n}^{k} \ \eta^{k} \exp(-n\eta), \tag{3.53}$$

$$\phi_{p}(\eta) = \sum_{n=0}^{\infty} \sum_{k=0}^{\infty} j_{m,n}^{k} \ \eta^{k} \exp(-n\eta), \tag{3.54}$$

in which $a_{m,n}^{k},\ b_{m,n}^{k}, c_{m,n}^{k}, d_{m,n}^{k}, e_{m,n}^{k}$ and $j_{m,n}^{k}$ symbolize the coefficients. Utilizing the rule of solution expression and the given boundary conditions, the initial guesses $f_0, F_0, \theta_0, \theta_{p_0}, \phi_0, \phi_{p_0}$ can be chosen as:

$$f_0(\eta) = (1+s) - \exp(-\eta), \tag{3.55}$$

$$F_0(\eta) = (1+s) - \exp(-\eta), \tag{3.56}$$

$$\theta_0(\eta) = \exp(-\eta), \tag{3.57}$$

$$\theta_{p_0}(\eta) = \exp(-\eta), \tag{3.58}$$

$$\phi_0(\eta) = \exp(-\eta), \tag{3.59}$$

$$\phi_{p_0}(\eta) = \exp(-\eta). \tag{3.60}$$

The auxiliary linear operators are

$$\mathcal{L}_f = \frac{d^3}{d\eta^3} - \frac{d}{d\eta}, \tag{3.61}$$

$$\mathcal{L}_F = \frac{d^2}{d\eta^2} - \frac{d}{d\eta}, \tag{3.62}$$

$$\mathcal{L}_\theta = \frac{d^2}{d\eta^2} - 1, \tag{3.63}$$

$$\mathcal{L}_{\theta_p} = \frac{d}{d\eta} - 1, \tag{3.64}$$

$$\mathcal{L}_\phi = \frac{d^2}{d\eta^2} - 1, \tag{3.65}$$

$$\mathcal{L}_{\phi_p} = \frac{d^2}{d\eta^2} - \frac{d}{d\eta}, \tag{3.66}$$

which satisfy

$$\mathcal{L}_f \left[c_1 + c_2 \exp(\eta) + c_3 \exp(-\eta)\right] = 0, \tag{3.67}$$

$$\mathcal{L}_F \left[c_4 + c_5 \exp(\eta)\right] = 0, \tag{3.68}$$

$$\mathcal{L}_\theta \left[c_6 \exp(\eta) + c_7 \exp(-\eta)\right] = 0, \tag{3.69}$$

$$\mathcal{L}_{\theta_p} \left[c_8 \exp(\eta)\right] = 0, \tag{3.70}$$

$$\mathcal{L}_\phi \left[c_9 \exp(\eta) + c_{10} \exp(-\eta)\right] = 0, \tag{3.71}$$

$$\mathcal{L}_{\phi_p} \left[c_{11} + c_{12} \exp(\eta)\right] = 0. \tag{3.72}$$

where $c_i\,(i = 1 - 12)$ are arbitrary constants. If we define $p \in [0, 1]$ as an embedding parameter and $\hbar_f, \hbar_F, \hbar_\theta, \hbar_{\theta_p}, \hbar_\phi, \hbar_{\phi_p}$ represent the non-zero auxiliary parameters, we can define the zeroth order deformation problems as

$$(1-p)\,\mathcal{L}_f \left[\widehat{f}(\eta;p) - \widehat{f}_0(\eta)\right] = p\hbar_f N_f \left[\widehat{f}(\eta;p), \widehat{F}(\eta;p)\right] \ , \tag{3.73}$$

$$(1-p)\,\mathcal{L}_F \left[\widehat{F}(\eta;p) - \widehat{F}_0(\eta)\right] = p\hbar_F N_F \left[\widehat{f}(\eta;p), \widehat{F}(\eta;p)\right], \tag{3.74}$$

$$(1-p)\,\mathcal{L}_\theta \left[\widehat{\theta}(\eta;p) - \widehat{\theta}_0(\eta)\right] = p\hbar_\theta N_\theta \left[\widehat{f}(\eta;p), \widehat{F}(\eta;p),\ \widehat{\theta}(\eta;p),\ \widehat{\theta_p}(\eta;p)\ \right], \tag{3.75}$$

$$(1-p)\,\mathcal{L}_{\theta_p} \left[\widehat{\theta_p}(\eta;p) - \widehat{\theta_p}_0(\eta)\right] = p\hbar_{\theta_p} N_{\theta_p} \left[\widehat{F}(\eta;p),\ \widehat{\theta}(\eta;p),\ \widehat{\theta_p}(\eta;p)\ \right], \tag{3.76}$$

$$(1-p)\,\mathcal{L}_\phi \left[\widehat{\phi}(\eta;p) - \widehat{\phi}_0(\eta)\right] = p\hbar_\phi N_\phi \left[\widehat{f}(\eta;p),\ \widehat{\theta}(\eta;p),\ \widehat{\phi}(\eta;p)\ \right], \tag{3.77}$$

$$(1-p)\,\mathcal{L}_{\phi_p} \left[\widehat{\phi_p}(\eta;p) - \widehat{\phi_p}_0(\eta)\right] = p\hbar_{\phi_p} N_{\phi_p} \left[\widehat{F}(\eta;p),\ \widehat{\phi_p}(\eta;p)\ \right]. \tag{3.78}$$

CASE 1:

$$\widehat{f}'(0;p) = 1 = \widehat{\theta}(0;p)\ = \widehat{\phi}(0;p),\ \widehat{f}(0;p) = S \tag{3.79}$$

$$\begin{aligned}
\widehat{f}'(\infty;p) &= \widehat{\phi}(\infty;p) = \widehat{\phi_p}(\infty;p) = \widehat{\phi_p'}(\infty;p) = 0 \\
\widehat{F}'(\infty;p) &= \widehat{\theta}(\infty;p) = \widehat{\theta_p}(\infty;p) = 0, \\
\widehat{F}(\infty;p) &= \widehat{f}(\infty;p) + \eta\widehat{f}'(\infty;p) - \eta\widehat{F}'(\infty;p)\Big|_{\eta=\infty}.
\end{aligned} \tag{3.80}$$

CASE 2:

$$\widehat{f}'(0;p) = 1, \widehat{\theta}(0;p)\ = \widehat{\phi}(0;p) = -1, \widehat{f}(0;p) = S, \tag{3.81}$$

$$
\begin{aligned}
\widehat{f}'(\infty;p) &= \widehat{\phi}(\infty;p) = \widehat{\phi_p}(\infty;p) = \widehat{\phi'_p}(\infty;p) = 0, \\
\widehat{F}'(\infty;p) &= \widehat{\theta}(\infty;p) = \widehat{\theta}_p(\infty;p) = 0, \\
\widehat{F}(\infty;p) &= \widehat{f}(\infty;p) + \eta\widehat{f}'(\infty;p) - \eta\widehat{F}'(\infty;p)\Big|_{\eta=\infty},
\end{aligned}
\tag{3.82}
$$

in which

$$
\begin{aligned}
N_f\left[\widehat{f}(\eta;p),\widehat{F}(\eta;p)\right] &= \frac{\partial^3\widehat{f}(\eta;p)}{\partial\eta^3} + \widehat{f}(\eta;p)\frac{\partial^2\widehat{f}(\eta;p)}{\partial\eta^2} - M\left(\frac{\partial\widehat{f}(\eta;p)}{\partial\eta}\right) \\
&\quad +2l\beta\left[\frac{\partial\widehat{F}(\eta;p)}{\partial\eta} - \frac{\partial\widehat{f}(\eta;p)}{\partial\eta}\right] - 2\left(\frac{\partial\widehat{f}(\eta;p)}{\partial\eta}\right)^2 \\
&\quad -A\left[2\left(\frac{\partial\widehat{f}(\eta;p)}{\partial\eta}\right) + \eta\left(\frac{\partial^2\widehat{f}(\eta;p)}{\partial\eta^2}\right)\right],
\end{aligned}
\tag{3.83}
$$

$$
\begin{aligned}
N_F\left[\widehat{f}(\eta;p),\widehat{F}(\eta;p)\right] &= \widehat{F}(\eta;p)\frac{\partial^2\widehat{F}(\eta;p)}{\partial\eta^2} - 2\left(\frac{\partial\widehat{F}(\eta;p)}{\partial\eta}\right)^2 \\
&\quad +2\beta\left[\frac{\partial\widehat{f}(\eta;p)}{\partial\eta} - \frac{\partial\widehat{F}(\eta;p)}{\partial\eta}\right] \\
&\quad -A\left[\eta\left(\frac{\partial^2\widehat{F}(\eta;p)}{\partial\eta^2}\right) + 2\left(\frac{\partial\widehat{F}(\eta;p)}{\partial\eta}\right)\right],
\end{aligned}
\tag{3.84}
$$

$$
\begin{aligned}
N_\theta\left[\widehat{\theta}(\eta;p),\widehat{f}(\eta;p),\widehat{F}(\eta;p),\widehat{\theta}_p(\eta;p)\right] &= \left(1+\frac{4R}{3}\right)\frac{\partial^2\widehat{\theta}(\eta;p)}{\partial\eta^2} + 2\frac{N}{\rho}\beta_T\Pr\left[\widehat{\theta_p}(\eta;p) - \widehat{\theta}(\eta;p)\right] \\
&\quad +\Pr\left[\widehat{f}(\eta;p)\frac{\partial\widehat{\theta}(\eta;p)}{\partial\eta} - c_1\frac{\partial\widehat{f}(\eta;p)}{\partial\eta}\widehat{\theta}(\eta;p)\right] + 2\lambda\Pr\widehat{\theta}(\eta;p) \\
&\quad +2\frac{N}{\rho}\beta\Pr Ec\left[\frac{\partial\widehat{F}(\eta;p)}{\partial\eta} - \frac{\partial\widehat{f}(\eta;p)}{\partial\eta}\right]^2 \\
&\quad -A\Pr\left[\eta\frac{\partial\widehat{\theta}(\eta;p)}{\partial\eta} + 4\widehat{\theta}(\eta;p)\right] + \Pr Ec\left[\frac{\partial^2\widehat{f}(\eta;p)}{\partial\eta^2}\right]^2 \\
&\quad +\Pr\left[N_T\left(\frac{\partial\widehat{\theta}(\eta;p)}{\partial\eta}\right)^2 + N_b\frac{\partial\widehat{\phi}(\eta;p)}{\partial\eta}\frac{\partial\widehat{\theta}(\eta;p)}{\partial\eta}\right],
\end{aligned}
\tag{3.85}
$$

$$
\begin{aligned}
N_{\theta_p}\left[\widehat{\theta}_p(\eta;p),\widehat{\theta}(\eta;p),\widehat{F}(\eta;p)\right] &= c_1\frac{\partial\widehat{F}(\eta;p)}{\partial\eta}\widehat{\theta}_p(\eta;p) - F(\eta;p)\frac{\partial\widehat{\theta}(\eta;p)}{\partial\eta} \\
&\quad +2\gamma\beta_T\left[\widehat{\theta}_p(\eta;p)-\widehat{\theta}(\eta;p)\right] \\
&\quad +A\left[\eta\frac{\partial\widehat{\theta}_p(\eta;p)}{\partial\eta}+4\widehat{\theta}_p(\eta;p)\right],
\end{aligned} \tag{3.86}
$$

$$
\begin{aligned}
N_{\phi}\left[\widehat{\phi}(\eta;p),\widehat{\theta}(\eta;p),\widehat{f}(\eta;p)\right] &= \frac{\partial^2\widehat{\phi}(\eta;p)}{\partial\eta^2}+\frac{N_T}{N_B}\frac{\partial^2\widehat{\theta}(\eta;p)}{\partial\eta^2} \\
&\quad -ASc\left[4\widehat{\phi}(\eta;p)+\eta\frac{\partial\widehat{\phi}(\eta;p)}{\partial\eta}\right] \\
&\quad +Sc\left[\widehat{f}(\eta;p)\frac{\partial\widehat{\phi}(\eta;p)}{\partial\eta}-c_1\frac{\partial\widehat{f}(\eta;p)}{\partial\eta}\widehat{\phi}(\eta;p)\right],
\end{aligned} \tag{3.87}
$$

$$
\begin{aligned}
N_{\phi_p}\left[\widehat{\phi_p}(\eta;p),\widehat{F}(\eta;p)\right] &= \frac{\partial^2\widehat{\phi_p}(\eta;p)}{\partial\eta^2}-ASc\left[4\widehat{\phi_p}(\eta;p)+\eta\frac{\partial\widehat{\phi_p}(\eta;p)}{\partial\eta}\right] \\
&\quad +Sc\left[\widehat{F}(\eta;p)\frac{\partial\widehat{\phi_p}(\eta;p)}{\partial\eta}-c_1\frac{\partial\widehat{F}(\eta;p)}{\partial\eta}\widehat{\phi_p}(\eta;p)\right].
\end{aligned} \tag{3.88}
$$

For $p=0$ and $p=1$, we have,

$$\widehat{f}(\eta;0)=f_0(\eta)\ ,\ \widehat{f}(\eta;1)=f(\eta), \tag{3.89}$$

$$\widehat{F}(\eta;0)=F_0(\eta)\ ,\ \widehat{F}(\eta;1)=F(\eta), \tag{3.90}$$

$$\widehat{\theta}(\eta;0)=\theta_0(\eta)\ ,\ \widehat{\theta}(\eta;1)=\theta(\eta), \tag{3.91}$$

$$\widehat{\theta}_p(\eta;0)=\theta_{p_0}(\eta)\ ,\ \widehat{\theta}_p(\eta;1)=\theta_p(\eta), \tag{3.92}$$

$$\widehat{\phi}(\eta;0)=\phi_0(\eta)\ ,\ \widehat{\phi}(\eta;1)=\phi(\eta), \tag{3.93}$$

$$\widehat{\phi_p}(\eta;0)=\phi_{p_0}(\eta)\ ,\ \widehat{\phi_p}(\eta;1)=\phi_p(\eta), \tag{3.94}$$

By Taylor theorem

$$\widehat{f}(\eta;p)=f_0(\eta)+\sum_{m=1}^{\infty}f_m(\eta)p^m, \tag{3.95}$$

$$\widehat{F}(\eta;p) = F_0(\eta) + \sum_{m=1}^{\infty} F_m(\eta)p^m, \tag{3.96}$$

$$\widehat{\theta}(\eta;p) = \theta_0(\eta) + \sum_{m=1}^{\infty} \theta_m(\eta)p^m, \tag{3.97}$$

$$\widehat{\theta_p}(\eta;p) = \theta_{p_0}(\eta) + \sum_{m=1}^{\infty} \theta_{p_m}(\eta)p^m, \tag{3.98}$$

$$\widehat{\phi}(\eta;p) = \phi_0(\eta) + \sum_{m=1}^{\infty} \phi_m(\eta)p^m, \tag{3.99}$$

$$\widehat{\phi_p}(\eta;p) = \phi_0(\eta) + \sum_{m=1}^{\infty} \phi_{p_m}(\eta)p^m, \tag{3.100}$$

$$f_m(\eta) = \frac{1}{m!}\left.\frac{\partial^m \widehat{f}(\eta;p)}{\partial \eta^m}\right|_{p=0}, \; F_m(\eta) = \frac{1}{m!}\left.\frac{\partial^m \widehat{F}(\eta;p)}{\partial \eta^m}\right|_{p=0}, \tag{3.101}$$

$$\theta_m(\eta) = \frac{1}{m!}\left.\frac{\partial^m \widehat{\theta}(\eta;p)}{\partial \eta^m}\right|_{p=0}, \; \theta_{p_m}(\eta) = \frac{1}{m!}\left.\frac{\partial^m \widehat{\theta_p}(\eta;p)}{\partial \eta^m}\right|_{p=0}, \tag{3.102}$$

$$\phi_m(\eta) = \frac{1}{m!}\left.\frac{\partial^m \widehat{\phi}(\eta;p)}{\partial \eta^m}\right|_{p=0}, \phi_{p_m}(\eta) = \frac{1}{m!}\left.\frac{\partial^m \widehat{\phi_p}(\eta;p)}{\partial \eta^m}\right|_{p=0}, \tag{3.103}$$

and

$$f(\eta) = f_0(\eta) + \sum_{m=1}^{\infty} f_m(\eta), \tag{3.104}$$

$$F(\eta) = F_0(\eta) + \sum_{m=1}^{\infty} F_m(\eta), \tag{3.105}$$

$$\theta(\eta) = \theta_0(\eta) + \sum_{m=1}^{\infty} \theta_m(\eta), \tag{3.106}$$

$$\theta_p(\eta) = \theta_{p_0}(\eta) + \sum_{m=1}^{\infty} \theta_{p_m}(\eta), \tag{3.107}$$

$$\phi(\eta) = \phi_0(\eta) + \sum_{m=1}^{\infty} \phi_m(\eta), \tag{3.108}$$

$$\phi_p(\eta) = \phi_{p_0}(\eta) + \sum_{m=1}^{\infty} \phi_{p_m}(\eta), \tag{3.109}$$

The mth-order deformation problems are defined as

$$\mathcal{L}[f_m(\eta) - \chi_m f_{m-1}(\eta)] = \hbar_f R_m^f(\eta), \tag{3.110}$$

$$\mathcal{L}[F_m(\eta) - \chi_m F_{m-1}(\eta)] = \hbar_F R_m^F(\eta), \tag{3.111}$$

$$\mathcal{L}[\theta_m(\eta) - \chi_m \theta_{m-1}(\eta)] = \hbar_\theta R_m^\theta(\eta), \tag{3.112}$$

$$\mathcal{L}[\theta_{p_m}(\eta) - \chi_m \theta_{p_{m-1}}(\eta)] = \hbar_{\theta_p} R_m^{\theta_p}(\eta), \tag{3.113}$$

$$\mathcal{L}[\phi_m(\eta) - \chi_m \phi_{m-1}(\eta)] = \hbar_\phi R_m^\phi(\eta), \tag{3.114}$$

$$\mathcal{L}[\phi_{p_m}(\eta) - \chi_m \phi_{p_{m-1}}(\eta)] = \hbar_{\phi_p} R_m^{\phi_p}(\eta), \tag{3.115}$$

CASE 1:

$$f_m(0) = f'_m(0) = \theta_m(0) = \phi_m(0) = 0, \tag{3.116}$$

$$f'_m(\infty) = F'_m(\infty) = \theta_m(\infty) = \theta_{p_m}(\infty) = \ \phi_m(\infty) = \phi_{p_m}(\infty) = \phi'_{p_m}(\infty) = 0, \tag{3.117}$$

$$F_m(\infty) - \ f_m(\infty) + \eta f'_m(\infty) - \eta F'_m(\infty)\big|_{\eta=\infty} = 0 \tag{3.118}$$

CASE 2:

$$f_m(0) = f'_m(0) = \theta'_m(0) = \phi'_m(0) = 0, \tag{3.119}$$

$$f'_m(\infty) = F'_m(\infty) = \theta_m(\infty) = \theta_{p_m}(\infty) = \ \phi_m(\infty) = \phi_{p_m}(\infty) = \phi'_{p_m}(\infty) = 0, \tag{3.120}$$

$$F_m(\infty) - \ f_m(\infty) + \eta f'_m(\infty) - \eta F'_m(\infty)\big|_{\eta=\infty} = 0$$

where

$$\begin{aligned} R_m^f(\eta) \ &= \ f'''_{m-1} + \sum_{k=0}^{m-1} f'_k f''_{m-1-k} - 2\sum_{k=0}^{m-1} f'_k f'_{m-1-k} && (3.121)\\ &\quad +2l\beta[F'_{m-1} - f'_{m-1}] - A[2f'_{m-1} + \eta f''_{m-1}] - M f'_{m-1}, && (3.122) \end{aligned}$$

$$R_m^F(\eta) = \sum_{k=0}^{m-1} F'_k F''_{m-1-k} - 2\sum_{k=0}^{m-1} F'_k F'_{m-1-k} + 2\beta[f'_{m-1} - F'_{m-1}] - A[2F'_{m-1} + \eta F''_{m-1}], \tag{3.123}$$

$$
\begin{aligned}
R_m^{\theta}(\eta) &= \left(1+\frac{4R}{3}\right)\theta''_{m-1} + \Pr\left[\sum_{k=0}^{m-1} f_k\theta'_{m-1-k} - c_1\sum_{k=0}^{m-1}\theta_k f'_{m-1-k}\right] \\
&\quad +2\frac{N}{\rho}\beta_T \Pr\left[\theta_{p_{m-1}} - \theta_{m-1}\right] - A\Pr\left[\eta\theta'_{m-1} + 4\theta_{m-1}\right] \\
&\quad +2\frac{N}{\rho}\beta \Pr Ec\left[\sum_{k=0}^{m-1} F'_k F'_{m-1-k} - \sum_{k=0}^{m-1} f'_k F'_{m-1-k} + \sum_{k=0}^{m-1} f'_k f'_{m-1-k}\right] \\
&\quad +2\lambda \Pr\theta_{m-1} + \Pr Ec\left[\sum_{k=0}^{m-1} f''_k f''_{m-1-k}\right],
\end{aligned} \tag{3.124}
$$

$$
\begin{aligned}
R_m^{\theta_p}(\eta) &= c_1\sum_{k=0}^{m-1}\theta_{p_k}F'_{m-1-k} - \sum_{k=0}^{m-1} F_k\theta'_{p_{m-1-k}} \\
&\quad +2\gamma\beta_T\left[\theta_{p_{m-1}} - \theta_{m-1}\right] + A\left[\eta\theta'_{p_{m-1}} + 4\theta_{p_{m-1}}\right],
\end{aligned} \tag{3.125}
$$

$$
\begin{aligned}
R_m^{\phi}(\eta) &= \phi''_{m-1} + \frac{N_T}{N_B}\theta''_{m-1} + Sc\left[\sum_{k=0}^{m-1} f_k\phi'_{m-1-k} - c_1\sum_{k=0}^{m-1}\phi_k f'_{m-1-k}\right] \\
&\quad -ASc\left[4\phi_{m-1} + \eta\phi'_{m-1}\right],
\end{aligned} \tag{3.126}
$$

$$
\begin{aligned}
R_m^{\phi_p}(\eta) &= \phi''_{p_{m-1}} + Sc\left[\sum_{k=0}^{m-1} F_k\phi'_{p_{m-1-k}} - c_1\sum_{k=0}^{m-1}\phi_{p_k}F'_{m-1-k}\right] \\
&\quad -ASc\left[4\phi_{p_{m-1}} + \eta\phi'_{p_{m-1}}\right],
\end{aligned} \tag{3.127}
$$

$$
\chi_m = \begin{cases} 0; & m \le 1, \\ 1; & m > 1. \end{cases} \tag{3.128}
$$

The general solutions of the given equations can be expressed as

$$
f_m(\eta) = f_m^*(\eta) + c_1 + c_2\exp(\eta) + c_3\exp(-\eta), \tag{3.129}
$$

$$
F_m(\eta) = F_m^*(\eta) + c_4 + c_5\exp(\eta), \tag{3.130}
$$

$$
\theta_m(\eta) = \theta_m^*(\eta) + c_6\exp(\eta) + c_7\exp(-\eta), \tag{3.131}
$$

$$\theta_{p_m}(\eta) = \theta^*_{p_m}(\eta) + c_8 \exp(\eta), \tag{3.132}$$

$$\phi_m(\eta) = \phi^*_m(\eta) + c_9 \exp(\eta) + c_{10} \exp(-\eta), \tag{3.133}$$

$$\phi_{p_m}(\eta) = \phi^*_{p_m}(\eta) + c_{11} + c_{12} \exp(\eta), \tag{3.134}$$

where $f^*_m(\eta), F^*_m(\eta), \theta^*_m(\eta), \theta^*_{p_m}(\eta), \phi^*_m(\eta)$ and $\phi^*_{p_m}(\eta)$ are the special solutions.

3.5 Optimal convergence-control parameters

Homotopy analysis solutions consists of the non-zero auxiliary parameters c_0^f, c_0^F, c_0^θ, $c_0^{\theta_p}$, c_0^ϕ and $c_0^{\phi_p}$ which act as helping tool in determining the region of convergence and rate of the homotopy series solution. By finding the so-called average residual errors [43] we get the optimal values of c_0^f, c_0^F, c_0^θ, $c_0^{\theta_p}$, c_0^ϕ and $c_0^{\phi_p}$ Tables (3.1) and (3.2) present the values for several optimal convergence control parameters and reveals the fact that the total averaged squared residual errors decrease as the order of approximation increases, which proves that the solution is convergent at higher order approximations. Hence, Optimal Homotopy Analysis Method provides us a proper way to select any set of local optimal convergence control parameters to attain the convergent solutions.

$\frac{values\rightarrow}{m\downarrow}$	c_0^f	c_0^F	c_0^θ	$c_0^{\theta_p}$	c_0^ϕ	$c_0^{\phi_p}$	ε_m^t	CPU time $[s]$
2	-0.558	-0.490	-0.467	0.468	-0.916	0.791	2.537×10^{-2}	10.81
4	-0.560	-0.589	-0.705	0.470	-0.635	.732	1.352×10^{-3}	139.96
6	-0.556	-0.627	-0.768	0.499	-0.565	0.644	2.072×10^{-4}	1177.21
8	-0.567	-0.542	-0.894	0.512	-0.630	0.504	1.365×10^{-4}	10637.1

Table.3.1 Total averaged squared residual errors using BVPh 2.0. (VEST Case)

$\frac{values\rightarrow}{m\downarrow}$	c_0^f	c_0^F	c_0^θ	$c_0^{\theta_p}$	c_0^ϕ	$c_0^{\phi_p}$	ε_m^t	CPU time $[s]$
2	-0.561	-0.494	-0.594	0.399	-0.639	0.790	2.31×10^{-2}	11.55
4	-0.570	-0.570	-0.670	0.486	-0.674	0.723	1.835×10^{-3}	139.83
6	-0.565	-0.560	-0.793	0.504	-0.470	0.630	3.836×10^{-4}	2020.91
8	-0.576	-0.537	-0.852	0.503	-0.455	0.501	1.869×10^{-4}	10032.7

Table.3.2 Total averaged squared residual errors using BVPh 2.0. (VEHF Case)

where ε_m^t is the total squared residual error.

Table (3.3) and Fig. (3.1) depict that the individual averaged squared residual errors also decrease as the order of approximation increases, proving that the solution is convergent

m	ε_m^f	ε_m^F	ε_m^θ	$\varepsilon_m^{\theta_p}$	ε_m^ϕ	$\varepsilon_m^{\phi_p}$	CPU time $[s]$
4	3.416×10^{-4}	3.02×10^{-4}	2.180×10^{-4}	1.610×10^{-4}	8.69×10^{-4}	6.236×10^{-4}	9.99
8	1.029×10^{-6}	1.466×10^{-5}	2.809×10^{-5}	2.901×10^{-5}	1.955×10^{-4}	2.863×10^{-4}	73.37
12	7.872×10^{-9}	1.015×10^{-6}	5.949×10^{-6}	6.274×10^{-6}	7.705×10^{-5}	3.260×10^{-5}	262.09
16	2.772×10^{-10}	8.601×10^{-8}	1.578×10^{-6}	1.577×10^{-6}	3.447×10^{-5}	2.701×10^{-6}	669.55

Table.3.3.Individual averaged squared residual errors using optimal values at $m = 2$.(VEST Case)

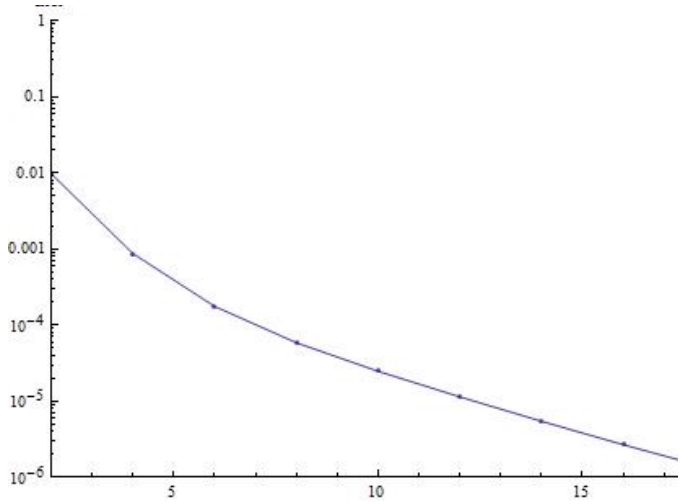

Fig 3.1 Individual squared residual error when m=2

3.6 Graphical results and discussion

The non-linear ordinary differential equations $(3.21 - 3.22$ and $3.36 - 3.39)$ along with the boundary conditions (3.23), (3.40) and (3.42) have been solved analytically by using the OHAM. The influence of various parameters on the temperature and concentration profiles are presented graphically in $Figs.3.2 - 3.20$. Different properties of fluid at the surface are investigated for skin friction coefficient, temperature gradient $\theta'(0)$ and concentration gradient $\phi'(0)$ in case of VEST and temperature $\theta(0)$ and concentration $\phi(0)$ in VEHF case, which are presented in $Table$ 3.4, 3.5.and 3.6. The values of $\beta_T = 0.6, c_1 = 1, \rho = 1, \gamma = 1.4$ and $l = 0.1$ are used in our calculations.

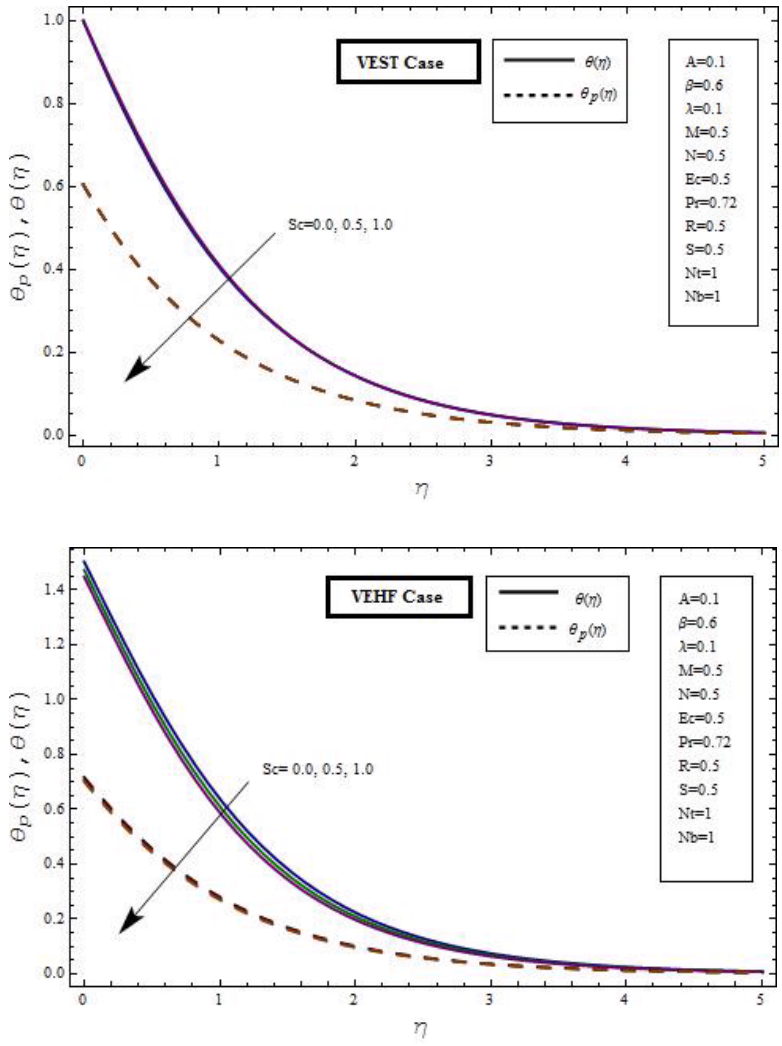

Fig. 3.2 Influence of Sc on temperature distribution for both VEST and VEHF cases.

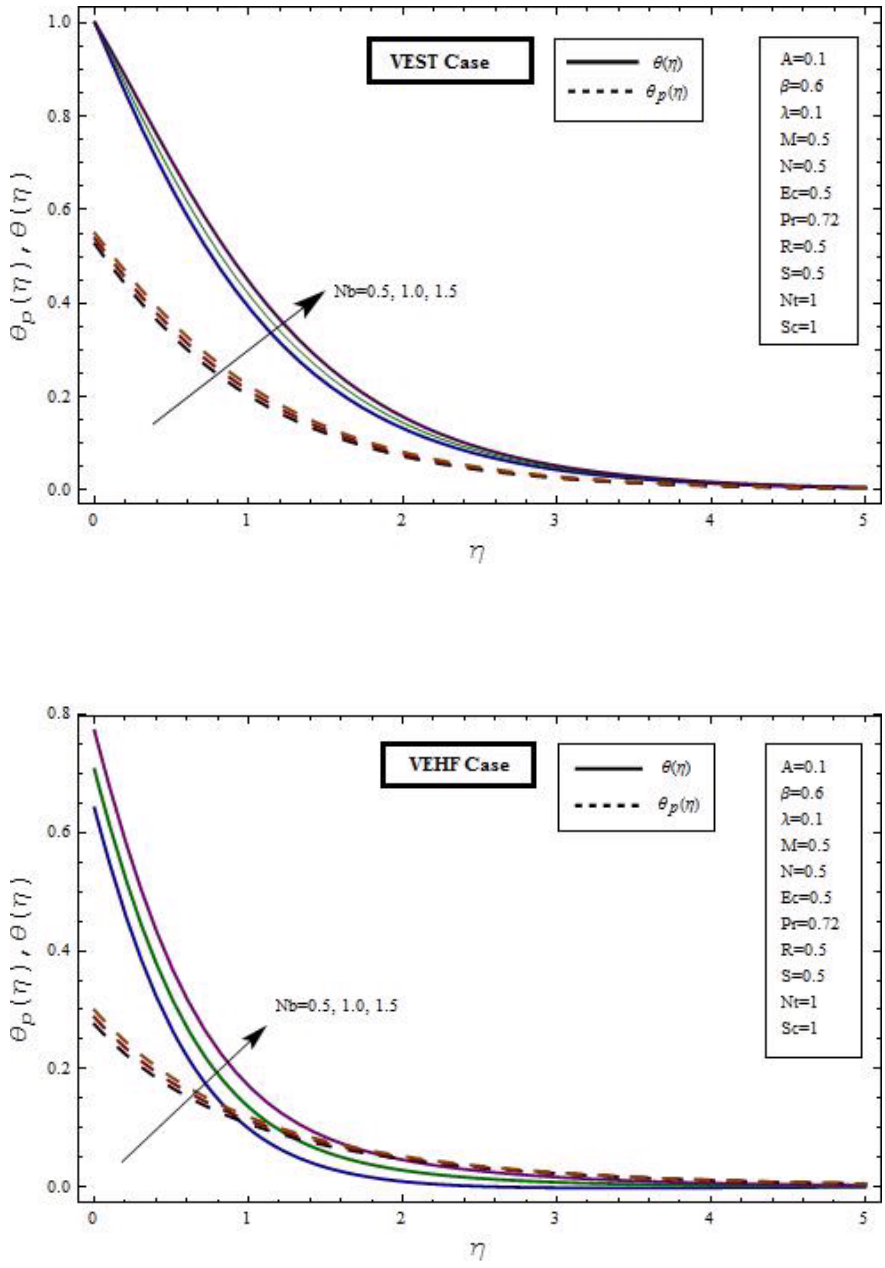

Fig.3.3 Influence of N_b on temperature distribution for both VEST and VEHF cases.

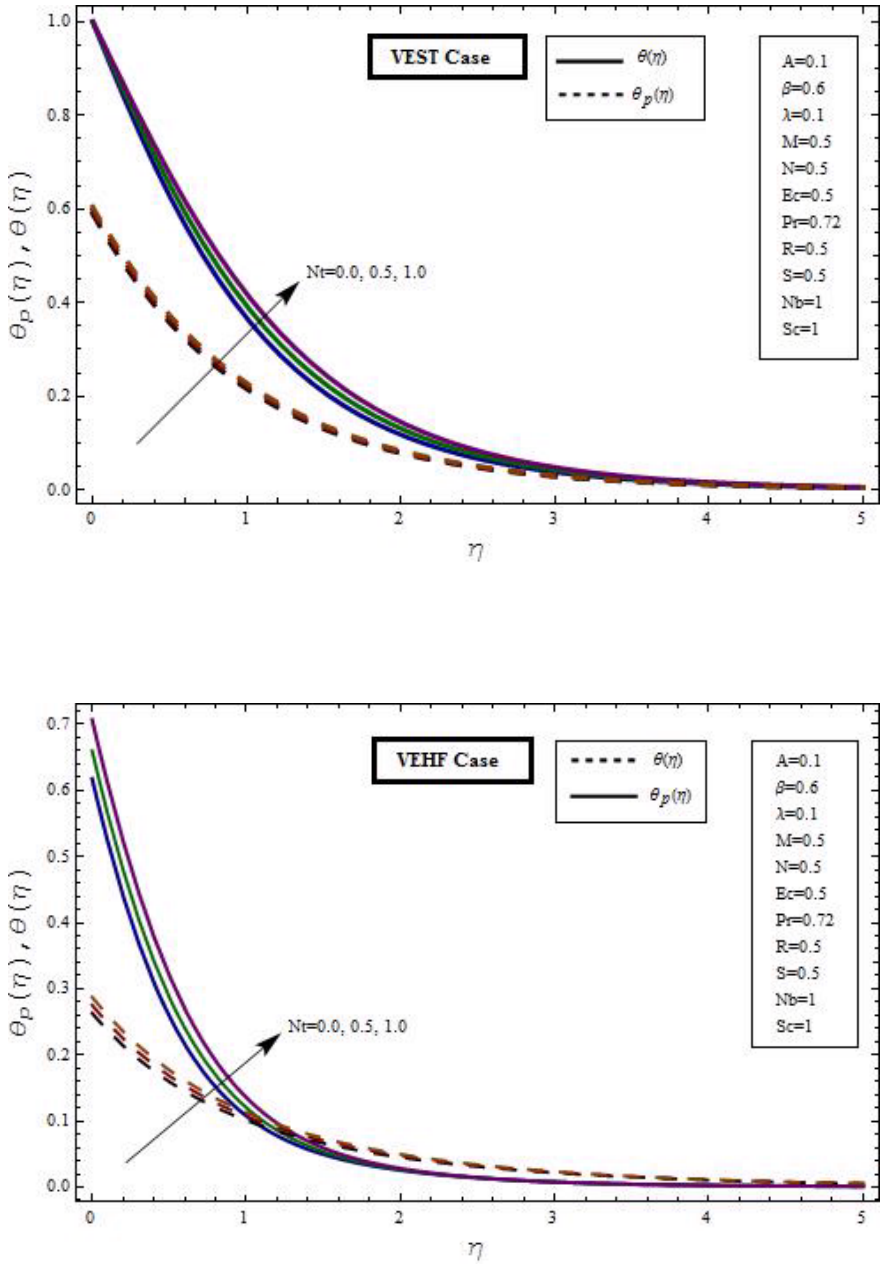

Fig.3.4 Influence of N_t on temperature distribution for both VEST and VEHF cases.

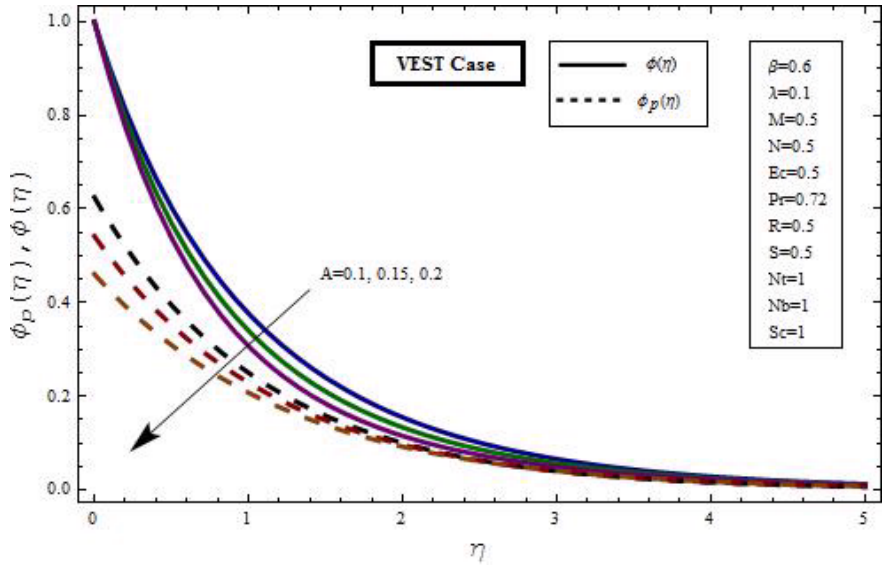

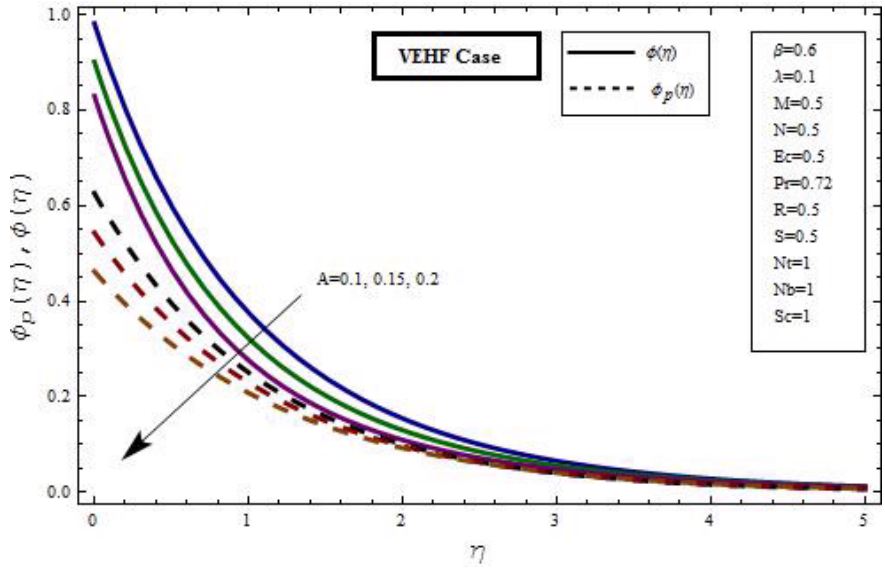

Fig.3.5 Influence of A on concentration profiles for both VEST and VEHF cases.

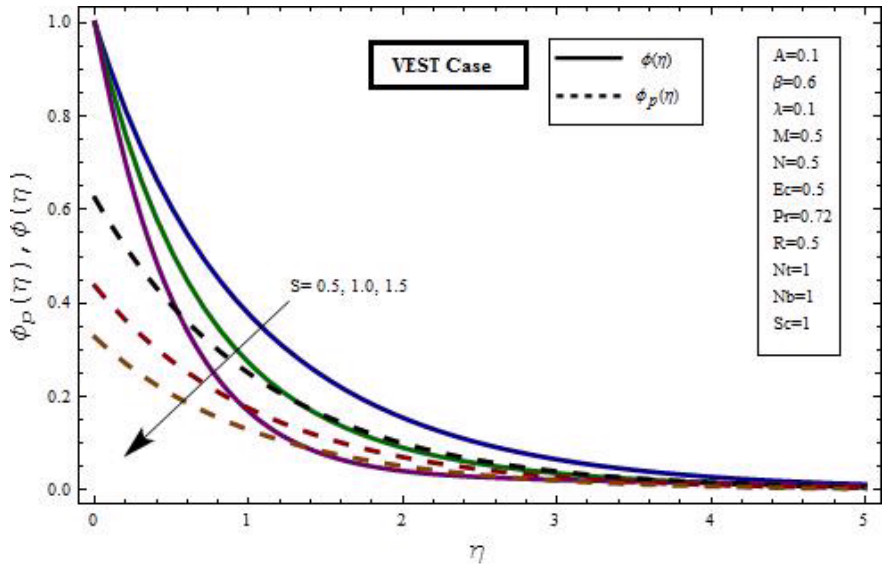

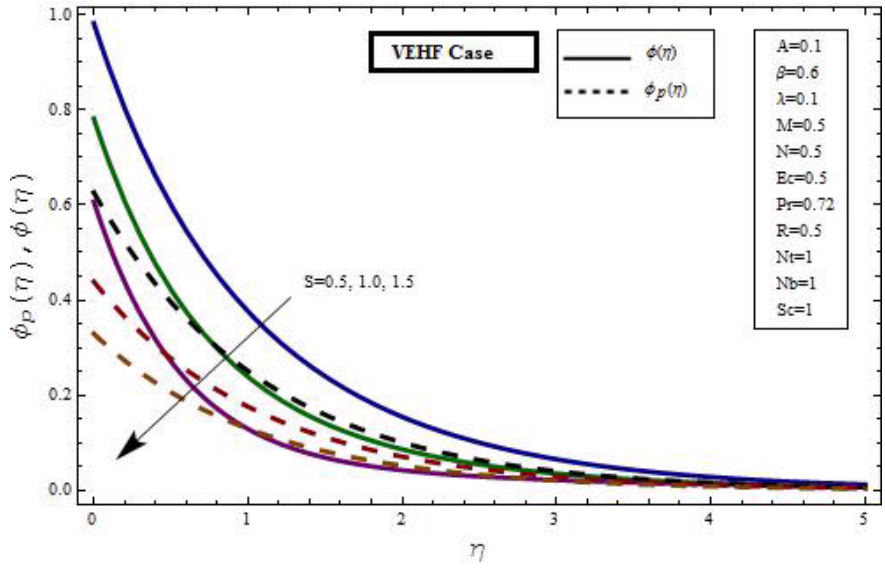

Fig.3.6 Influence of S on concentration profiles for both VEST and VEHF cases.

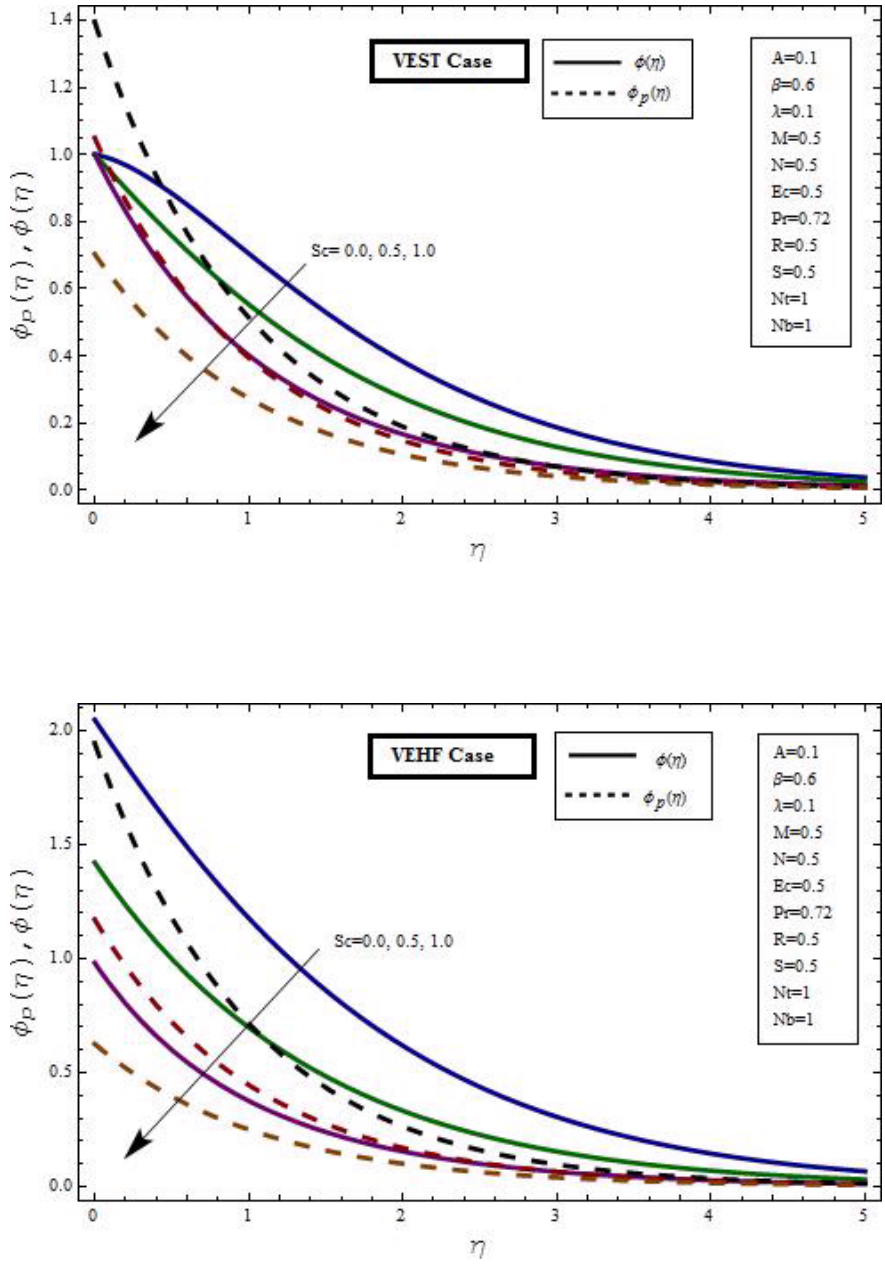

Fig 3.7 Influence of Sc on concentration profiles for both VEST and VEHF cases.

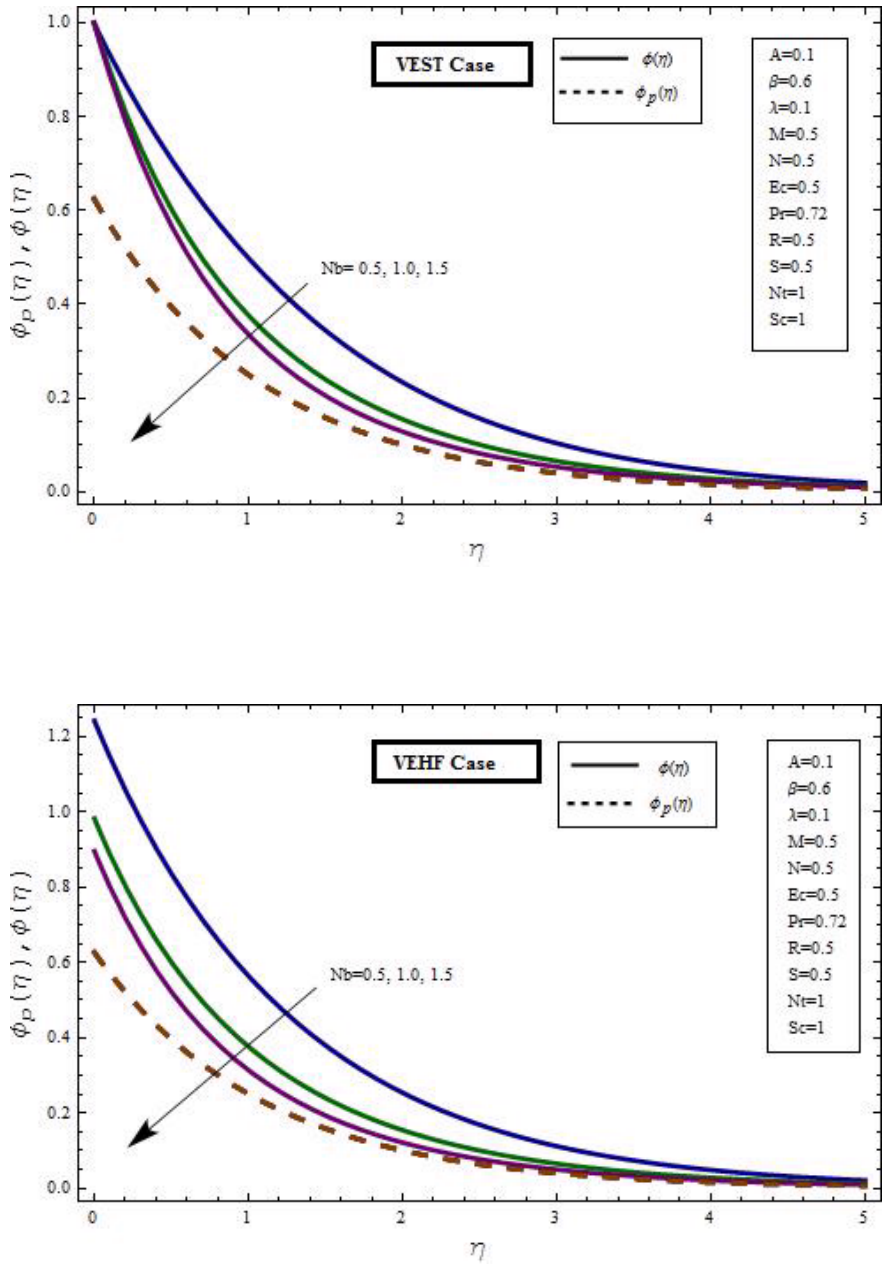

Fig.3.8 Influence of N_b on concentration profiles for both VEST and VEHF cases.

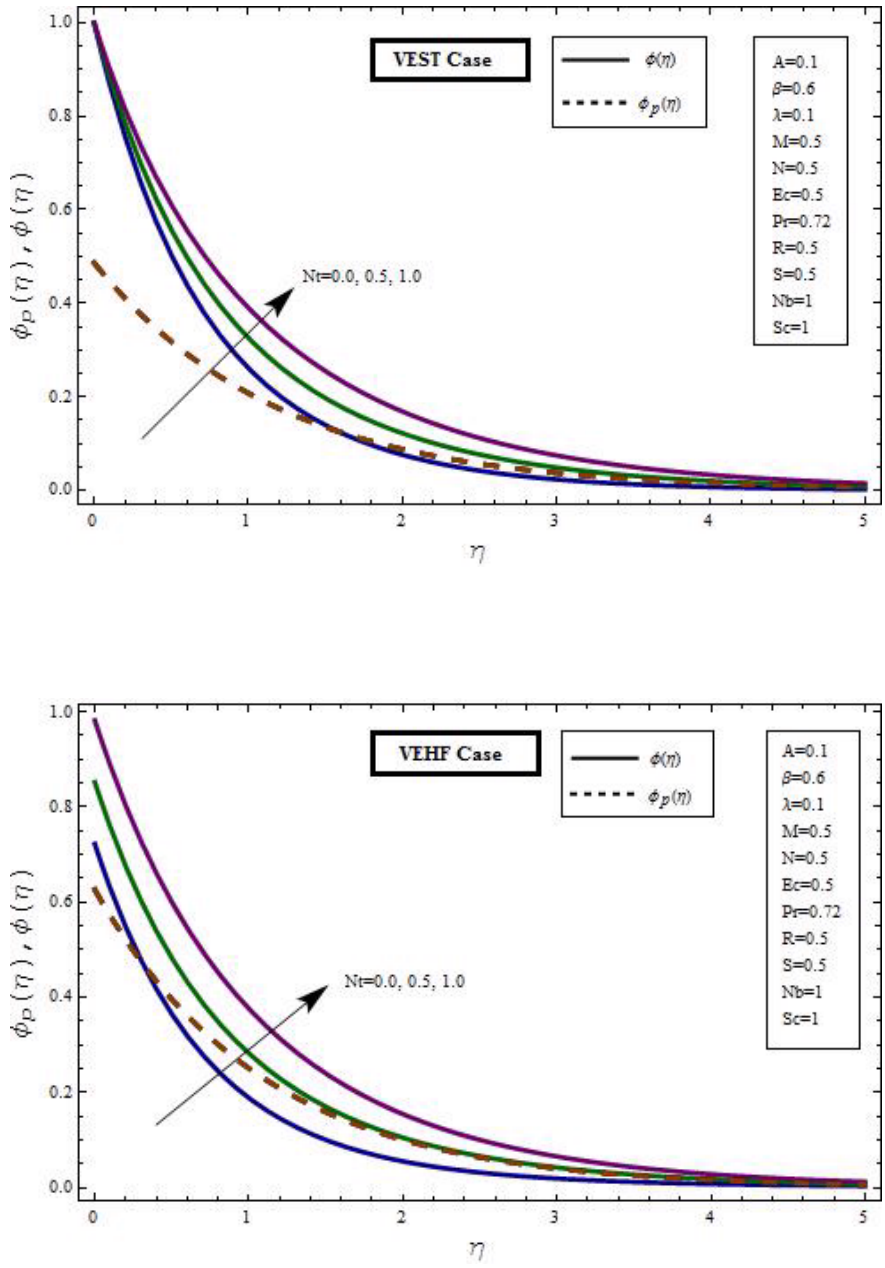

Fig. 3.9 Influence of N_t on concentration profiles for both VEST and VEHF cases

Table 3.4: Effect of different parameters on heat and mass transfer coefficients $\theta'(0)$ and $\phi'(0)$ in VEST case and $\theta(0)$ and $\phi(0)$ in VEHF case.

N_t	N_b	Sc	$\theta'(0)(VEST)$	$\theta(0)(VEHF)$	$\phi'(0)(VEST)$	$\phi(0)(VEHF)$
0.1			-1.0209	0.8634	-1.0411	0.9812
0.3	1	1	-0.8512	0.9408	-0.8721	1.4921
0.5			-0.6648	1.0323	-0.5628	2.0388
	0.1		-1.0209	0.8634	-1.0411	0.9812
1	0.3	1	-0.9247	0.9208	-1.2817	0.8081
	0.5		-0.8411	0.9801	-1.3320	0.7728
		0.3	-0.9104	0.8721	-0.6353	2.2561
1	1	0.5	-0.9672	0.8694	-0.8425	1.6182
		1	-1.0209	0.8634	-1.0411	0.9812

Effects of Schmidt number (Sc), Thermophoretic parameter (N_T) and Brownian motion parameter (N_B) on temperature fields of fluid and dust phase are analyzed in $Figs.(3.2-3.4)$ Increase in N_T and N_B increase the temperature distribution of fluid and dust phase as they both increase the surface temperature. While increase in Sc, decreases the temperature profiles and thermal boundary layer thickness in both the cases. This is because increase in Sc reduces the molecular diffusivity which lowers the temperature.

In $Figs.$ $(3.5-3.9)$, the concentration profiles $\phi(\eta)$ and $\phi_p(\eta)$ are plotted for different parameters involved in our study. When we increase the unsteady parameter (A) and suction parameter (S) there is a decrease in the concentration profiles of both fluid and dust particles. Through $Figs.(3.7-3.9)$ it is observed that by increase in the values of N_t, the thermophoretic parameter, there is an increase in concentration profiles. Whereas increase in Schmidt number (Sc) and Brownian motion parameter (N_b) decrease the concentration as the thickness of the concentration boundary layer decreases. This is because that an increase in Sc implies a decrease in the molecular diffusivity.

$Table$.3.4 represents the influence of Thermophoresis parameter, Brownian motion parameter and Schmidt number on heat and mass transfer coefficients.

3.7 Concluding Remarks

- Dust phase temperature and concentration is lower than that of fluid phase.
- Increase in unsteadiness parameter and suction parameter decreases the concentration of nanofluid.
- While viscous dissipation, thermal radiation and the number density of dust particles have no effect on the concentration.
- Nanofluid increases the rate of heat transfer.
- Thermophoresis parameter and Brownian motion parameter increase the temperature profile while Schmidt number decreases temperature.
- Concentration increases with an increase in Thermophoresis parameter whereas it reduces when we increase Brownian motion parameter and Schmidt number.
- The Nusselt number decreases with an increase in Thermophoresis parameter and Brownian motion parameter whereas it increases with an increase in Prandtl number and Schmidt number.
- Sherwood number decreases with an increase in Thermophoresis parameter while increases with an increase in Brownian motion parameter and Schmidt number.

Bibliography

[1] Sakiadis, B. C. (1961). Boundary-layer behavior on continuous solid surfaces: I. Boundary-layer equations for two-dimensional and axisymmetric flow. AIChE Journal, 7(1), 26-28.

[2] Tsou, F. K., Sparrow, E. M., & Goldstein, R. J. (1967). Flow and heat transfer in the boundary layer on a continuous moving surface. International Journal of Heat and Mass Transfer, 10(2), 219-235.

[3] Gupta, P. S., & Gupta, A. S. (1977). Heat and mass transfer on a stretching sheet with suction or blowing. The Canadian Journal of Chemical Engineering,55(6), 744-746.

[4] Mustafa, M., Khan, J. A., Hayat, T., & Alsaedi, A. (2015). Boundary Layer Flow of Nanofluid Over a Nonlinearly Stretching Sheet With Convective Boundary Condition. IEEE Transactions On Nanotechnology, 14(1), 159.

[5] Mabood, F., Khan, W. A., & Ismail, A. I. M. (2015). MHD boundary layer flow and heat transfer of nanofluids over a nonlinear stretching sheet: A numerical study. Journal of Magnetism and Magnetic Materials, 374, 569-576.

[6] Magyari, E., & Keller, B. (1999). Heat and mass transfer in the boundary layers on an exponentially stretching continuous surface. Journal of Physics D: Applied Physics, 32(5), 577.

[7] Nadeem, S., Haq, R. U., & Khan, Z. H. (2014). Heat transfer analysis of water-based nanofluid over an exponentially stretching sheet. Alexandria Engineering Journal, 53(1), 219-224.

[8] Ibrahim, W., & Shanker, B. (2015). MHD Boundary Layer Flow and Heat Transfer Due to a Nanofluid Over an Exponentially Stretching Non-Isothermal Sheet. Journal of Nanofluids, 4(1), 16-27.

[9] Grubka, L. J., & Bobba, K. M. (1985). Heat transfer characteristics of a continuous, stretching surface with variable temperature. Journal of Heat Transfer, 107(1), 248-250.

[10] Char, M. I. (1988). Heat transfer of a continuous, stretching surface with suction or blowing. Journal of Mathematical Analysis and Applications, 135(2), 568-580.

[11] Elbashbeshy, E. M. A., & Bazid, M. A. A. (2004). Heat transfer over an unsteady stretching surface. Heat and Mass Transfer, 41(1), 1-4.

[12] Malvandi, A., Hedayati, F., & Ganji, D. D. (2015). Boundary Layer Slip Flow and Heat Transfer of Nanofluid Induced by a Permeable Stretching Sheet with Convective Boundary Condition. Journal of Applied Fluid Mechanics, 8(1).

[13] Partha, M. K., Murthy, P. V. S. N., & Rajasekhar, G. P. (2005). Effect of viscous dissipation on the mixed convection heat transfer from an exponentially stretching surface. Heat and mass transfer, 41(4), 360-366.

[14] Dhanai, R., Rana, P., & Kumar, L. (2015). Dual Solutions in MHD Boundary Layer Nanofluid Flow and Heat Transfer with Heat Source/Sink considering Viscous Dissipation. Research Journal of Engineering and Technology, 6(1), 142-148.

[15] Hussain, T., Shehzad, S. A., Alsaedi, A., Hayat, T., & Ramzan, M. (2015). Flow of Casson nanofluid with viscous dissipation and convective conditions: A mathematical model. Journal of Central South University, 22(3), 1132-1140.

[16] Pal, D., & Mandal, G. (2015). Mixed convection–radiation on stagnation-point flow of nanofluids over a stretching/shrinking sheet in a porous medium with heat generation and viscous dissipation. Journal of Petroleum Science and Engineering, 126, 16-25.

[17] Awais, M., Hayat, T., Iram, S., Siddiqa, S., & Alsaedi, A. (2015). Thermophoresis and Heat Generation/Absorption in Flow of Third Grade Nanofluid. Current Nanoscience, 11(3), 394-401.

[18] Sajid, M., & Hayat, T. (2008). Influence of thermal radiation on the boundary layer flow due to an exponentially stretching sheet. International Communications in Heat and Mass Transfer, 35(3), 347-356.

[19] Biliana, B., & Roslinda, N. (2009). Numerical solution of the boundary layer flow over an exponentially stretching sheet with thermal radiation.

[20] Hayat, T., Muhammad, T., Shehzad, S. A., & Alsaedi, A. (2015). Similarity solution to three dimensional boundary layer flow of second grade nanofluid past a stretching surface with thermal radiation and heat source/sink. AIP Advances, 5(1), 017107.

[21] Sheikholeslami, M., Ganji, D. D., Javed, M. Y., & Ellahi, R. (2015). Effect of thermal radiation on magnetohydrodynamics nanofluid flow and heat transfer by means of two phase model. Journal of Magnetism and Magnetic Materials, 374, 36-43.

[22] Andersson, V. P. H. (1992). MHD flow of a viscoelastic fluid past a stretching surface. Acta Mechanica, 95(1-4), 227-230.

[23] Damseh, R. (2006). Thermal boundary layer on an exponentially stretching continous surface in the presence of magnetic field effect. Int. J. of Applied Mechanics and Engineering, 11(2), 289-299.

[24] Ishak, A. (2011). MHD boundary layer flow due to an exponentially stretching sheet with radiation effect. Sains Malaysiana, 40(4), 391-395.

[25] Ahmad, I., Sajid, M., Awan, W., Rafique, M., Aziz, W., Ahmed, M., ... & Taj, M. (2014). MHD flow of a viscous fluid over an exponentially stretching sheet in a porous medium. Journal of Applied Mathematics, 2014.

[26] Chaudhary, S., & Kumar, P. (2015). Magnetohydrodynamic Boundary Layer Flow over an Exponentially Stretching Sheet with Radiation Effects. Applied Mathematical Sciences, 9(23), 1097-1106.

[27] Elbashbeshy, E. M., Emam, T. G., & Abdelgaber, K. M. (2012). Effects of thermal radiation and magnetic field on unsteady mixed convection flow and heat transfer over an exponen-

tially stretching surface with suction in the presence of internal heat generation/absorption. Journal of the Egyptian Mathematical Society, 20(3), 215-222.

[28] Mansur, S., & Ishak, A. (2014, June). Unsteady boundary layer flow and heat transfer over a stretching sheet with a convective boundary condition in a nanofluid. In Proceedings Of The 3rd International Conference On Mathematical Sciences (Vol. 1602, pp. 311-316). AIP Publishing.

[29] Saffman, P. G. (1962). On the stability of laminar flow of a dusty gas. Journal of fluid mechanics, 13(01), 120-128.

[30] Vajravelu, K., & Nayfeh, J. (1992). Hydromagnetic flow of a dusty fluid over a stretching sheet. International journal of non-linear mechanics, 27(6), 937-945.

[31] Pavithra, G. M., & Gireesha, B. J. (2014). Unsteady flow and heat transfer of a fluid-particle suspension over an exponentially stretching sheet. Ain Shams Engineering Journal, 5(2), 613-624.

[32] Gireesha, B. J., Mahanthesh, B., & Gorla, R. S. R. (2014). Suspended Particle Effect on Nanofluid Boundary Layer Flow Past a Stretching Surface. Journal of Nanofluids, 3(3), 267-277.

[33] Ramesh, G. K., Gireesha, B. J., & Gorla, R. S. R. (2015). Boundary layer flow past a stretching sheet with fluid-particle suspension and convective boundary condition. Heat and Mass Transfer, 1-6.

[34] Choi, S. U. S. Enhancing thermal conductivity of fluids with nanoparticles. ASME-Publications-Fed 231 (1995): 99-106.

[35] Buongiorno, J. (2006). Convective transport in nanofluids. Journal of Heat Transfer, 128(3), 240-250.

[36] Nadeem, S., & Lee, C. (2012). Boundary layer flow of nanofluid over an exponentially stretching surface. Nanoscale research letters, 7(1), 1-6.

[37] Bachok, N., Ishak, A., & Pop, I. (2012). Unsteady boundary-layer flow and heat transfer of a nanofluid over a permeable stretching/shrinking sheet.International Journal of Heat and Mass Transfer, 55(7), 2102-2109.

[38] Naramgari, S., & Sulochana, C. (2015). Dual solutions of radiative MHD nanofluid flow over an exponentially stretching sheet with heat generation/absorption. Applied Nanoscience, 1-9.

[39] Haq, R. U., Nadeem, S., Khan, Z. H., & Akbar, N. S. (2015). Thermal radiation and slip effects on MHD stagnation point flow of nanofluid over a stretching sheet. Physica E: Low-dimensional Systems and Nanostructures, 65, 17-23.

[40] Nadeem, S., Mehmood, R., & Akbar, N. S. (2015). Partial slip effect on non-aligned stagnation point nanofluid over a stretching convective surface.Chinese Physics B, 24(1), 014702.

[41] Gireesha, B. J., Chamkha, A. J., Rudraswamy, N. G., & Krishnamurthy, M. R. (2015). MHD Flow and Heat Transfer of a Nanofluid Embedded with Dust Particles Over a Stretching Sheet. Journal of Nanofluids, 4(1), 66-72.

[42] Yabushita, K., Yamashita, M., & Tsuboi, K. (2007). An analytic solution of projectile motion with the quadratic resistance law using the homotopy analysis method. Journal of Physics A: Mathematical and theoretical, 40(29), 8403.

[43] Liao, S. (2010). An optimal homotopy-analysis approach for strongly nonlinear differential equations. Communications in Nonlinear Science and Numerical Simulation, 15(8), 2003-2016.